Roles for the Polycomb Group Protein BMI1 in Lung Adenocarcinoma Progression and Maintenance

by

Daniel Louis Karl

B.A. History and English
Northwestern University (2004)

Submitted to the Department of Biology
in Partial Fulfillment of the Requirements for the Degree of

Doctor of Philosophy

at the

MASSACHUSETTS INSTITUTE OF TECHNOLOGY

July 26, 2016 [September 2016]

Signature redacted

Signature of Author.....
Department of Biology
July 26, 2016

Signature redacted

Certified by .....
Jacqueline Lees
Professor of Biology
Thesis Supervisor

Signature redacted

Accepted by .....
Michael Hemann
Professor of Biology
Chair, Committee for Graduate Students

Roles for the Polycomb Group Protein Bmi1 in Lung Adenocarcinoma Initiation, Progression and Maintenance

by

Daniel Louis Karl

Submitted to the Department of Biology on July 26, 2016 in Partial Fulfillment of the Requirements for the Degree of Doctor of Philosophy in Molecular Biology

ABSTRACT

The B lymphoma Mo-MLV insertion region 1 homolog (Bmi1) protein is implicated as an oncogene in a variety of human cancers. During normal development, Bmi1 acts as part of a transcriptional repressive complex that regulates processes such as stem cell self-renewal, cell-fate commitment, and proliferation. During tumorigenesis, many cancers co-opt these core Bmi1 functions. A subset of these malignancies demonstrates an increased dependence on Bmi1, revealing a window of vulnerability that could be exploited for the therapeutic benefit of patients. With the advent of cancer genomics, we have begun to appreciate the complex molecular determinants that inform these therapeutic windows. Indeed, Bmi1 is now understood to play unique roles depending on the underlying genetic contexts of tissue type, developmental stage, and of individual tumors. With this in mind, in this thesis I used mouse models of oncogenic Kras driven lung cancer to explore the potential dependence of lung adenocarcinoma, among the deadliest of cancers, on Bmi1 for tumor initiation, progression, and maintenance. Specifically, I demonstrate that Bmi1 is dispensable for tumor initiation but mediates the transition to advanced disease and thereby impacts the overall survival of tumor bearing animals. I show that Bmi1 is required to sustain the proliferative capacity of Kras driven lung adenomas. In part, it does so by enforcing efficient progression through the cell cycle independent of a canonical target, the $p19^{ARF}$-p53 tumor suppressive axis. This creates a large potential therapeutic window, as half of all lung adenocarcinoma patients display p53 mutations. My gene expression analyses further establishes a critical role for Bmi1 in the repression of developmental regulators, which may contribute to the atypical differentiation state of tumors as they adapt to the loss of Bmi1. Finally, using both mouse models and cell lines, I present evidence that a subset of advanced tumors are sensitive to the loss of Bmi1. Overall, this thesis advances our understanding of the genetic dependencies of Bmi1 in lung cancers and reveals novel mechanisms that potentially can be exploited to combat this deadly of disease.

Thesis Supervisor: Jacqueline A. Lees
Title: Professor of Biology

ACKNOWLEDGEMENTS

While I was in the fortunate position to be the one to commit this body of work to paper, this thesis was a village's effort and I would like to spend a few words of thanks here.

First, I would like to thank my advisor and mentor Dr. Jacqueline Lees for her support through my graduate career. She has been a constant source of encouragement, ideas, and understanding, helping shape me as a student and scientist. I would also like to thank the entire Lees Lab that created an exciting and engaging environment in which to pursue my scientific interests. I treasure the friendship and camaraderie that we built, and I owe much of my scientific growth to my interactions with all of you. In particular I want to thank Paul Danielian for spearheading this effort with me. Rachit Neupane, Anna Kuperman, Stephanie Riocci, Jenny Tadros, and Arjun Bhutkar were instrumental in driving this work forward - thank you all. Personally, I want to thank Monica Stanciu for her generosity, advice, and close friendship through the years, as well as Roberta Ferretti and Tiziana Parisi for their unwavering friendship and guidance. All of you enriched my time here at MIT as well as my life beyond. Exclamations cannot fully represent my gratitude!

I would also like to thank my classmates. I formed life-long friendships with so many of you and hope that as we scatter across the country we maintain the sense of community that began here. I look forward to following the amazing things that you will accomplish.

Finally, I want to thank my family. My journey to and through graduate school included more than a few sharp turns. I am certain that my parents gasped through all of it, and I am grateful that their voices were constant cries of inspiration and support. I hope that when it is my turn to gasp as a parent that I will live up to your example. To all my family scattered throughout the world, each of you has informed a part of my life for the better and you may be surprised to know that even little things find their way into this thesis. I share this accomplishment with all of you.

Haley, Micah and Emme: If exclamations cannot fully represent gratitude, then words cannot capture the depth of love, appreciation, happiness and understanding that I glean from you every day. Thank you for sharing your lives with me and for buttressing me as a student, father and husband through all of mine.

TABLE OF CONTENTS

CHAPTER 1: INTRODUCTION

The B lymphoma Mo-MLV insertion region 1 homolog (BMI1) protein has been implicated as an oncogene in a variety of cancers. It functions as part of a transcriptional repressive complex that regulates many processes during normal development including cell-fate commitment, stem cell self-renewal, and cell proliferation. Using mouse models of lung adenocarcinoma, I have established Bmi1 as an important regulator in the progression of tumors to advanced disease. In this chapter, I will introduce Bmi1, both as an epigenetic regulator in development and differentiation and then, more specifically, in the context of lung cancer. However, first I will briefly introduce epigenetic regulators and their importance to cancer biology.

I. AN OVERVIEW OF EPIGENETIC REGULATORS IN TUMORIGENESIS

1. Genetic and epigenetic determinants of cancer

Genetic endowment, from parent to child or cell to progeny, inaugurates and perpetuates life. This idea seems foundational to our understanding of biology, evolution, and organismal development, yet at its origins it remains intimately linked to our first insights into the deadly nature of cancer. In a series of seminal experiments in 1902, Theodor Boveri, with his wife and collaborator Marcella[1], made the first observations that sea urchin sperm and egg impart equal genetic material to the next generation (Boveri 1902). These observations, coupled with evidence presented by Walter Sutton that same year, prompted the widespread acceptance of chromosomal theory as the fundamental mechanism for Mendelian inheritance (McKusick 1985). Within a year - and three years before William Bateson coined the term "Genetics" -

[1] Marcella O'Grady Boveri was the first woman to earn a biology PhD from MIT in 1885.

Boveri also noticed that the misallocation of chromosomes occasionally caused the developing sea urchin embryo to grow abnormally (Boveri 1903). This spurred Boveri to speculate that perhaps cancer is rooted in abnormal transmission of genetic information (reviewed in Balmain 2001). Over a hundred years of inquiry into genetics has largely validated Boveri's chromosomal theory of inheritance as well as his speculation that the abnormal transfer of genetic material is a critical determinant of cancer (Boveri 1914 , translated in Boveri 1929; Boveri 2008).

For much of the last half century, cancer biologists focused on the role of individual genes in cancer, and only more recently began to appreciate epigenetic contributions. In the late 1970s, key discoveries by Varmus and Bishop that individual genes can cause cellular transformation paved the way for the long hunt to find cancer causing genes (Stehelin et al. 1976). In fact, the first human genetic driver of cancer - the oncogene *Hras* - was identified only a few years later and shown to be pro-tumorigenic due to a key mutation in its gene sequence (Reddy et al. 1982; Taparowsky et al. 1982). By contrast, epigenetic inheritance can be broadly defined as the transfer of cellular information outside of the DNA sequence itself (Waddington 1953; Feinberg and Tycko 2004). Adding a methyl group to a cytosine nucleotide, for example, does not change the DNA sequence, but it can induce a heritable biological outcome (Johnson and Coghill 1925; Pollack et al. 1980; and reviewed in Franchini et al. 2012). Though Waddington popularized epigenetics more broadly in the middle of the 1900s, it was not until the 1980s that Feinberg and Vogelstein first demonstrated that some cancers were globally hypomethylated (Feinberg and Vogelstein 1983). That epigenetic changes likely contributed to cancer was shown in the 1990s, when several groups found that

promoter hypermethylation and the subsequent repression of tumor suppressor genes such as pRB and $p16^{INK4A}$ are critical events in cancer (Greger et al. 1989; Sakai et al. 1991; Gonzalez-Zulueta et al. 1995; Merlo et al. 1995). Since the 1990s, countless other epigenetic alterations have been identified in various cancer types. Today, the community of cancer biologists is keenly aware of the need to better understand the vastly complex genetic and epigenetic determinants of cancer in order to develop durable responses to this deadly set of diseases.

2. DNA Methylation in cancer

Much is now known about the common epigenetic alterations that frequently arise in cancer. As described above, the first observable epigenetic differences between normal and cancer cells were global changes in DNA methylation. This modification is almost exclusively found in the context of stretches of CpG dinucleotides, called CpG islands, near the promoters of genes (Franchini et al. 2012). Catalyzed by one of three DNA methyltransferases (DNMT1-3), a methyl group is covalently bound to the C5 position of a cytosine, this mark correlates with repression of the nearby gene. The methyl group can serve either as a recruitment signal for a number of proteins that together inhibit the active transcription of the genes, or potentially by sterically blocking the ability of certain transcription factors (such as MYC) to bind and drive transcription (Prendergast et al. 1991). Importantly, it was shown that DNA methylation is a heritable event, where after DNA synthesis, DNMT1 catalyzes the methylation of newly synthesized CpGs based on the methylation status of the opposite strand (Bestor et al. 1988; Li et al. 1992; Franchini et al. 2012). In this way, the locus in the daughter cell will remain repressed, potentially through the lifetime of the organism.

Paradoxically, both global hypermethylation and hypomethylation have been observed in cancer and may contribute to tumorigenesis. As mentioned previously, hypermethylation can enforce the repression of tumor suppressor genes such as pRB and $p16^{INK4A}$ and other cell cycle inhibitors. This was shown to be critical to tumorigenesis in a number of preclinical studies that demonstrated that inhibition of DNMT1 led to reactivation of these genes in some cancers and tumor regression (Laird et al. 1995; Cheng et al. 2003). In fact, this was the principle by which several chemotherapeutic agents (notably 5-azacytidine) have now been approved for use against several myelodisplasia disorders. However, it has recently been observed that DNMT1 inhibition in patients may have the unintended consequence of derepressing a set of other targets - such as endogenous retroviruses - that may contribute to the tumor suppressive effects of DNMT inhibition (Chiappinelli et al. 2015; Roulois et al. 2015). Conversely, hypomethylation has been shown to lead to genomic instability, a phenomenon that is well understood in other contexts to be a driver of tumor progression (Chen et al. 1998; reviewed in Robertson 2005). Hypomethylation has been implicated as a cause for the rearrangement of large portions of pericentromeric heterochromatin and the activation of transposable elements (Mertens et al. 1997; Walsh et al. 1998). However, this may also be due in part to the expression of oncogenes such as Myc or Ras in cancer (Vafa et al. 2002; Denko et al. 1994). Nevertheless, CpG methylation status contributes to tumorigenesis even though the requirements for targeting unique loci are less well understood. This lack of specificity may ultimately impact our ability to target methylated DNA loci in cancers using broad DNMT inhibitors.

3. Understanding and targeting the Histone Code

Epigenetic contributions to cancer are not limited to the covalent modification of DNA. Various species of RNAs, from long-noncoding RNAs to post-transcriptional processing and handling of transcripts, can influence gene expression in ways that alter the gene expression of cancer cells without modifying the DNA sequence (Sahu et al. 2015; Hayes et al. 2014). Beyond RNA, alterations in chromatin - the three dimensional DNA-protein structure that collectively packages genetic material - have emerged as important mediators of tumorigenesis by regulating gene expression (Garraway and Lander 2013; Audia and Campbell 2016; Ahuja et al. 2016). Targeting chromatin regulators has gained more traction as potential targets for therapeutic intervention partially because it is technically easier to deliver small molecules that inhibit the enzymatic modification of chromatin. Furthermore, the preponderance of specific modifications with functionally narrow biological outputs has the potential to limit unintended adverse effects on gene expression.

The diversity of modified chromatin can largely be thought of as an integrated system classically referred to as the 'histone code' (Jenuwein and Allis 2001). Histones, including an H3-H4 tetramer and two H2A-H2B dimers, are the main protein components of nucleosomes that are the primary packagers of DNA. While the core of this octamer serves as a molecular spool for DNA, the terminal histone tails project from the core and are extensively post-translationally modified. Histone methylation and acetylation are perhaps the best understood modifications, but histone tails can also be ubiquitylated, sumoylated, phosphorylated, citrullinated, ribosylated, deiminated, and crotonylated (Audia and Campbell 2016). The most well studied modifications are

those on the tail of histone H3, where lysine 4 (H3K4), lysine 9 (H3K9), lysine 27 (H3K27), and lysine 36 (H3K36) are variously methylated or acetylated correlating to gene activation (reviewed in Lawrence et al. 2016). Many studies, for instance, have implicated H3K4 tri-methylation (H3K4me3) along with H3K9 and H3K27 acetylation (H3K9Ac/H3K27Ac) with promoters undergoing active transcription. Conversely, tri-methylation of H3K9 and H3K27 correlates with transcriptional inactivation. The diverse set of histone modifications leads to complex and integrated biological responses in part by serving as recruitment factors for activators, sustainers or repressors of target nearby genes. They may also mediate the accessibility of the underlying DNA to DNA binding factors by sterically inhibiting access. As discussed in future sections, there are mechanisms to pass down the cellular decisions made at the histone level to subsequent generations. Ultimately, histones serve as a modifiable signaling platform that informs cellular decisions about the underlying genetic information.

The advent of tumor sequencing studies has demonstrated that mutations in histone modifiers are frequent events in many cancers and likely are functionally important for tumor maintenance (Garraway and Lander 2013). These mutations are often heterozygous loss of function mutations in the enzymes that catalyze the deposition or removal of histone modifications. For instance, histone acetyl transferase (HAT) proteins CREBP and EP300 are frequently mutated in cancer, as are histone lysine methytransferases (KMTs) and histone lysine demethylases (KDMs) (Garraway and Lander 2013). Since many of these are required for cell survival, inhibition may selectively target cancer cells. After the therapeutic targeting of DNMTs, inhibitors of

histone deacetylases (HDACs) are the most prominent epigenetic targets currently in the clinic (West and Johnstone 2014). HDAC inhibitors have been FDA approved for the treatment of T cell lymphomas; however, their exact method of tumor suppression remains elusive and may be partially independent of gene regulation through hyperascetylated histones. Clinical trials are currently underway for a number of inhibitors targeting other histone modifiers - notably Ezh2 that catalyzes H3K27me3 and will be discussed in more detail later in this introduction. Lastly, a preponderance of preclinical data suggests that 'histone readers' - proteins that are recruited to a locus by histone marks - are crucial for tumor maintenance. For example, over-expression of BRD4, which recognizes histone lysine acetylation to assist in transcriptional activation, can lead to inappropriate activation of Myc targets. Small molecule inhibitors of BRD4 are now in clinical trials after showing efficacy in preclinical studies (Delmore et al. 2011; Dawson et al. 2011; Zuber et al. 2011). Together these studies emphasize the importance of chromatin as a modifiable regulator for gene regulation, including those that may directly impact tumorigenesis.

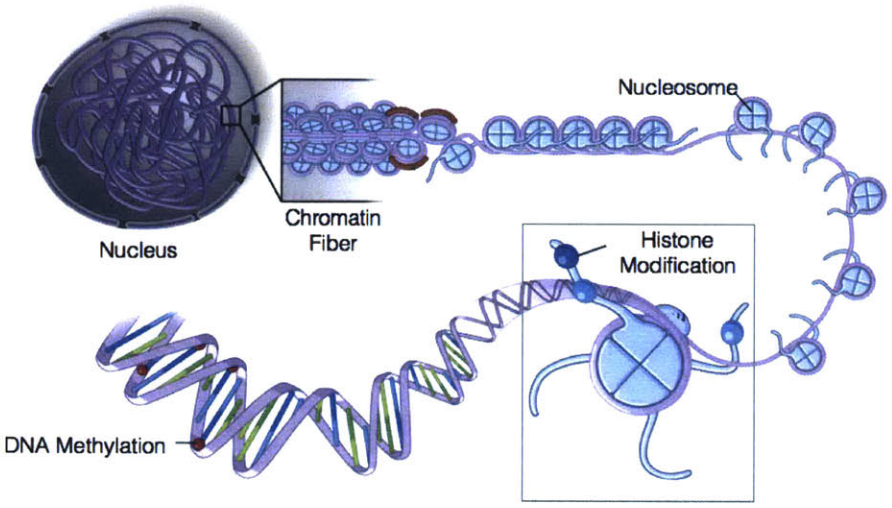

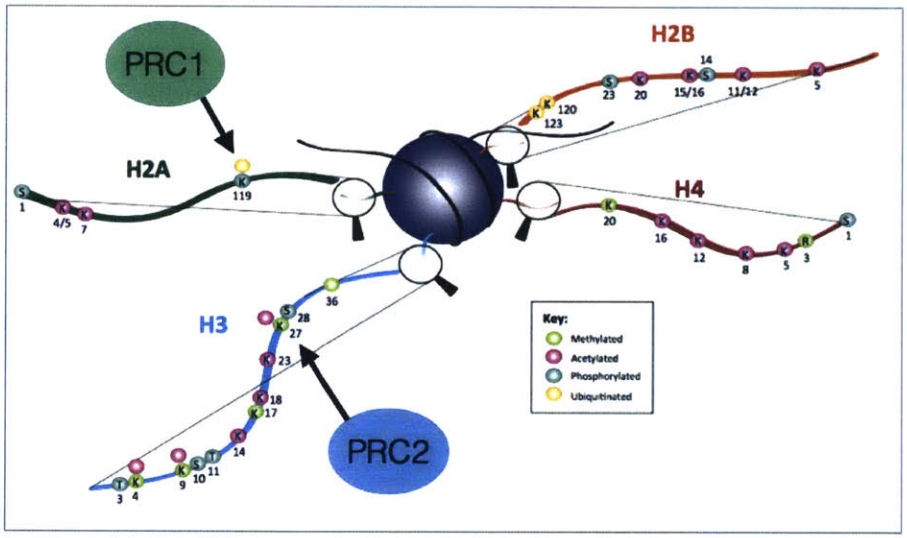

adapted from Yan MSC et al. *J Appl Physiol* 2010 and Lawrence M, et al. *Trends in Genetics* 2016

Figure 1. Schematic illustrating higher order chromatin organization in the nucleus, including chromatin fibers and individual nucleosomes. Below, common sites of covalent modification of histone tails are depicted.Polycomb Repressive Complex 1 (PRC1) catalyzes the ubiquitination of lysine 119 (K119) on the tail of histone H2A. Polycomb Repressive Complex 2 (PRC2) mediates the methylation of lysine 27 (K27) on histone H3. Letters indicate amino acids (K=lysine, R=arginine, S=serine, T=threonine), and numbers represent amino acid position.

II. MECHANISMS OF EPIGENETIC REGULATION BY BMI1 THROUGH THE POLYCOMB REPRESSIVE COMPLEX 1

1. Polycomb group proteins repress transcriptional activity

The Polycomb Group proteins (PcGs) were originally identified as mutant alleles in *Drosophila melanogaster* - the common fruit fly. In 1947, P.H. Lewis first described an x-ray induced dominant mutant that resulted in a number of developmental transformations, including extra hairs (called sex combs) on the second and third sets of legs in addition to the first (Lewis 1947). He named the mutant Polycomb (Pc). Subsequent studies using this allele confirmed that Pc repressed several "substances" that specified thoracic and abdominal segmentation during development (Lewis 1978). These "substances" - later understood to be transcription factors - were activated from a clustered array of genes collectively called the bithorax and antennapedia complexes (BX-C and ANT-C). The genes along these arrays were active in a manner that was co-linear with the insect's body segment, thereby controlling the unique patterns of development for each segment. Loss of Pc resulted in the inappropriate release of these genes leading to homeotic transformations during development. We now know that BX-C and ANT-C together encode the *Hox* transcription factors that are critical determinants of body patterning in both vertebrates and invertebrates. In 1995, EB Lewis won the Nobel Prize in part for the accomplishment of teasing apart the complex interrelationships of these gene clusters and their regulators.

Although Polycomb (Pc) was the first allele discovered that encodes a repressor for the *Hox* genes, it quickly became obvious that it was the founding member of a large group of genes that display similar phenotypes when mutated (Jürgens 1985). Together

their products became known collectively as the Polycomb Group Proteins (PcGs). In particular, several of the mutants cooperated directly with Pc or phenocopied its segmentation defects in *Drosophila*. Among them, Posterior sex combs (Psc), Polyhomeotic (Ph), and Sex combs extra (Sce) were present in equal stoichiometric amounts, appeared to co-localize, and also biochemically fractionated together as a complex (Zink and Paro 1989; Franke et al. 1992; Francis et al. 2001). These four components became known as the core of the Polycomb Repressive Complex 1. Future screens identified additional polycomb genes that enhanced PcG phenotypes (Sato and Denell 1985). One such screen looked for modifiers of a *zeste-white* phenotype and identified Enhancer of zeste E(z) and Suppressor of zeste Su(z)12, both of which caused homeotic transformations (Persson 1976; Wu et al. 1989). Future experiments implicated these two genes, along with Extra Sex Combs (esc), as the core components of a second canonical group - the Polycomb Repressive Complex 2(Struhl 1981; Jones et al. 1998). Together, PRC1 and PRC2 are the most studied and well understood polycomb complexes, are conserved in vertebrates, and are critical for the repression of their target genes.

2. Mammalian PRC1 is a dynamic complex involving many interchangeable subunits

While the *Drosophila* and mammalian PRC2 consist of a similar number of core proteins, the mammalian PRC1 evolved to include multiple genes for each *Drosophila* core PRC1 subunit. There are at least 5 orthologs of the original *Drosophila* Pc gene (called Cbx2,4,6,7,8); 3 PH proteins (in mouse called Phc1-3); 6 PSC orthologs (Pcgf1-6); and 2 orthologs of Sce (Ring1a/b)(reviewed in Gil and O'Loghlen 2014). In addition,

we now understand that various core PRC1 components can be substituted with other proteins to form non-canonical PRC1 complexes. Canonical PRC1 includes a Ring1 along with PCGF2 (Mel18) and PCGF4 (Bmi1) along with one of the Cbx proteins. In non-canonical PRC1, RYBP and YAF2 can take the place of the Cbx proteins and together with Ring1 and PCGFs, can be found with E2F6, KDM2b, L3MBTL and the BCOR complex (Trimarchi et al. 2001; Gao et al. 2012). While much of the diversification of the PRC1 seems to be due to duplication events during mammalian evolution, such as with the Cbxs and Pcgfs, the extensive integration of novel polycomb proteins into different PRC1 complexes hints at a dynamic role for PRC1 in target specification.

The plethora of mammalian PRC1 complexes raises a number of interesting questions regarding the differential functionality of each sub-complex. Genetic studies, for instance, have demonstrated that certain subunits are partially redundant. For example, mice deficient for either Mel18 (PCGF2) or Bmi1 (PCGF4) are viable and display similar posterior skeletal transformations, reminiscent of Polycomb phenotypes in *Drosophila,* but mice deficient of both do not survive embryogenesis (van der Lugt et al. 1994; Akasaka et al. 1996; 2001). Meanwhile, Ring1b deficiency is also an embryonic lethal phenotype, implicating Ring1b as a required component of PRC1 with Mel18 and Bmi1 sharing at least partial functional redundancy in the complex (Voncken et al. 2003). While Mel18 and Bmi1 regulate some common pathways in a dose dependent manner, the individual knockout mice nevertheless display some unique phenotypes suggesting that these proteins have specialized roles during development (Akasaka et al. 2001; Morey et al. 2015). Bmi1 null mice, for instance, display unique neurological

abnormalities, while Mel18 null mice develop smooth and cardiac muscle deficiencies. These differences, cannot entirely be explained by differential expression of these proteins in different tissues or developmental stages.

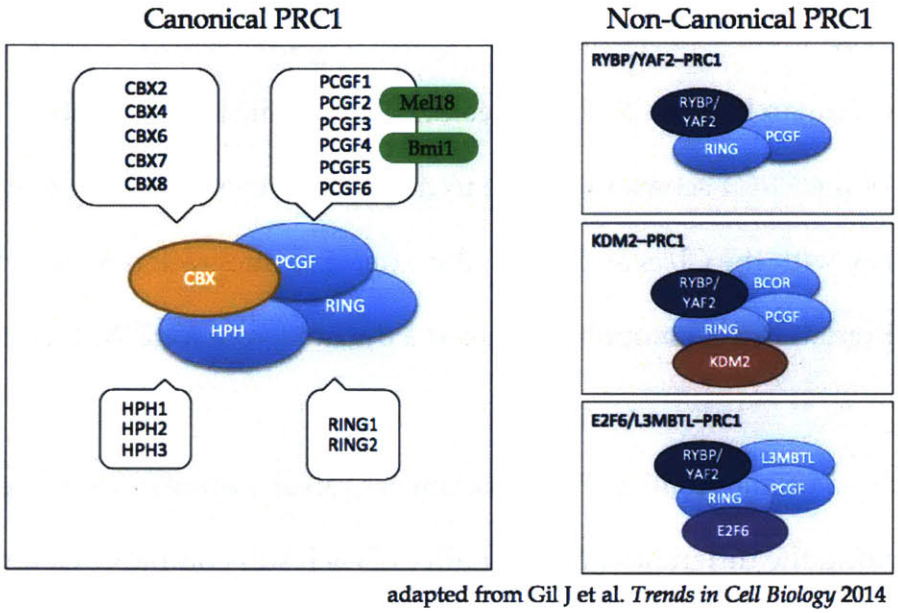

adapted from Gil J et al. *Trends in Cell Biology* 2014

Figure 2. Polycomb Repressive Complex 1 (PRC1) Diversity
Interchangeable subunit proteins in the canonical and non-canonical PRC1 complexes. Cbx proteins define the canonical complex. A PCGF such as Bmi1 or Mel18 and a Ring ligase comprise the core subunits in both types of PRC1 complexes.

Inherent in the diversity and specialization of PRC1 components is the notion that alternative subunits are recruited to a unique set of targets depending PRC1 sub-complex. Supporting this claim, RYBP and Cbx7 can both be expressed in the same cell type but mediate different biological functions (Morey et al. 2012a; Tavares et al. 2012). Furthermore, most Cbx proteins are recruited to methylated histones such as H3K27me3 through their chromodomains, while RYBP binds DNA directly (Taverna et al. 2007; Gil and O'Loghlen 2014). In fact, even different Cbx proteins have been shown

to have preferential binding to methylated histones and gene targets (Kaustov et al. 2010; Klauke et al. 2013). Nevertheless, the extent of diversity of these potentially competing complexes within the same cell is not clearly understood. The coexistence of alternative PRC1 complexes within the same cell also raises the possibility that the dosage of the subunits may play an important role. This underscores the highly complex nature of PRC1. While the picture of PRC1 diversity in mammals is not entirely clear, its is becoming increasingly well understood that this dynamic set of interchangeable proteins may allow for fine-tuned homing of polycomb mediated repression based on variable contextual cues.

3. Mechanisms of transcriptional repression by PRC1

Polycomb group proteins mediate transcriptional repression through various mechanisms that directly impact the underlying chromatin. For many years repression of target loci by PRC1 was thought to be largely mediated by the enzymatic activity of Ring1b (Wang et al. 2004a; Wei et al. 2006). Ring1b is an E3 ubiquitin ligase that catalyzes the covalent attachment of a ubiquitin protein of many substrates. Mono-ubiquitination of lysine 119 on histone H2A (H2AK119ub) seems to correlate closely with target repression (Wang et al. 2004a; Jian Cao 2012). H2AK119ub deposition may be required for transcriptional silencing by PRC1 and was shown to occur both *in vitro* and *in vivo* (Nakagawa et al. 2008; Cao et al. 2005). That H2AK119ub leads to transcriptional repression was buoyed by evidence that loss of this mark by H2A de-ubiqutinases results in gene re-expression (Joo et al. 2007). Intriguingly, in some instances, specific PRC1 may localize to actively transcribed genes (Brookes et al. 2012).

Nevertheless, there is broad acceptance that the primary role for PRC1 at target loci is transcriptional repression.

Though the exact mechanisms by which H2AK119ub mediate repression are not entirely elucidated, it may directly interact with the transcriptional machinery. The first evidence for this was found in 1982, when it was shown that a poised gene contained much more ubiquitinated H2A than permanently non-transcribed DNA (Levinger and Varshavsky 1982). Moreover, ubiquitinated H2A can be found in DNAse sensitive regions, suggesting that the chromatin is amenable to transcription in its presence (Dawson et al. 1991; Zhang 2003). Indeed, H2AK119ub may be important for restraining an engaged and poised RNA Polymerase II at promoters (Zhou et al. 2008; Brookes et al. 2012; Stock et al. 2007). This could either be due to a physical interaction with RNA Pol II itself, or perhaps by preventing the recruitment of elongation factors from engaging with the transcriptional machinery (Nakagawa et al. 2008; Simon and Kingston 2013). H2AK119ub, then, may serve as a signaling module in order to fine tune transcriptional repression at various poised loci.

Despite the focus on transcriptional repression through H2AK119ub, PRC1 can also mediate repression independent of its ubiquitinase activity. It has been suggested that a primary role for stable PRC1 mediated repression is through the compaction of chromatin into compressed heterochromatin unsuitable for active transcription. This was demonstrated *in vitro* without histone ubiquitination (Francis et al. 2004). PRC1 components appear to localize to heterochromatin in nuclear foci, and that localization specified transcriptional repression (Bantignies et al. 2011). Interestingly, Bmi1 may play a critical role in mediating this PRC1 function (Francis et al. 2004; Abdouh et al.

2016). In this model, PRC1 induces a closed chromatin environment inaccessible to transcriptional machinery. Other studies have since shown that catalytically inactive PRC1 can nevertheless maintain the repression of canonical *Hox* genes (Pengelly et al. 2015). Despite the tremendous insights into the diversity of roles for PRC1 in transcription, the factors that influence the circumstances governing these choices remain largely unknown.

4. The targeting and heritability of transcriptional silencing by PRC1

The classical model of PRC1 gene targeting involves the sequential recruitment of PRC2 and subsequently PRC1 to a locus (Wang et al. 2004b). In this scheme, Ezh2 catalyzes the deposition of methyl groups on lysine 27 of histone H3, which serves as a recruiting platform for PRC1 (Min 2003; Blackledge et al. 2015). Specifically, the chromodomains of the Cbx proteins recognize and bind H3K27me3 and PRC1 recruitment is secondary to PRC2 localization (Boyer et al. 2006). Other factors, such as the long non-coding RNAs, may help recruit PRC2 or directly bridge PRC1 during locus targeting (reviewed in Brockdorff 2013). However, this hierarchical model does not entirely explain why PRC1 and PRC2, as well as their respective histone marks, do not always overlap in the genome (Ku et al. 2008a). In fact, more than one study has shown that PRC1 may be involved in the recruitment of PRC2 rather than vice versa (Blackledge et al. 2014; Cooper et al. 2014). It is also clear that PRC1 inhabits a set of genes independent of PRC2 (Tavares et al. 2012). This seems to occur through non-canonical PRC1 variants, such as those containing RYBP which presumably recruits the complex through direct DNA binding. Perhaps this should not be surprising given that specific DNA sequences coined Polycomb Responsive Elements (PRE) have been

identified in *Drosophila*, even though similar bona-fide PREs have remained elusive in the mammalian genome (Müller and Kassis 2006). Several transcription factors - including Max, Rest, and Runx1 - bind PRC1 components and may assist in recruitment (Ogawa et al. 2002; Dietrich et al. 2012; Yu et al. 2012; Arnold et al. 2013). Nevertheless, it appears that distinct PRC1 components and their binding partners may help explain the diversity and specificity of PRC1 localization.

Regardless of the actual mechanism of PRC1 targeting and repression, PcGs appear to be important for maintaining heritable transcriptional repression. It has recently been shown that histone marks do in fact constitute a stable form of epigenetic inheritance, much like DNA methylation, and that it is not dependent on DNA sequence, DNA methylation, or RNA interference (Ragunathan et al. 2015; Audergon et al. 2015). For Polycomb mediated epigenetic repression, Polycomb or Polycomb-dependent marks must be inherited on the daughter strand during DNA synthesis (Beuchle et al. 2001). In part this occurs after histone eviction during DNA synthesis, when parental histones are randomly distributed to parental and daughter strands along with newly synthesized histones (Jackson 1988). Histone marks can then be inherited and must be duplicated on newly synthesize histones after deposition, though much more is known about the inheritance of methylation marks than ubiquitin (reviewed in Groth et al. 2007). However, histone H3-H4 tetramers are a much more stable resident of the nucleosome than H2A or H2B, which complicates the picture of H2AK119ub heritability. Furthermore, that ubiquitinated H2A levels change dramatically during the cell cycle also implies that this mark is more transient than histone methylation and may have to be redeposited based on site context after the cell

cycle (Joo et al. 2007). It is possible that the sustained presence of PRC1 proteins mediates a heritable form of heterochromatin independent of its enzymatic activity, thereby maintaining repression or redepositing ubiquitin after synthesis (Francis et al. 2009; Aoto et al. 2008). In *Drosophila*, PRC1 may form a platform on which to directly bridge new PRC1 complexes onto newly synthesized DNA and histones (Lo et al. 2012). Therefore, whether in combination with PRC2 or direct bridging with PRC1, PRC1 can mediate transcriptional repression through the cell cycle and therefore to progeny along a lineage.

5. Mammalian PRC1 is a critical regulator of development and differentiation

Appreciation for the indispensable role of PRC1 during organismal development and differentiation dates back to its original characterization in *Drosophila*. Yet for many years it was thought that PRC1 was restricted to controlling development through long-term repression of *Hox* genes. We now know that mammalian PRC1 is more broadly involved in tissue development, lineage specification and differentiation. Mice deficient of the main PRC1 catalytic subunit Ring1b are embryonic lethal due to arrest during gastrulation, a critical time for lineage specification into one of the three germ layers (Voncken et al. 2003). This phenotype underscores the important role for PRC1 during differentiation. More recently, PRC1 was found to occupy a diverse set of developmental targets, including many transcription factors (Bracken et al. 2006; Boyer et al. 2006). These targets are important regulators of tissue differentiation programs, buttressing the hypothesis that PRC1 is important for stably repressing factors that drive alternative lineages. As a result, PRC1 is crucial for enforcing a cell's commitment to a specific cell type or developmental pathway. This has since been validated in

several other tissue types and *in vivo*, and may be one of the critical functions of PRC1 for organismal maintenance (Chiacchiera et al. 2016; Brookes et al. 2012).

In addition to repressing alternative fate choices, PRC1 directly influences differentiation. Loss of various PRC1 components such as Ring1b in embryonic stem cells result in the inability to differentiate or express appropriate committed markers in embryoid bodies (Leeb and Wutz 2007). Subsequent studies examining PRC1 in embryonic stem (ES) cell differentiation found that Cbx7 was a critical component in ES cell maintenance, but that Cbx4 and Cbx2 were up-regulated during differentiation (Morey et al. 2012b; O'Loghlen et al. 2012). In this case, Cbx2 and 4 targets PRC1 to a set of pluripotency genes, thereby shutting them off and allowing for ES cell differentiation. Genetic studies looking closely at the Cbx proteins in hematopoietic stem cells similarly identified that differential Cbx proteins are required for adult stem cell maintenance and differentiation (Klauke et al. 2013). Together, these data demonstrate an important role for PRC1 for stem cell maintenance and differentiation.

6. Bmi1 is a core PRC1 member involved in development and tissue homeostasis

Bmi1 (Pcgf4) is the defining member of one of the canonical PRC1 sub-complexes and may be the most studied PCGF owing to its varying roles during normal development and pathological conditions. It was originally discovered as a common viral insertion site in a screen identifying c-Myc cooperators in a mouse model of lymphomagenesis (van Lohuizen et al. 1991b). Later that year, the same group identified Bmi1 as the mammalian ortholog of PSC in *Drosophila* (van Lohuizen et al. 1991a). Future experiments validated that a BMI1 containing mammalian Polycomb complex regulates *Hox* genes (van der Lugt et al. 1996). Shortly after its identification,

viable mouse models were developed with either germline deletion or over-expression of Bmi1, which together highlighted important roles for Bmi1 during development and tissue maintenance (van der Lugt et al. 1994; Alkema et al. 1995). For instance, mice deficient of Bmi1 are anemic, have a partially compromised immune system. In particular, Bmi1 null mice display severe defects in the lymphoid and myeloid lineages, resulting in the reduction of mature B and T cells, and a loss of cellularity in the thymus and spleen. These mice also display a number of severe neurological deficiencies. Together, these phenotypes have been attributed to an important role for Bmi1 in maintaining homeostasis in stem and progenitor compartment of these tissues.

Dynamic regulation of Bmi1 expression and activity suggests that it has important spacial and temporal functions. Signaling events through the PI3K/Akt or p38 pathways control Bmi1 phosphorylation and accessibility to chromatin (Liu et al. 2012; Voncken et al. 2005). Phosphorylation may also modulate Bmi1 activity throughout the cell cycle (Voncken et al. 1999). These events suggest that cells require the ability to rapidly alter Bmi1 dependent function based on various stimuli. Intriguingly, Bmi1 may autoregulate itself, both through ubiquitination and transcriptional repression (Taherbhoy et al. 2015, and unpublished observations). Other PRC1 subunits can also regulated Bmi1, either directly at its promoter or indirectly through repressing activators such as Myc (Qian et al. 2010). Together, these complicated regulatory schemes emphasize the need for tuning Bmi1 dosage and rapidly changing its accessibility to chromatin.

6.1 Bmi1 maintains stem cell self renewal

Bmi1 regulates stem and progenitor cell self renewal, in part, by sustaining the repression of cell cycle inhibitors that lead to stem cell exhaustion. Murine embryonic fibroblasts derived from Bmi1 germline mutant mice were observed to have a delay in entering the S phase of the cell cycle (Jacobs et al. 1999a). Two cell cycle inhibitors expressed from the same genetic locus *Cdkn2a*, $p16^{INK4A}$ and ARF ($p19^{ARF}$ in mice and $p14^{ARF}$ in humans), were found to be derepressed in these fibroblasts. Furthermore, *Ink4a* deficient mice appeared to ameliorate many of the severe phenotypes associated with the BMI1 null mice, particularly some of the hematological and neurological defects. Subsequent studies further pinned *Cdkn2a* as a pivotal target of Bmi1, with the deregulation of the locus a critical event leading to the depletion of hematopoietic, neural, and cerebellar stem cells in Bmi1 deficient mice (Molofsky 2005).

Derepression of the *Cdkn2a* locus has been closely associated with stem cell exhaustion in a variety of contexts (reviewed in Martin et al. 2014). Expression of $p16^{INK4A}$ leads to cell cycle arrest largely by inhibiting CyclinD1/CDK4/6 mediated phosphorylation of pRB, a critical checkpoint event for cell cycle entry. This, then, would inhibit the capacity of stem cells to continually divide. Arf also plays various roles that impinge on progression through the cell cycle (reviewed in Kim and Sharpless 2006). Classically, Arf is known to sequester MDM2 resulting in p53-p21 mediated cell cycle arrest or apoptosis, however it has been shown to act independently of p53 to mediate other biological functions (Weber et al. 2000; Sherr 2006; Lessard et al. 2010). Derepression of *Cdkn2a* in a variety of tissues can induce senescence - an irreversible

exit from the cell cycle (Lobo et al. 2007; Sousa-Victor et al. 2014). Together, this locus appears to be particularly primed to disrupt stem cell self renewal when expressed.

Despite the common role for Bmi1 in hematopoietic and neuronal stem cell self renewal through *Cdkn2a* repression, Bmi1 may regulated stem cell biology in various ways depending on the tissue. In the prostate, for instance, Bmi1 sustains self-renewal by regulating β-catenin signaling without altering $p16^{INK4A}$ or Arf transcript levels (Lukacs et al. 2010). In fact, recent studies have uncovered roles of Bmi1 in hematopoietic stem cell (HSC) biology independent of $p16^{INK4A}$ or Arf. Loss of Bmi1 in HSCs led to mitochondrial dysfunction and altered redox state that may contribute to senescence (Liu et al. 2009; Nakamura et al. 2012). Another set of experiments identified a potential role for Bmi1 early in DNA damage response signaling, which contributed to Bmi1 mediated HSC self-renewal (Chagraoui et al. 2011). *Cdkn2a* independent roles for BMI1 in maintaining neural stem cell self renewal have also been identified. It inhibits differentiation pathways in neural stem cells engaged in active self-renewal signals (Gargiulo et al. 2013). It also directly regulates the cell cycle inhibitor p21 in order to regulate neuronal and cerebellar stem cell self-renewal (Fasano et al. 2007; Subkhankulova et al. 2010). Lastly, a recent study also implicated a role for PRC1 in regulating murine embryonic fibroblast through the cooperation with MDM2 in repressing developmental genes (Wienken et al. 2016). Interestingly, most of the studies that pinpoint *Cdkn2a* as the principle target of Bmi1 are conducted with a mouse that lacks Bmi1 throughout development as the primary experimental tool. Given the known interrelationships between polycomb and methylation during development, Bmi1 may have an unappreciated role in establishing stable repression of *Cdkn2a* at

some point in development. The uncoupling of these events would be entirely consistent with these varied phenotypes. Even though the exact mechanisms may be context or tissue specific, these data argue that the Bmi1 containing PRC1 complex has evolved to play a prominent role in maintaining self-renewal capacity in a number of different tissues.

6.2 Bmi1 specifies fate choice during differentiation

The emergence of a prominent role for Bmi1 in stem cell biology spurred examination of Bmi1 during lineage commitment and fate choice specification. In many ways this was expected since PRC1 more broadly was found to largely restrain differentiation factors (Bracken et al. 2006). Chromatin immunoprecipitation followed by sequencing confirmed that Bmi1 dependent ubiquitinated H2A largely overlapped with developmental regulators (Kallin et al. 2009). Therefore, Bmi1 might serve as part of a PRC1 signaling module that selectively restrains specific targets based on external cues. This idea is consistent with known roles for PcGs in embryonic stem cell differentiation where certain lineage specific factors are poised for transcription (Bernstein et al. 2006; Boyer et al. 2006). Promoters at these loci are termed "bivalent" if they contain both activating and repressive marks - notably the activating H3K4me3 mark as well as repressive H3K27me3 mark deposited by PRC2 (Bernstein et al. 2006). These promoters contain core transcription factor machinery and engaged RNA pol II (Guenther et al. 2007; Min et al. 2011). A hallmark of bivalent promoters is that they can be resolved one of two ways, toward productive elongation or long term repression depending on the lineage to which the cell commits. Importantly, PRC1 was shown to occupy a number of PRC2 marked bivalent promoters in mouse ES cells and that these

were highly enriched for developmental transcription factors (Boyer et al. 2006; Ku et al. 2008b). Furthermore, these PRC1 marked domains can be resolved toward transcriptional activation (Richly et al. 2010). This pinpoints PRC1 at the convergence point for cellular decisions to express developmental transcription factors involved in lineage specification.

Bmi1 has been shown to have analogous functions during lineage commitment in adult stem and progenitor cell compartments. Specifically, Bmi1 was shown to be critically important for maintaining bivalent domains at B-cell lineage developmental regulator genes *Ebf1* and *Pax5* in multi-potent progenitors (Oguro et al. 2010). Loss of Bmi1 resulted in the resolution of bivalent domains at those to loci and the subsequent improper expression of lymphoid driving factors. This also resulted to the depletion of the hematopoietic stem cell and multi-potent progenitor cell pools towards the B cell lineage, independent of *Cdkn2a* expression. Other recent studies have also highlighted Bmi1s role in fate choice specification. For instance, loss of Bmi1 alters goblet cell lineage differentiation in the small intestine through modulation of Notch signaling (Lopez-Arribillaga et al. 2014). Bmi1 also restrains non-muscle transcription factors during myogenesis (Asp et al. 2011). More recently, Bmi1 was found restrain cardiac specific transcription factors in fibroblasts (Zhou et al. 2016). Interestingly, knockdown of Bmi1 led to the reacquisition of bivalency at the promoters of these cardiac transcription factors *Gata4, Tbx20, Isl1,* and *Pitx2* and their eventual re-expression along with the depletion of H2AK119ub. Thus, Bmi1 plays a prominent role in cellular decisions regarding fate-choice by poising transcription at the promoters of selective developmental regulators.

7. Diverse roles for Bmi1 in human cancers

Given the consistent and wide-spread role for Bmi1 in maintaining stem cell compartments - whether by restraining cell cycle inhibitors and differentiation factors, or maintaining redox balance and DNA damage signaling - it is unsurprising that Bmi1 has been associated with cancers. In many ways, cancers can be thought of as diseases driven by inappropriate self-renewal as well as over-proliferation. Cancers are often described as hijacking stem cell biology, both in hierarchical structure as well as the seemingly inexhaustible capacity to self-renewal (Visvader and Lindeman 2008). The extent to which different cancers adhere to a stem like hierarchy is still a matter of active debate. Nevertheless, described roles in repressing tumor suppressor genes classify Bmi1 as a potential oncogene.

Since its identification as a cooperating factor in a mouse model of lymphomagenesis, there has been intensive scrutiny of Bmi1 as a proto-oncogene. Many of the early studies focused on potential roles for Bmi1 in tissue compartments in which Bmi1 was shown to critically regulate stem cells - the hematological and neuronal compartments. Shortly after the Bmi1 null mouse was generated, it was found that Bmi1 cooperated with c-Myc, in part, by inhibiting a p53-dependent pro-apoptotic arm of c-Myc overexpression in lymphomagenesis (Jacobs et al. 1999b). These findings were later extended more broadly to indicate a critical requirement in the maintenance of many leukemic cells (Lessard and Sauvageau 2003). Several studies have also implicated Bmi1 in neurological malignancies including medulloblastomas, neuroblastomas, and glioblastomas (Leung et al. 2004; Nowak 2006; Bruggeman et al. 2007). Importantly, Bmi1 was shown to be either over-expressed in human

malignancies in these tissues or correlated with poor prognosis (Mihara et al. 2006; Xu et al. 2011; Mohty et al. 2007; Leung et al. 2004; Abdouh et al. 2009).

Broad interest following the pinpointing of Bmi1 as an oncogene led to its widespread examination in other malignancies. Among the first studies linking Bmi1 to solid tumors in humans was in Non-Small Cell Lung Cancer (NSCLC), which I will review more extensively in the next section (Vonlanthen et al. 2001). Bmi1 is also connected with multiple other cancers including those in the breast, stomach, ovary, pancreas, prostate, and colon; and numerous preclinical studies have validated functional roles for Bmi1 in promoting tumor growth (Koppens and van Lohuizen 2015; Hoenerhoff et al. 2009; Martínez-Romero et al. 2009; Bednar et al. 2015; Maynard et al. 2014). Additionally, *de novo* preclinical models have suggested potential roles for Bmi1 in the progression or maintenance of hepatocellular carcinoma, melanoma, pituitary tumors, as well as several sarcomas (Wang et al. 2008; Ferretti et al. 2016; Westerman et al. 2012; Douglas et al. 2008). Indeed, there is mounting evidence that Bmi1 functions as a bone-fide oncogene in a variety of tissue contexts and might serve as a meaningful therapeutic target. In fact, recent interest in targeting Bmi1 has led to the development of at least one published small molecule inhibitor that showed efficacy in a pre-clinical model of colorectal cancer (Kreso et al. 2014).

7.1 Mechanisms of the oncogene BMI1 oncogene

Considering the diverse set of functions attributed to Bmi1 in normal development and tissue homeostasis, it is unsurprising that there does not appear to be one common mode by which Bmi1 exerts its oncogenic effects. Nevertheless, the first mechanistic insights into Bmi1 focused on its role in suppressing the *Cdkn2a* locus in

lymphomas (Jacobs et al. 1999b). This leads to MDM2 sequestration of p53 and the suppression of a Myc driven apoptotic cascade. A similar role was also suggested for Bmi1 in other tumor types, which also implicated restraint of $p16^{INK4A}$ by Bmi1 as a critical factor in promoting tumor cell proliferation and inhibiting senescence (Park et al. 2004). Myc, a known driver of *Cdkn2a*, plays a fundamental role in many of these tumors and together these data may indicate that Bmi1 is particularly relevant for poised, Myc driven loci (Guney 2006). Interestingly, Myc has been broadly implicated in the release of poised RNA Pol II (Rahl et al. 2010). It is tempting to consider that Bmi1 might be involved in restraining a larger set of Myc targets in addition to *Cdkn2a*. In many ways, the field still focuses on *Cdkn2a* repression as a likely mechanism by which Bmi1 exerts its pro-tumorignic effects.

Despite the focus on *Cdkn2a*, it is clear that tissue context is a key determinant in the specification of Bmi1's oncogenic roles in any given tumor type. In neuronal lineages, for instance, neither $p16^{INK4A}$ nor Arf appear to be integral roles for BMI1 as an oncogene, despite their prominence as targets in maintaining normal stem cells. In medulloblastoma, Bmi1 impinges on sonic hedgehog signaling to mediate self-renewal (Leung et al. 2004; Bruggeman et al. 2005). Furthermore, in mouse models of glioma, Bmi1 loss impacts glioma progression and differentiation in and *Ink4a/Arf* null background (Bruggeman et al. 2007). More recently, an RNAi screen implicated Bmi1 in restraining a tumor suppressor downstream of ER stress signaling to mediate glioma maintenance (Gargiulo et al. 2013). The differences observed in these various neuronal malignancies highlight that Bmi1 targets are tissue and lineage specific and may change based on cellular context during tumorigenesis.

That Bmi1 expression specifies PRC1 in a context specific manner may in part explain the preponderance of different phenotypes that result from the loss of BMI1 in various tumors. For instance, the *Cdkn1a* locus that encodes the cell cycle inhibitor p21 has been identified as a target for Bmi1 in a several different cancer types (Hu et al. 2014). A role for Bmi1 in maintaining redox state and regulating reactive oxygen species (ROS) is involved in tumorigenesis in the pancreas and prostate (Nacerddine et al. 2012; Bednar et al. 2015). Furthermore, Bmi1 may stabilize YAP activity in Ewing sarcoma and repress WWOX and Foxc1 expression in small cell lung cancer and breast cancer, respectively (Hsu and Lawlor 2011; Kimura et al. 2011). In a broad sense, it is entirely possible that abundance of seemingly disparate Bmi1-dependent tumorigenic pathways are ultimately secondary to a fundamental, and as yet unappreciated, role for Bmi1 in cell biology. A more likely explanation, though, is that Bmi1 acts largely like other described epigenetic regulators - integrating a variety of inputs based on chromatin state, external signaling cues, active and poised promoters to target various different loci and restrain transcription.

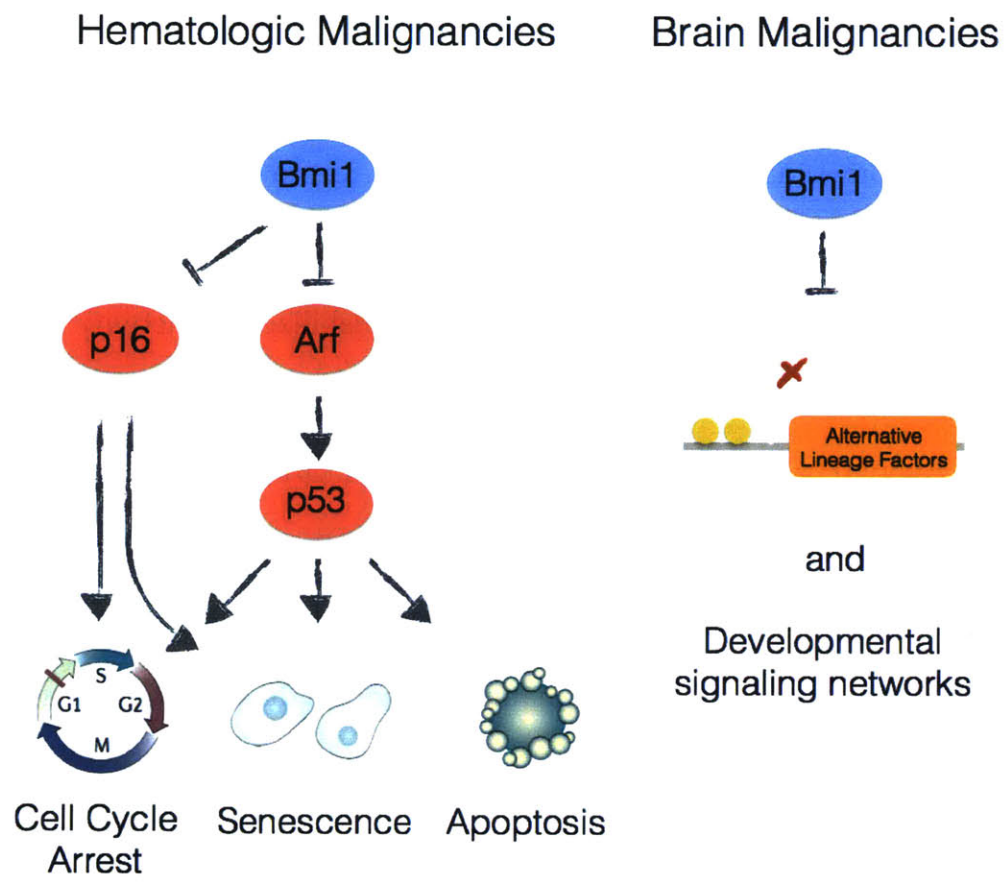

Figure 3. Bmi1 plays differential roles dependent on cancer type in adult mice. In hematological malignancies, Bmi1 is critical for maintaining the transcriptional repression of the CDKN2A locus that encodes the tumor suppressors p16 and Arf. These tumors suppressors modulate tumor cell proliferation and survival. In brain malignancies, Bmi1 can modulate tumorigenesis independent of the CDKN2A locus by regulating alternative lineage factors and signaling networks.

III. GENETIC AND EPIGENETIC DRIVERS IN LUNG ADENOCARCINOMA

In 2015, the deadliest cancers arose in the lung and bronchial airways - comprising an estimated 27% of cancer related deaths despite representing only 14% of new cancer cases (Siegel et al. 2015). The gross disparity between these two numbers highlights one of the central difficulties in treating pulmonary cancers, their frequency to relapse following treatment. Despite tremendous progress identifying and targeting molecular drivers, it is becoming increasingly well understood that the inherent high mutational burden in this disease leads to highly multi-clonal lesions that may serve as a storehouse of genetic insults, some of which may confer resistance to therapies (Kandoth et al. 2013; McGranahan et al. 2015; Piotrowska et al. 2015). Thus, the majority of patients present with incurable disease, leaving broad acting platinum-based chemotherapies as the standard of care for the most patients (Schiller et al. 2002). Recent progress on identifying epigenetic drivers in lung cancer has led to increasing interest in whether these reversible events can be modulated for the therapeutic benefit of these cancer patients (reviewed in Jakopovic et al. 2013).

1. Molecular drivers in lung adenocarcinoma

The vast majority of lung cancers are phenotypically classified as Non-Small Cell Lung Carcinomas (NSCLC), of which lung adenocarcinoma is the largest subtype (Chen et al. 2014). Cigarette smoking is one of the leading environmental causes of lung cancer and it appears to preferentially lead to the development of adenocarcinomas in the distal airway. While lesions from smokers are well known to have high mutational rates compared to other tumor types, even tumors from non-smokers have an exceptionally high rate of mutations (Alexandrov et al. 2013; Collisson et al. 2014;

Govindan et al. 2012). Broadly, adenocarcinomas are epithelial neoplasias that display glandular characteristics or are from a glandular origin; and in the lung tend to occur in the peripheral alveolar spaces. Nevertheless, the classification of lung adenocarcinoma incorporates a variety of different histological subtypes that are frequently being redefined based on accumulating molecular evidence of their origins and/or characteristics (Travis et al. 2011; 2015).

Despite the predominant reliance on chemotherapies, patient outcome has improved slightly due to the emergence of therapies targeting specific drivers in lung adenocarcinoma (Reck et al. 2013). Over-active Epidermal Growth Factor Receptor (EGFR) signaling is now understood to be a key event in tumorigenesis for a subset of lung adenocarcinomas, and small molecule inhibition of this receptor, in combination with chemotherapy, improves overall outcome of patients harboring EGFR mutations (Mok et al. 2009). Roughly 5% of lung adenocarcinoma patients present with an EML4-ALK fusion gene that results in inappropriate signaling through Anaplastic Lymphoma Kinase (ALK). These patients often respond better when treated with targeted ALK inhibitors (Kwak et al. 2010). Many other potential drivers have also been identified - such as ROS1 rearrangements, Met, Braf, Her2 mutations among others - some of which are targetable (Reck et al. 2013; Chen et al. 2014). In addition to these therapies, it is clear that a subset of patients durably respond to immune checkpoint therapies that harness the patients own immune system to fight cancer (Brahmer et al. 2015; Kazandjian et al. 2016). This suggests that immune evasion or cooption can be a critical determinant of lung tumorigenesis. Combined with improved diagnostic and staging

techniques, better histological classifications and biomarkers have improved the overall survival rate for lung adenocarcinoma patients (Reck et al. 2013; Chen et al. 2014).

Perhaps the most well studied molecular driver of lung adenocarcinoma is oncogenic signaling through various Kras mutants. Mutated in nearly 30% of lung adenocarcinomas, various Kras mutants have been identified that ultimately all enhance signaling through this small GTPase (Collisson et al. 2014). Active Kras signaling - when Kras is GTP bound - leads to downstream activation of the MAPK pathway and/ or the PI3K-AKT pathway, which are implicated in tumor cell proliferation and survival (Rajalingam et al. 2007). Though there have been many attempts to develop small molecule inhibitors of Kras, nothing has made it successfully into the clinic (Spiegel et al. 2014; Patricelli et al. 2016). Furthermore, various Kras mutations appear to confer differential sensitivity to chemotherapies, complicating a frontline clinical response (Pao et al. 2005; Janakiraman et al. 2010). This class of patients, then, remains the largest identifiable subset without a targeted therapeutic option. As a result, there is a particular interest in better understanding the biology of lung adenocarcinomas driven by Kras mutations.

While Kras mutations are common oncogenic drivers in lung adenocarcinoma, the transcription factor p53 is the most frequently mutated - being targeted in roughly 50% of all tumors, including those that are Kras mutant (Collisson et al. 2014). First identified in 1979, it is considered one of the classic tumor suppressors and is mutated or lost in a wide variety of cancers (Lane and Crawford 1979; Linzer and Levine 1979; Vogelstein et al. 2000). In response to cellular stresses, such as DNA damage or other oncogenic stressors, p53 is either induced or stabilized. When active, it can lead to the

expression of a large set of genes including those that lead to apoptosis or cell cycle arrest (Bieging et al. 2014). For instance, if Arf is expressed it binds and sequesters MDM2 and prevents it from repressing p53 (Pomerantz et al. 1998; Zhang et al. 1998). In other words, Arf expression can lead to cell cycle arrest or apoptosis indirectly through p53 dependent transcriptional activation. In lung cancers, p53 mutations often lead to the disruption of DNA binding, and this is followed by loss of heterozygosity of the second allele. This results in the inability of p53 to activate downstream tumor suppressive pathways. Additionally, various studies have suggested that some of these p53 mutants confer gain of function tumorigenic properties (Dittmer et al. 1993; Mello and Attardi 2013). Mouse models of lung adenocarcinoma have implicated a prominent role for p53 in regulating tumor progression, chemotherapeutic resistance and apoptosis (Feldser et al. 2010; Oliver et al. 2010; Singh et al. 2010).

2. Lung adenocarcinoma subtypes may reflect tumor cell of origin or tumor progression

Lung adenocarcinomas typically develop in the distal airways and are thought to arise from one of several tumor initiating cell types. However, it remains unclear whether the histological diversity is the result of the specific biological context of a tumor cell of origin, or whether stochastic events during progression predisposes a tumor toward a certain phenotype. This question has critical implications for whether histological subtyping reflects a fundamental difference of the underlying biology and whether it may be predictive of therapeutic response (Chen et al. 2014).

Resident adult lung stem cells are frequently proposed to be candidate tumor initiating cell populations. This would be consistent with the hypothesis that a cell with

high self-renewal potential has increased chance of acquiring sufficient tumor initiating events during its lifetime, or that of its progenitor. Many of the most convincing studies identifying distal lung stem cells used mouse models combined with various lineage tracers and injury models. The mouse alveoli and bronchiole are comprised of a number of distinct cell types with specialized functions (Rackley and Stripp 2012). The alveoli are the gas exchange sacs that are critical for re-oxigenating the blood and are largely comprised of Type I (AT1) cells that mediate the gas exchange with blood vessels and the Type II (ATII) cells that secrete protective mucins such as Surfactant Protein C (SPC or Sftpc). Alveoli are also occupied by resident macrophages that assist in clearing potentially harmful factors from the environment. Terminal bronchioles are linearly organized and comprised of a more diverse set of cells including neuroendocrine cells, secretory Goblet cells, basal cells, ciliated cells, and non-ciliated club cells - a prominent cell type that secretes a surfactant binding protein called the club cell secretory protein (CCSP, CC10 or Scgb1a1). More recently another cell type has been identified, variously termed the Bronchi-alveolar Stem Cell (BASC) or double positive cell, that exists at the bronchi-alveolar boundary and specified by the dual expression of SPC and CCSP. Several of these populations have been implicated as adult stem cell populations in the lung capable of regenerating the bronchiole or the alveoli following injury including BASCs, ATII cells, club cells, basal cells, as well as other less well characterized cell types (Kim et al. 2005; Barkauskas et al. 2013; Rawlins et al. 2009; Kumar et al. 2011; Zuo et al. 2015; Kajstura et al. 2011). While the diverse nature of lung stem cells is still actively being studied, these putative stem cell populations have been the focus of attempts to understand the tumor cell of origin for lung adenocarcinoma.

Mouse models have proven to be a valuable tool for studying lung stem cell biology and the origin of lung adenocarcinoma (Kwon and Berns 2013). Using a mouse model of lung tumorigenesis, BASCs were identified as a cell population that expanded soon after the lung epithelium was challenged with an oncogenic allele of Kras (Jackson et al. 2001; Kim et al. 2005). This was the first evidence to directly identify a putative stem cell population as a tumor initiating cell in the lung. Since then, various lineage specific Cre alleles have been used to drive oncogenic Kras in various cell types. It is now clear that ATII and club cells can be cells of origin in mouse models of Kras driven lung adenocarcinomas. (Sutherland et al. 2014; Xu et al. 2012; Desai et al. 2014). These findings support an argument among some in the pathology community that a prominent histological subtype - papillary adenocarcinoma - arises from club cells, and that solid adenocarcinomas arise from ATII cells (Thaete and Malkinson 1991; Sato and Kauffman 1980; Kauffman et al. 1979). As an alternative model, there is also strong evidence that papillary tumors arise within preexisting solid lesions and are thus instead a marker of adenoma progression (Rehm et al. 1988; Belinsky et al. 1992). Recent lineage tracing experiments also further support this latter hypothesis as Cre driven from more differentiated ATII marker is sufficient to drive papillary adenomas (Desai et al. 2014). It is possible that some of the controversy in this field may be broadly caused by the fluid nature of histological grading. For instance, a papillary adenoma launched in the bronchiole lumen may have a distinct origin from advanced papillary-like lesions that arise within peripheral solid adenomas despite their convergence on similar histological phenotypes (Sutherland et al. 2014; Desai et al. 2014). It remains to be determined if they are also converging on similar underlying

biology. Lastly, it is also now clear that the presence of or absence of inflammation, whether virally induced or otherwise, may alter the histological spectrum of initiated tumors (Rowbotham and Kim 2014). This may either reflect changes in tumor fate choice or a differential requirement for environmental factors by tumor initiating cells. Overall, the diversity of tumor initiating cell populations and histological subytpes in lung adenomagenesis may reflect biological propensities to respond to different therapies.

3. Dedifferentiation is a route to progression to advanced disease

In broad terms, cancer may be described as a failure to maintain a proper balance between a stem-like states and a terminally differentiated post-mitotic cell states. This often occurs due to the misappropriation of stem cell or developmental networks (Ben-Porath et al. 2008; Abad et al. 2013; Kho et al. 2004). In fact, the acquisition of a histologically dedifferentiated lesion is considered a hallmark of highly advanced disease for nearly all cancer types (Fusenig et al. 1995; Gabbert et al. 1985). In lung cancers in particular, the acquisition of more developmentally primitive cell states correlates with poorer outcome (Liu et al. 2006; Cheung and Nguyen 2015). This is also evidenced by recent changes to lung adenocarcinoma classification system, where the prominence of certain pathologically relevant features of differentiation is a key determinant for staging and outcome (Travis et al. 2015; 2011). Therefore, accumulating evidence suggests that the precise control of these networks is crucial for tumor progression and may be exploited in order to alter tumor fate.

In lung adenocarcinoma, the re-expression of developmental transcription factors or embryonal markers correlates with tumor dedifferentiation and advanced disease. In

particular, the embryonal factor Hmga2 is expressed in advanced disease may have functional roles in tumor growth (Sarhadi et al. 2006; Lee and Dutta 2007). Furthermore, the expression of transcription factors associated with lung-related developmental lineages correlates with a dedifferentiation phenotype and tumor progression (Li et al. 2015; Snyder et al. 2013). This may imply that a tumor derives benefit from uncovering common developmental or progenitor-like transcriptional networks. Lastly, lung specific transcription factors, such as Nkx2.1, that support differentiated cell types in the adult lung are tumor suppressive in part by impeding the acquisition of cryptic progenitor programs (Winslow et al. 2011; Snyder et al. 2013). For instance, Nkx2.1 restrains another transcription factor, Foxa2, from activating gastric related programs (Snyder et al. 2013). These programs correlate with a prominent mucinous form of lung adenocarcinoma that together with Foxa2 correlate with tumor progression. These recent advances in the molecular understanding of these transitions underscore that histological characterizations may be relevant to molecular determinants of these subtypes. They also suggest that deregulated differentiation networks are integral for tumor progression in lung adenocarcinoma.

4. Epigenetic regulators are drivers lung adenocarcinoma

As described above, much is known about the major genetic drivers of lung adenocarcinoma and the mutations that appear to initiate them. In contrast we are only beginning to fully appreciate the diverse epigenetic events that participate in lung tumorigenesis. As discussed in Part I of this chapter, DNA methylation is one of the major epigenetic events that regulates tissue homeostasis and organ development, and they may be deregulated in lung adenocarcinoma (Schrump 2013). For instance, DNA

methyltransferase (DNMT) expression is elevated in advanced lung tumors generated in mice that were exposed to tobacco-smoke (Belinsky et al. 1996). DNMT expression in lung cancer is also correlated to hypermethylation in humans (Kim et al. 2006; Lin et al. 2007; 2010). Furthermore, several studies suggested that a subset of patients display a CpG Island Methylator Phenotype (CIMP) characterized by global hypermethylation including various tumor suppressor loci such as *Cdkn2a*, *Gata4*, *Hoxd13* and *Hoxa9* (Shinjo et al. 2012; Collisson et al. 2014). Nearly a quarter of all lung adenocarcinomas can be classified as CIMP-high, with another third of patients having intermediate CIMP. Of note, Myc over-expression appears to correlate with CIMP, which may be indicative of a general need to broadly silence tumor suppressors in the presence of a general transcriptional activator (Collisson et al. 2014; Castro et al. 2013). By contrast, globally induced hypomethylation is known to derepress endogenous retroviruses (ERVs) and imprinting genes such as the growth factor Igf2 or the tumor suppressor p57 (Jaenisch et al. 1985; Feinberg et al. 2002; Holm et al. 2005). Both ERVs and imprinted genes can be reactivated in lung cancer (Yi and Kim 2007; Kohda et al. 2001). Overall, changes in DNA methylation in lung adenocarcinoma suggests that modulating epigenetic events may impact tumor growth. In fact, combination epigenetic therapy has shown efficacy in advanced non-small cell lung cancer clinical trials (Ramalingam et al. 2010; Juergens et al. 2011).

4.1 Complicated roles for PRC2 in lung adenocarcinoma

There has been tremendous interest in establishing the roles for PRC2 in lung adenocarcinoma, in part due to suspected oncogenic activities in other tumor types (Varambally et al. 2002). Increasingly, inhibiting the enzymatic activity of Ezh2, which

deposits H3K27me3, has shown efficacy in activating suppressed genes to yield a therapeutic response (McCabe et al. 2012). The availability of a small molecule PRC2 inhibitors for clinical trials has further spurred interest in understanding PRC2 in lung tumor biology. Interestingly, PRC2 was shown to target many of the same differentiation factors that are hypermethylated in various cancers, perhaps implicating PRC2 as an orthologous epigenetic mechanism to DNA methylation during tumorigenesis (Widschwendter et al. 2007). Indeed, polycomb targets appear more likely to undergo DNA hypermethylation in response to cigarette smoke condensate in lung adenocarcionma cell lines (Liu et al. 2010; Schrump 2013). However, much of the early data on PRC2 in lung adenocarcinoma were correlative. For instance, one study demonstrated that elevated Ezh2 protein expression correlated with poor prognosis and poor differentiation in human non-small cell lung cancer samples (Kikuchi et al. 2010). Similarly, loss of miR-101 correlated with Ezh2 expression in lung tumorigenesis (Varambally et al. 2008; Zhang et al. 2011). Two elegant recent studies examined PRC2 more closely during lung adenomagenesis and demonstrated that targeting the complex may be efficacious in a subset of tumors. In one, Ezh2 inhibition was found to be highly tumor suppressive dependent on the underlying genetic landscape (Fillmore et al. 2015). In another, PRC2 appeared to regulate tumor fate choice by repressing developmental regulators based on dosage and p53 status (Serresi et al. 2016). Together, these studies highlight the complex context dependent manner by which PRC2 can regulate lung adenocarcinoma and may inform when therapeutic intervention would be particularly advantageous.

4.2 Known roles for BMI1 in lung adenomagenesis and progression

PRC1, and BMI1 in particular, has been linked more broadly as a direct oncogene in lung adenocarcinoma than PRC2. In 2001, immunohistochemical analysis suggested that BMI1 expression anti-correlated with $p16^{INK4A}$ and Arf expression in human tumors (Vonlanthen et al. 2001). Later, a microarray analysis of tumor transcripts linked a Bmi1-driven 11 gene expression signature to poor survival in several tumor types, including NSCLC (Glinsky et al. 2005). BMI1 protein expression was also determined to be a marker of poor prognosis in an independent set of 172 NSCLCs - with a large fraction of tumors staining for BMI1 (Vrzalikova et al. 2008). Together, these data implicated that Bmi1 acts as an oncogene in lung cancer, perhaps by restraining the *Cdkn2a* locus.

Correlative studies using human NSCLC samples triggered further interest in understanding the genetic and epigenetic underpinnings of Bmi1 in lung adenocarcinoma. Using mice that were deficient for Bmi1 throughout development, two studies showed it to be a critical mediator of lung adenoma growth and progression in mice (Dovey et al. 2008; Becker et al. 2009). Both of these studies pinpointed Arf deregulation as a downstream effector of tumor exhaustion in Bmi1 deficient adenomas. Of note, Bmi1 deficient tumors that were driven by oncogenic Kras developed fewer tumors than wildtype controls, while tumors bearing oncogenic Braf did not display any defects in tumor initiation. Subsequently, Bmi1 was found to be enriched at the Arf promoter in lung adenomas, along with PRC2 dependent H3K27me3, and knockdown of Bmi1 in tumors increased expression from Arf (Young and Jacks 2010). These findings dovetailed with other data suggesting that Bmi1 is

critical for maintaining the self renewal capacity of at least one of the putative lung stem cells, the BASCs. BASCs isolated from Bmi1 deficient mice quickly exhaust both *in vitro* and *in vivo* when challenged in self-renewal assays (Dovey et al. 2008). In a separate study, BASCs derived from Bmi1 deficient mice also derepressed many imprinted loci leading to the dramatic up-regulation of p57, along with other imprinted genes, that together hampered stem cell self renewal (Zacharek et al. 2011). Together, these data argue that Bmi1 is important for maintaining the self renewal capacity of cancer cells by restraining tumor suppressors.

4.3 Synthesizing the potential for therapeutically targeting BMI1 in lung adenocarcinoma

While synthesizing the wealth of knowledge about epigenetic regulators in lung cancer two key conclusion stand out: 1) modifying reversible epigenetic events impacts tumor biology and may be a viable treatment strategy, and 2) we still have much to learn about the underlying contextual factors in lung tumors and how they impact the target specificity of epigenetic regulators. This remains the case particularly for understanding the implications of targeting Bmi1 in lung adenocarcinomas. Tissue and context specificity is clearly a critical determinant for Bmi1's role in mediating stemness as discussed in the second part of this chapter. So, too, does the mutational landscape appear to be critical for other polycomb regulators in lung adenocarcinoma. Therefore, it is reasonable to speculate that Bmi1 may also be critical for restraining targets at different stages of tumorigenesis depending on the cellular context. Tumor initiating cells and established tumor cells are likely sustained by different mechanisms that we are still identifying, and modulating Bmi1 may have variable consequences in each

background. Furthermore, it is also clear that there is phenotypic and genetic diversity in established lung tumors that might lead to differential Bmi1 targets in any given tumor. Elucidating Bmi1's variable requirements, as well as its specificity in these settings, remains an unmet need in the field. This is particularly relevant given the active interest in developing therapeutics that target Bmi1 and other polycomb group proteins in cancer.

In this thesis, I critically evaluate roles for Bmi1 at various stages of lung tumorigenesis and maintenance. I find that Bmi1 is broadly oncogenic by mediating the transition from lower grade tumors to advanced disease. I then provide evidence that a subset of tumors may be sensitive to the loss of Bmi1, which may inform a therapeutic window for targeted intervention. Overall, this thesis suggests that a critical understanding of the genetic dependencies of Bmi1 in lung cancers may reveal novel mechanisms by which to combat this disease.

REFERENCES

Abad M, Mosteiro L, Pantoja C, Cañamero M, Rayon T, Ors I, Graña O, Megías D, Domínguez O, Martínez D, et al. 2013. Reprogramming in vivo produces teratomas and iPS cells with totipotency features. *Nature* **502**: 340–345.

Abdouh M, Facchino S, Chatoo W, Balasingam V, Ferreira J, Bernier G. 2009. BMI1 sustains human glioblastoma multiforme stem cell renewal. *J Neurosci* **29**: 8884–8896.

Abdouh M, Hanna R, Hajjar El J, Flamier A, Bernier G. 2016. The Polycomb Repressive Complex 1 Protein BMI1 Is Required for Constitutive Heterochromatin Formation and Silencing in Mammalian Somatic Cells. *Journal of Biological Chemistry* **291**: 182–197.

Ahuja N, Sharma AR, Baylin SB. 2016. Epigenetic Therapeutics: A New Weapon in the War Against Cancer. *Annu Rev Med* **67**: 73–89.

Akasaka T, Kanno M, Balling R, Mieza MA, Taniguchi M, Koseki H. 1996. A role for mel-18, a Polycomb group-related vertebrate gene, during theanteroposterior specification of the axial skeleton. *Development* **122**: 1513–1522.

Akasaka T, van Lohuizen M, Van der Lugt N, Mizutani-Koseki Y, Kanno M, Taniguchi M, Vidal M, Alkema M, Berns A, Koseki H. 2001. Mice doubly deficient for the Polycomb Group genes Mel18 and Bmi1 reveal synergy and requirement for maintenance but not initiation of Hox gene expression. *Development* **128**: 1587–1597.

Alexandrov LB, Nik-Zainal S, Wedge DC, Aparicio SAJR, Behjati S, Biankin AV, Bignell GR, Bolli N, Borg A, Børresen-Dale A-L, et al. 2013. Signatures of mutational processes in human cancer. *Nature* **500**: 415–421.

Alkema MJ, van der Lugt NMT, Bobeldijk RC, Berns A, van Lohuizen M. 1995. Transformation of axial skeleton due to overexpression of bmi-1 in transgenic mice. *Nature* **374**: 724–727.

Aoto T, Saitoh N, Sakamoto Y, Watanabe S, Nakao M. 2008. Polycomb group protein-associated chromatin is reproduced in post-mitotic G1 phase and is required for S phase progression. *J Biol Chem* **283**: 18905–18915.

Arnold P, Schöler A, Pachkov M, Balwierz PJ, Jørgensen H, Stadler MB, van Nimwegen E, Schübeler D. 2013. Modeling of epigenome dynamics identifies transcription factors that mediate Polycomb targeting. *Genome Research* **23**: 60–73.

Asp P, Blum R, Vethantham V, Parisi F, Micsinai M, Cheng J, Bowman C, Kluger Y, Dynlacht BD. 2011. PNAS Plus: Genome-wide remodeling of the epigenetic landscape during myogenic differentiation. *Proc Natl Acad Sci USA*.

Audergon PNCB, Catania S, Kagansky A, Tong P, Shukla M, Pidoux AL, Allshire RC. 2015. Restricted epigenetic inheritance of H3K9 methylation. *Science* **348**: 132–135.

Audia JE, Campbell RM. 2016. Histone Modifications and Cancer. *Cold Spring Harb Perspect Biol* **8**: a019521.

Balmain A. 2001. Cancer genetics: from Boveri and Mendel to microarrays. *Nat Rev Cancer* **1**: 77–82.

Bantignies F, Roure V, Comet I, Leblanc B, Schuettengruber B, Bonnet J, Tixier V, Mas A, Cavalli G. 2011. Polycomb-dependent regulatory contacts between distant Hox loci in Drosophila. *Cell* **144**: 214–226.

Barkauskas CE, Cronce MJ, Rackley CR, Bowie EJ, Keene DR, Stripp BR, Randell SH, Noble PW, Hogan BLM. 2013. Type 2 alveolar cells are stem cells in adult lung. *J Clin Invest* **123**: 3025–3036.

Barker N. 2014. Adult intestinal stem cells: critical drivers of epithelial homeostasis and regeneration. *Nat Rev Mol Cell Biol* **15**: 19–33.

Becker M, Korn C, Sienerth AR, Voswinckel R, Luetkenhaus K, Ceteci F, Rapp UR. 2009. Polycomb group protein Bmi1 is required for growth of RAF driven non-small-cell lung cancer. *PLoS ONE* **4**: e4230.

Bednar F, Schofield HK, Collins MA, Yan W, Zhang Y, Shyam N, Eberle JA, Almada LL, Olive KP, Bardeesy N, et al. 2015. Bmi1 is required for the initiation of pancreatic cancer through an Ink4a-independent mechanism. *Carcinogenesis* **36**: 730–738.

Belinsky SA, Devereux TR, Foley JF, Maronpot RR, Anderson MW. 1992. Role of the alveolar type II cell in the development and progression of pulmonary tumors induced by 4-(methylnitrosamino)-1-(3-pyridyl)-1-butanone in the A/J mouse. **52**: 3164–3173.

Belinsky SA, Nikula KJ, Baylin SB, Issa JP. 1996. Increased cytosine DNA-methyltransferase activity is target-cell-specific and an early event in lung cancer. *Proc Natl Acad Sci USA* **93**: 4045–4050.

Ben-Porath I, Thomson MW, Carey VJ, Ge R, Bell GW, Regev A, Weinberg RA. 2008. An embryonic stem cell-like gene expression signature in poorly differentiated aggressive human tumors. *Nat Genet* **40**: 499–507.

Bernstein BE, Mikkelsen TS, Xie X, Kamal M, Huebert DJ, Cuff J, Fry B, Meissner A, Wernig M, Plath K, et al. 2006. A Bivalent Chromatin Structure Marks Key Developmental Genes in Embryonic Stem Cells. *Cell* **125**: 315–326.

Bestor T, Laudano A, Mattaliano R, Ingram V. 1988. Cloning and sequencing of a cDNA encoding DNA methyltransferase of mouse cells. The carboxyl-terminal domain of the mammalian enzymes is related to bacterial restriction methyltransferases. *J Mol Biol* **203**: 971–983.

Beuchle D, Struhl G, Müller J. 2001. Polycomb group proteins and heritable silencing of Drosophila Hox genes. *Development* **128**: 993–1004.

Bieging KT, Mello SS, Attardi LD. 2014. Unravelling mechanisms of p53-mediated tumour suppression. *Nat Rev Cancer* **14**: 359–370.

Blackledge NP, Farcas AM, Kondo T, King HW, McGouran JF, Hanssen LLP, Ito S, Cooper S, Kondo K, Koseki Y, et al. 2014. Variant PRC1 complex-dependent H2A ubiquitylation drives PRC2 recruitment and polycomb domain formation. *Cell* **157**: 1445–1459.

Blackledge NP, Rose NR, Klose RJ. 2015. Targeting Polycomb systems to regulate gene expression: modifications to a complex story. *Nat Rev Mol Cell Biol* **16**: 643–649.

Boveri M. 1903. *Boveri: Über Mitosen bei einseitiger Chromosomenbindung....* Naturwiss. Bd. XXXVII.

Boveri T. 1902. On multipolar mitosis as a means of analysis of the cell Nucleus *Foundations of experimental embryology* (1964 translation ed.) 74-97.

Boveri T. 1914. *Zur Frage der Entstehung maligner Tumoren.* Verlag von Gustav Fischer.

Boveri T. 2008. Concerning the Origin of Malignant Tumours by Theodor Boveri. Translated and annotated by Henry Harris. *J Cell Sci* **121**: 1–84.

Boveri T. 1929. *The Origin of Malignant Tumors.* Williams & Wilkins, Baltimore.

Boyer LA, Plath K, Zeitlinger J, Brambrink T, Medeiros LA, Lee TI, Levine SS, Wernig M, Tajonar A, Ray MK, et al. 2006. Polycomb complexes repress developmental regulators in murine embryonic stem cells. *Nature* **441**: 349–353.

Bracken AP, Dietrich N, Pasini D, Hansen KH, Helin K. 2006. Genome-wide mapping of Polycomb target genes unravels their roles in cell fate transitions. *Genes Dev* **20**: 1123–1136.

Brahmer J, Reckamp KL, Baas P, Crinò L, Eberhardt WEE, Poddubskaya E, Antonia S, Pluzanski A, Vokes EE, Holgado E, et al. 2015. Nivolumab versus Docetaxel in Advanced Squamous-Cell Non-Small-Cell Lung Cancer. *N Engl J Med* **373**: 123–135.

Brockdorff N. 2013. Noncoding RNA and Polycomb recruitment. *RNA* **19**: 429–442.

Brookes E, de Santiago I, Hebenstreit D, Morris KJ, Carroll T, Xie SQ, Stock JK, Heidemann M, Eick D, Nozaki N, et al. 2012. Polycomb Associates Genome-wide with a Specific RNA Polymerase II Variant, and Regulates Metabolic Genes in ESCs. *Cell Stem Cell* **10**: 157–170.

Bruggeman SWM, Hulsman D, Tanger E, Buckle T, Blom M, Zevenhoven J, van Tellingen O, van Lohuizen M. 2007. Bmi1 Controls Tumor Development in an Ink4a/Arf-Independent Manner in a Mouse Model for Glioma. *Cancer Cell* **12**: 328–341.

Bruggeman SWM, Valk-Lingbeek ME, van der Stoop PPM, Jacobs JJL, Kieboom K, Tanger E, Hulsman D, Leung C, Arsenijevic Y, Marino S, et al. 2005. Ink4a and Arf differentially affect cell proliferation and neural stem cell self-renewal in Bmi1-deficient mice. *Genes Dev* **19**: 1438–1443.

Cao R, Tsukada Y-I, Zhang Y. 2005. Role of Bmi-1 and Ring1A in H2A Ubiquitylation and Hox Gene Silencing. *Mol Cell* **20**: 845–854.

Castro IC, Breiling A, Luetkenhaus K, Ceteci F, Hausmann S, Kress S, Lyko F, Rudel T, Rapp UR. 2013. MYC-induced epigenetic activation of GATA4 in lung adenocarcinoma. - PubMed - NCBI. *Mol Cancer Res* **11**: 161–172.

Chagraoui J, Hébert J, Girard S, Sauvageau G. 2011. An anticlastogenic function for the Polycomb Group gene Bmi1. *Proc Natl Acad Sci USA* **108**: 5284–5289.

Chen RZ, Pettersson U, Beard C, Jackson-Grusby L, Jaenisch R. 1998. DNA hypomethylation leads to elevated mutation rates. *Nature* **395**: 89–93.

Chen Z, Fillmore CM, Hammerman PS, Kim CF, Wong K-K. 2014. Non-small-cell lung cancers: a heterogeneous set of diseases. *Nat Rev Cancer* **14**: 535–546.

Cheng JC, Matsen CB, Gonzales FA, Ye W, Greer S, Marquez VE, Jones PA, Selker EU. 2003. Inhibition of DNA methylation and reactivation of silenced genes by zebularine. *J Natl Cancer Inst* **95**: 399–409.

Cheung WKC, Nguyen DX. 2015. Lineage factors and differentiation states in lung cancer progression. *Oncogene* **34**: 5771–5780.

Chiacchiera F, Rossi A, Jammula S, Piunti A, Scelfo A, Ordóñez-Morán P, Huelsken J, Koseki H, Pasini D. 2016. Polycomb Complex PRC1 Preserves

Intestinal Stem Cell Identity by Sustaining Wnt/β-Catenin Transcriptional Activity. *Stem Cell* **18**: 91–103.

Chiappinelli KB, Strissel PL, Desrichard A, Li H, Henke C, Akman B, Hein A, Rote NS, Cope LM, Snyder A, et al. 2015. Inhibiting DNA Methylation Causes an Interferon Response in Cancer via dsRNA Including Endogenous Retroviruses. *Cell* **162**: 974–986.

Collisson EA, Network TCGAR, Campbell JD, Brooks AN, Berger AH, Lee W, Chmielecki J, Beer DG, Cope L, Creighton CJ, et al. 2014. Comprehensive molecular profiling of lung adenocarcinoma. *Nature* **511**: 543–550.

Cooper S, Dienstbier M, Hassan R, Schermelleh L, Sharif J, Blackledge NP, De Marco V, Elderkin S, Koseki H, Klose R, et al. 2014. Targeting polycomb to pericentric heterochromatin in embryonic stem cells reveals a role for H2AK119u1 in PRC2 recruitment. *Cell Reports* **7**: 1456–1470.

Dawson BA, Herman T, Haas AL, Lough J. 1991. Affinity isolation of active murine erythroleukemia cell chromatin: uniform distribution of ubiquitinated histone H2A between active and inactive fractions. *J Cell Biochem* **46**: 166–173.

Dawson MA, Prinjha RK, Dittmann A, Giotopoulos G, Bantscheff M, Chan W-I, Robson SC, Chung C-W, Hopf C, Savitski MM, et al. 2011. Inhibition of BET recruitment to chromatin as an effective treatment for MLL-fusion leukaemia. *Nature* **478**: 529–533.

Delmore JE, Issa GC, Lemieux ME, Rahl PB, Shi J, Jacobs HM, Kastritis E, Gilpatrick T, Paranal RM, Qi J, et al. 2011. BET Bromodomain Inhibition as a Therapeutic Strategy to Target c-Myc. *Cell* **146**: 904–917.

Denko NC, Giaccia AJ, Stringer JR, Stambrook PJ. 1994. The human Ha-ras oncogene induces genomic instability in murine fibroblasts within one cell cycle. *Proc Natl Acad Sci USA* **91**: 5124–5128.

Desai TJ, Brownfield DG, Krasnow MA. 2014. Alveolar progenitor and stem cells in lung development, renewal and cancer. *Nature* **507**: 190–194.

Dietrich N, Lerdrup M, Landt E, Agrawal-Singh S, Bak M, Tommerup N, Rappsilber J, Södersten E, Hansen K. 2012. REST-mediated recruitment of polycomb repressor complexes in mammalian cells. ed. H.D. Madhani. *PLoS Genet* **8**: e1002494.

Dittmer D, Pati S, Zambetti G, Chu S, Teresky AK, Moore M, Finlay C, Levine AJ. 1993. Gain of function mutations in p53. *Nat Genet* **4**: 42–46.

Douglas D, Hsu JH-R, Hung L, Cooper A, Abdueva D, van Doorninck J, Peng G, Shimada H, Triche TJ, Lawlor ER. 2008. BMI-1 promotes ewing sarcoma tumorigenicity independent of CDKN2A repression. *Cancer Res* **68**: 6507–6515.

Dovey JS, Zacharek SJ, Kim CF, Lees JA. 2008. Bmi1 is critical for lung tumorigenesis and bronchioalveolar stem cell expansion. *Proc Natl Acad Sci USA* **105**: 11857–11862.

Fasano CA, Dimos JT, Ivanova NB, Lowry N, Lemischka IR, Temple S. 2007. shRNA Knockdown of Bmi-1 Reveals a Critical Role for p21-Rb Pathway in NSC Self-Renewal during Development. *Cell Stem Cell* **1**: 87–99.

Feinberg AP, Cui H, Ohlsson R. 2002. DNA methylation and genomic imprinting: insights from cancer into epigenetic mechanisms. *Semin Cancer Biol* **12**: 389–398.

Feinberg AP, Tycko B. 2004. The history of cancer epigenetics. *Nat Rev Cancer* **4**: 143–153.

Feinberg AP, Vogelstein B. 1983. Hypomethylation distinguishes genes of some human cancers from their normal counterparts. *Nature* **301**: 89–92.

Feldser DM, Kostova KK, Winslow MM, Taylor SE, Cashman C, Whittaker CA, Sanchez-Rivera FJ, Resnick R, Bronson R, Hemann MT, et al. 2010. Stage-specific sensitivity to p53 restoration during lung cancer progression. *Nature* **468**: 572–575.

Ferretti R, Bhutkar A, McNamara MC, Lees JA. 2016. BMI1 induces an invasive signature in melanoma that promotes metastasis and chemoresistance. *Genes Dev* **30**: 18–33.

Fillmore CM, Xu C, Desai PT, Berry JM, Rowbotham SP, Lin Y-J, Zhang H, Marquez VE, Hammerman PS, Wong K-K, et al. 2015. EZH2 inhibition sensitizes BRG1 and EGFR mutant lung tumours to TopoII inhibitors. *Nature* **520**: 239–242.

Franchini D-M, Schmitz K-M, Petersen-Mahrt SK. 2012. 5-Methylcytosine DNA demethylation: more than losing a methyl group. *Annu Rev Genet* **46**: 419–441.

Francis NJ, Follmer NE, Simon MD, Aghia G, Butler JD. 2009. Polycomb proteins remain bound to chromatin and DNA during DNA replication in vitro. *Cell* **137**: 110–122.

Francis NJ, Kingston RE, Woodcock CL. 2004. Chromatin compaction by a polycomb group protein complex. *Science* **306**: 1574–1577.

Francis NJ, Saurin AJ, Shao Z, Kingston RE. 2001. Reconstitution of a functional core polycomb repressive complex. *Mol Cell* **8**: 545–556.

Franke A, DeCamillis M, Zink D, Cheng N, Brock HW, Paro R. 1992. Polycomb and polyhomeotic are constituents of a multimeric protein complex in chromatin of Drosophila melanogaster. *EMBO J* **11**: 2941–2950.

Fusenig NE, Breitkreutz D, Boukamp P. 1995. Differentiation and tumor progression. *Recent results in Cancer Research* **139**: 1–19.

Gabbert H, Wagner R, Moll R, Gerharz C-D. 1985. Tumor dedifferentiation: An important step in tumor invasion. *Clin Exp Metastasis* **3**: 257–279.

Gao Z, Zhang J, Bonasio R, Strino F, Sawai A, Parisi F, Kluger Y, Reinberg D. 2012. PCGF Homologs, CBX Proteins, and RYBP Define Functionally Distinct PRC1 Family Complexes. *Mol Cell* **45**: 344–356.

Gargiulo G, Cesaroni M, Serresi M, de Vries N, Hulsman D, Bruggeman SW, Lancini C, van Lohuizen M. 2013. In vivo RNAi screen for BMI1 targets identifies TGF-β/BMP-ER stress pathways as key regulators of neural- and malignant glioma-stem cell homeostasis. **23**: 660–676.

Garraway LA, Lander ES. 2013. Lessons from the Cancer Genome. *Cell* **153**: 17–37.

Gil J, O'Loghlen A. 2014. PRC1 complex diversity: where is it taking us? *Trends Cell Biol* **24**: 632–641.

Glinsky GV, Berezovska O, Glinskii AB. 2005. Microarray analysis identifies a death-from-cancer signature predicting therapy failure in patients with multiple types of cancer. *J Clin Invest* **115**: 1503–1521.

Gonzalez-Zulueta M, Bender CM, Yang AS, Nguyen T, Beart RW, Van Tornout JM, Jones PA. 1995. Methylation of the 5' CpG island of the p16/CDKN2 tumor suppressor gene in normal and transformed human tissues correlates with gene silencing. **55**: 4531–4535.

Govindan R, Ding L, Griffith M, Subramanian J, Dees ND, Kanchi KL, Maher CA, Fulton R, Fulton L, Wallis J, et al. 2012. Genomic Landscape of Non-Small Cell Lung Cancer in Smokers and Never-Smokers. *Cell* **150**: 1121–1134.

Greger V, Passarge E, Höpping W, Messmer E, Horsthemke B. 1989. Epigenetic changes may contribute to the formation and spontaneous regression of retinoblastoma. *Hum Genet* **83**: 155–158.

Groth A, Rocha W, Verreault A, Almouzni G. 2007. Chromatin challenges during DNA replication and repair. *Cell* **128**: 721–733.

Guenther MG, Levine SS, Boyer LA, Jaenisch R, Young RA. 2007. A chromatin landmark and transcription initiation at most promoters in human cells. *Cell* **130**: 77–88.

Guney I. 2006. Reduced c-Myc signaling triggers telomere-independent senescence by regulating Bmi-1 and p16INK4a. *Proc Natl Acad Sci USA* **103**: 3645–3650.

Hayes J, Peruzzi PP, Lawler S. 2014. MicroRNAs in cancer: biomarkers, functions and therapy. *Trends in molecular medicine* **20**: 460–469.

Hoenerhoff MJ, Chu I, Barkan D, Liu Z-Y, Datta S, Dimri GP, Green JE. 2009. BMI1 cooperates with H-RAS to induce an aggressive breast cancer phenotype with brain metastases. *Oncogene* **28**: 3022–3032.

Holm TM, Jackson-Grusby L, Brambrink T, Yamada Y, Rideout WM III, Jaenisch R. 2005. Global loss of imprinting leads to widespread tumorigenesis in adult mice. **8**: 275–285.

Hsu JH, Lawlor ER. 2011. BMI-1 suppresses contact inhibition and stabilizes YAP in Ewing sarcoma. *Oncogene* **30**: 2077–2085.

Hu X, Feng Y, Zhang D, Zhao SD, Hu Z, Greshock J, Zhang Y, Yang L, Zhong X, Wang L-P, et al. 2014. A Functional Genomic Approach Identifies FAL1 as an Oncogenic Long Noncoding RNA that Associates with BMI1 and Represses p21 Expression in Cancer. **26**: 344–357.

Jackson EL, Willis N, Mercer K, Bronson RT, Crowley D, Montoya R, Jacks T, Tuveson DA. 2001. Analysis of lung tumor initiation and progression using conditional expression of oncogenic K-ras. *Genes Dev* **15**: 3243–3248.

Jackson V. 1988. Deposition of newly synthesized histones: hybrid nucleosomes are not tandemly arranged on daughter DNA strands. **27**: 2109–2120.

Jacobs JJ, Kieboom K, Marino S, DePinho RA, van Lohuizen M. 1999a. The oncogene and Polycomb-group gene bmi-1 regulates cell proliferation and senescence through the ink4a locus. *Nature* **397**: 164–168.

Jacobs JJ, Scheijen B, Voncken JW, Kieboom K, Berns A, van Lohuizen M. 1999b. Bmi-1 collaborates with c-Myc in tumorigenesis by inhibiting c-Myc-induced apoptosis via INK4a/ARF. *Genes Dev* **13**: 2678–2690.

Jaenisch R, Schnieke A, Harbers K. 1985. Treatment of mice with 5-azacytidine efficiently activates silent retroviral genomes in different tissues. *Proc Natl Acad Sci USA* **82**: 1451–1455.

Jakopovic M, Thomas A, Balasubramaniam S, Schrump D, Giaccone G, Bates SE. 2013. Targeting the Epigenome in Lung Cancer: Expanding Approaches to Epigenetic Therapy. *Frontiers in Oncology* **3**: 1–12.

Janakiraman M, Vakiani E, Zeng Z, Pratilas CA, Taylor BS, Chitale D, Halilovic E, Wilson M, Huberman K, Ricarte Filho JC, et al. 2010. Genomic and biological characterization of exon 4 KRAS mutations in human cancer. **70**: 5901–5911.

Jenuwein T, Allis CD. 2001. Translating the Histone Code. *Science* **293**: 1074–1080.

Jian Cao QY. 2012. Histone Ubiquitination and Deubiquitination in Transcription, DNA Damage Response, and Cancer. *Frontiers in Oncology* **2**: 26.

Johnson TB, Coghill RD. 1925. Researches on Pyrimidines. C111. The Discovery of 5-Methyl-Cytosine in Tuberculinic Acid, The Nucleic Acid of The Tubercle Bacillus 1. *J Am Chem Soc* **47**: 2838–2844.

Jones CA, Ng J, Peterson AJ, Morgan K, Simon J, Jones RS. 1998. The Drosophila esc and E(z) proteins are direct partners in polycomb group-mediated repression. *Mol Cell Biol* **18**: 2825–2834.

Joo H-Y, Zhai L, Yang C, Nie S, Erdjument-Bromage H, Tempst P, Chang C, Wang H. 2007. Regulation of cell cycle progression and gene expression by H2A deubiquitination. *Nature* **449**: 1068–1072.

Juergens RA, Wrangle J, Vendetti FP, Murphy SC, Zhao M, Coleman B, Sebree R, Rodgers K, Hooker CM, Franco N, et al. 2011. Combination Epigenetic Therapy Has Efficacy in Patients with Refractory Advanced Non-Small Cell Lung Cancer. *Cancer Discov* **1**: 598–607.

Jürgens G. 1985. A group of genes controlling the spatial expression of the bithorax complex in Drosophila. *Nature* **316**: 153–155.

Kajstura J, Rota M, Hall SR, Hosoda T, D'Amario D, Sanada F, Zheng H, Ogórek B, Rondon-Clavo C, Ferreira-Martins J, et al. 2011. Evidence for human lung stem cells. *N Engl J Med* **364**: 1795–1806.

Kallin EM, Cao R, Jothi R, Xia K, Cui K, Zhao K, Zhang Y. 2009. Genome-wide uH2A localization analysis highlights Bmi1-dependent deposition of the mark at repressed genes. *PLoS Genet* **5**: e1000506.

Kandoth C, McLellan MD, Vandin F, Ye K, Niu B, Lu C, Xie M, Zhang Q, McMichael JF, Wyczalkowski MA, et al. 2013. Mutational landscape and significance across 12 major cancer types. *Nature* **502**: 333–339.

Kauffman SL, Alexander L, Sass L. 1979. Histologic and ultrastructural features of the clara cell adenoma of the mouse lung. *Lab Invest* **40**: 708–716.

Kaustov L, Ouyang H, Amaya M, Lemak A, Nady N, Duan S, Wasney GA, Li Z, Vedadi M, Schapira M, et al. 2010. Recognition and Specificity Determinants of the Human Cbx Chromodomains. *J Biol Chem* **286**: 521–529.

Kazandjian D, Suzman DL, Blumenthal G, Mushti S, He K, Libeg M, Keegan P, Pazdur R. 2016. FDA Approval Summary: Nivolumab for the Treatment of Metastatic Non-Small Cell Lung Cancer With Progression On or After Platinum-Based Chemotherapy. *Oncologist* **21**: 634–642.

Kho AT, Zhao Q, Cai Z, Butte AJ, Kim JYH, Pomeroy SL, Rowitch DH, Kohane IS. 2004. Conserved mechanisms across development and tumorigenesis revealed by a mouse development perspective of human cancers. *Genes Dev* **18**: 629–640.

Kikuchi J, Kinoshita I, Shimizu Y, Kikuchi E, Konishi J, Oizumi S, Kaga K, Matsuno Y, Nishimura M, Dosaka-Akita H. 2010. Distinctive expression of the polycomb group proteins Bmi1 polycomb ring finger oncogene and enhancer of zeste homolog 2 in nonsmall cell lung cancers and their clinical and clinicopathologic significance. *Cancer* **116**: 3015–3024.

Kim CFB, Jackson EL, Woolfenden AE, Lawrence S, Babar I, Vogel S, Crowley D, Bronson RT, Jacks T. 2005. Identification of bronchioalveolar stem cells in normal lung and lung cancer. *Cell* **121**: 823–835.

Kim H, Kwon YM, Kim JS, Han J, Shim YM, Park J, Kim DH. 2006. Elevated mRNA levels of DNA methyltransferase-1 as an independent prognostic factor in primary nonsmall cell lung cancer. *Cancer* **107**: 1042–1049.

Kim WY, Sharpless NE. 2006. The Regulation of INK4/ARF in Cancer and Aging. *Cell* **127**: 265–275.

Kimura M, Takenobu H, Akita N, Nakazawa A, Ochiai H, Shimozato O, Fujimura Y-I, Koseki H, Yoshino I, Kimura H, et al. 2011. Bmi1 regulates cell fate via tumor suppressor WWOX repression in small-cell lung cancer cells. *Cancer Sci* **102**: 983–990.

Klauke K, Radulović V, Broekhuis M, Weersing E, Zwart E, Olthof S, Ritsema M, Bruggeman S, Wu X, Helin K, et al. 2013. Polycomb Cbx family members mediate the balance between haematopoietic stem cell self-renewal and differentiation. *Nat Cell Biol* **15**: 353–362.

Kohda M, Hoshiya H, Katoh M, Tanaka I, Masuda R, Takemura T, Fujiwara M, Oshimura M. 2001. Frequent loss of imprinting of IGF2 and MEST in lung adenocarcinoma. *Mol Carcinog* **31**: 184–191.

Koppens M, van Lohuizen M. 2016. Context-dependent actions of Polycomb repressors in cancer. *Oncogene* **35**: 1341–1352.

Kreso A, van Galen P, Pedley NM, Lima-Fernandes E, Frelin C, Davis T, Cao L, Baiazitov R, Du W, Sydorenko N, et al. 2014. Self-renewal as a therapeutic target in human colorectal cancer. *Nat Med* **20**: 29–36.

Ku M, Koche RP, Rheinbay E, Mendenhall EM, Endoh M, Mikkelsen TS, Presser A, Nusbaum C, Xie X, Chi AS, et al. 2008a. Genomewide Analysis of PRC1 and PRC2 Occupancy Identifies Two Classes of Bivalent Domains ed. B. Van Steensel. *PLoS Genet* **4**: e1000242.

Ku M, Koche RP, Rheinbay E, Mendenhall EM, Endoh M, Mikkelsen TS, Presser A, Nusbaum C, Xie X, Chi AS, et al. 2008b. Genomewide Analysis of PRC1 and PRC2 Occupancy Identifies Two Classes of Bivalent Domains ed. B. Van Steensel. *PLoS Genet* **4**: e1000242.

Kumar PA, Hu Y, Yamamoto Y, Hoe NB, Wei TS, Mu D, Sun Y, Joo LS, Dagher R, Zielonka EM, et al. 2011. Distal Airway Stem Cells Yield Alveoli In Vitro and during Lung Regeneration following H1N1 Influenza Infection. *Cell* **147**: 525–538.

Kwak EL, Bang Y-J, Camidge DR, Shaw AT, Solomon B, Maki RG, Ou S-HI, Dezube BJ, Jänne PA, Costa DB, et al. 2010. Anaplastic lymphoma kinase inhibition in non-small-cell lung cancer. *N Engl J Med* **363**: 1693–1703.

Kwon M-C, Berns A. 2013. Mouse models for lung cancer. *Molecular Oncology* **7**: 165–177.

Laird PW, Jackson-Grusby L, Fazeli A, Dickinson SL, Jung WE, Li E, Weinberg RA, Jaenisch R. 1995. Suppression of intestinal neoplasia by DNA hypomethylation. *Cell* **81**: 197–205.

Lane DP, Crawford LV. 1979. T antigen is bound to a host protein in SV40-transformed cells. *Nature* **278**: 261–263.

Lawrence M, Daujat S, Schneider R. 2016. Lateral Thinking: How Histone Modifications Regulate Gene Expression. *Trends in Genetics* **32**: 42–56.

Lee YS, Dutta A. 2007. The tumor suppressor microRNA let-7 represses the HMGA2 oncogene. *Genes Dev* **21**: 1025–1030.

Leeb M, Wutz A. 2007. Ring1B is crucial for the regulation of developmental control genes and PRC1 proteins but not X inactivation in embryonic cells. *J Cell Biol* **178**: 219–229.

Lessard F, Morin F, Ivanchuk S, Langlois F, Stefanovsky V, Rutka J, Moss T. 2010. The ARF tumor suppressor controls ribosome biogenesis by regulating the RNA polymerase I transcription factor TTF-I. *Mol Cell* **38**: 539–550.

Lessard J, Sauvageau G. 2003. Bmi-1 determines the proliferative capacity of normal and leukaemic stem cells. *Nature* **423**: 255–260.

Leung C, Lingbeek M, Shakhova O, Liu J, Tanger E, Saremaslani P, van Lohuizen M, Marino S. 2004. Bmi1 is essential for cerebellar development and is overexpressed in human medulloblastomas. *Nature* **428**: 337–341.

Levinger L, Varshavsky A. 1982. Selective arrangement of ubiquitinated and D1 protein-containing nucleosomes within the drosophila genome. *Cell* **28**: 375–385.

Lewis EB. 1978. A gene complex controlling segmentation in Drosophila. *Nature* **276**: 565–570.

Lewis PH. 1947. New mutants report. **21**: 69.

Li CM-C, Gocheva V, Oudin MJ, Bhutkar A, Wang SY, Date SR, Ng SR, Whittaker CA, Bronson RT, Snyder EL, et al. 2015. Foxa2 and Cdx2 cooperate with Nkx2-1 to inhibit lung adenocarcinoma metastasis. *Genes Dev* **29**: 1850–1862.

Li E, Bestor TH, Jaenisch R. 1992. Targeted mutation of the DNA methyltransferase gene results in embryonic lethality. *Cell* **69**: 915–926.

Lin R-K, Hsieh Y-S, Lin P, Hsu H-S, Chen C-Y, Tang Y-A, Lee C-F, Wang Y-C. 2010. The tobacco-specific carcinogen NNK induces DNA methyltransferase 1 accumulation and tumor suppressor gene hypermethylation in mice and lung cancer patients. *J Clin Invest* **120**: 521–532.

Lin R-K, Hsu H-S, Chang J-W, Chen C-Y, Chen J-T, Wang Y-C. 2007. Alteration of DNA methyltransferases contributes to 5'CpG methylation and poor prognosis in lung cancer. *Lung Cancer* **55**: 205–213.

Linzer DIH, Levine AJ. 1979. Characterization of a 54K Dalton cellular SV40 tumor antigen present in SV40-transformed cells and uninfected embryonal carcinoma cells. *Cell* **17**: 43–52.

Liu F, Killian JK, Yang M, Walker RL, Hong JA, Zhang M, Davis S, Zhang Y, Hussain M, Xi S, et al. 2010. Epigenomic alterations and gene expression profiles in respiratory epithelia exposed to cigarette smoke condensate. *Oncogene* **29**: 3650–3664.

Liu H, Kho AT, Kohane IS, Sun Y. 2006. Predicting survival within the lung cancer histopathological hierarchy using a multi-scale genomic model of development. *PLoS Med* **3**: e232.

Liu J, Cao L, Chen J, Song S, Lee IH, Quijano C, Liu H, Keyvanfar K, Chen H, Cao L-Y, et al. 2009. Bmi1 regulates mitochondrial function and the DNA damage response pathway. *Nature* **459**: 387–392.

Liu Y, Liu F, Yu H, Zhao X, Sashida G, Deblasio A, Harr M, She Q-B, Chen Z, Lin H-K, et al. 2012. Akt Phosphorylates the Transcriptional Repressor Bmi1 to Block Its Effects on the Tumor-Suppressing Ink4a-Arf Locus. *Science Signaling* **5**: ra77.

Lo SM, Follmer NE, Lengsfeld BM, Madamba EV, Seong S, Grau DJ, Francis NJ. 2012. A Bridging Model for Persistence of a Polycomb Group Protein Complex through DNA Replication In Vitro. *Mol Cell* **46**: 784–796.

Lobo NA, Shimono Y, Qian D, Clarke MF. 2007. The Biology of Cancer Stem Cells. *Annu Rev Cell Dev Biol* **23**: 675–699.

Lopez-Arribillaga E, Rodilla V, Pellegrinet L, Guiu J, Iglesias M, Roman AC, Gutarra S, Gonzalez S, Munoz-Canoves P, Fernandez-Salguero P, et al. 2014. Bmi1 regulates murine intestinal stem cell proliferation and self-renewal downstream of Notch. *Development* **142**: 41–50.

Lukacs RU, Memarzadeh S, Wu H, Witte ON. 2010. Bmi-1 Is a Crucial Regulator of Prostate Stem Cell Self-Renewal and Malignant Transformation. **7**: 682–693.

Martin N, Beach D, Gil J. 2014. Ageing as developmental decay: insights from p16INK4a. *Trends in molecular medicine* **20**: 667–674.

Martínez-Romero C, Rooman I, Skoudy A, Guerra C, Molero X, González A, Iglesias M, Lobato T, Bosch A, Barbacid M, et al. 2009. The epigenetic regulators Bmi1 and Ring1B are differentially regulated in pancreatitis and pancreatic ductal adenocarcinoma. **219**: 205–213.

Maynard MA, Ferretti R, Hilgendorf KI, Perret C, Whyte P, Lees JA. 2014. Bmi1 is required for tumorigenesis in a mouse model of intestinal cancer. *Oncogene* **33**: 3742–3747.

McCabe MT, Ott HM, Ganji G, Korenchuk S, Thompson C, Van Aller GS, Liu Y, Graves AP, Pietra Della A III, Diaz E, et al. 2012. EZH2 inhibition as a therapeutic strategy for lymphoma with EZH2-activating mutations. *Nature* **492**: 108–112.

McGranahan N, Favero F, de Bruin EC, Birkbak NJ, Szallasi Z, Swanton C. 2015. Clonal status of actionable driver events and the timing of mutational processes in cancer evolution. *Sci Transl Med* **7**: 283ra54–283ra54.

McKusick VA. 1985. Marcella O'Grady Boveri (1865-1950) and the chromosome theory of cancer. *J Med Genet* **22**: 431–440.

Mello SS, Attardi LD. 2013. Not all p53 gain-of-function mutants are created equal. *Cell Death Differ* **20**: 855–857.

Merlo A, Herman JG, Mao L, Lee DJ, Gabrielson E, Burger PC, Baylin SB, Sidransky D. 1995. 5 | [prime] | CpG island methylation is associated with transcriptional silencing of the tumour suppressor p16/CDKN2/MTS1 in human cancers. *Nat Med* **1**: 686–692.

Mertens F, Johansson B, Höglund M, Mitelman F. 1997. Chromosomal imbalance maps of malignant solid tumors: a cytogenetic survey of 3185 neoplasms. **57**: 2765–2780.

Mihara K, Chowdhury M, Nakaju N, Hidani S, Ihara A, Hyodo H, Yasunaga S, Takihara Y, Kimura A. 2006. Bmi-1 is useful as a novel molecular marker for predicting progression of myelodysplastic syndrome and patient prognosis. *Blood* **107**: 305–308.

Min IM, Waterfall JJ, Core LJ, Munroe RJ, Schimenti J, Lis JT. 2011. Regulating RNA polymerase pausing and transcription elongation in embryonic stem cells. *Genes Dev* **25**: 742–754.

Min J. 2003. Structural basis for specific binding of Polycomb chromodomain to histone H3 methylated at Lys 27. *Genes Dev* **17**: 1823–1828.

Mohty M, Yong ASM, Szydlo RM, Apperley JF, Melo JV. 2007. The polycomb group BMI1 gene is a molecular marker for predicting prognosis of chronic myeloid leukemia. *Blood* **110**: 380–383.

Mok TS, Wu Y-L, Thongprasert S, Yang C-H, Chu D-T, Saijo N, Sunpaweravong P, Han B, Margono B, Ichinose Y, et al. 2009. Gefitinib or Carboplatin–Paclitaxel in Pulmonary Adenocarcinoma. **361**: 947–957.

Molofsky AV. 2005. Bmi-1 promotes neural stem cell self-renewal and neural development but not mouse growth and survival by repressing the p16Ink4a and p19Arf senescence pathways. *Genes Dev* **19**: 1432–1437.

Morey L, Aloia L, Cozzuto L, Benitah SA, Di Croce L. 2013. RYBP and Cbx7 define specific biological functions of polycomb complexes in mouse embryonic stem cells. *Cell Reports* **3**: 60–69.

Morey L, Pascual G, Cozzuto L, Roma G, Wutz A, Benitah SA, Di Croce L. 2012b. Nonoverlapping Functions of the Polycomb Group Cbx Family of Proteins in Embryonic Stem Cells. *Cell Stem Cell* **10**: 47–62.

Morey L, Santanach A, Blanco E, Aloia L, Nora EP, Bruneau BG, Di Croce L. 2015. Polycomb Regulates Mesoderm Cell Fate-Specification in Embryonic Stem Cells through Activation and Repression Mechanisms. *Stem Cell* **17**: 300–315.

Müller J, Kassis JA. 2006. Polycomb response elements and targeting of Polycomb group proteins in Drosophila. *Curr Opin Genet Dev* **16**: 476–484.

Nacerddine K, Beaudry J-B, Ginjala V, Westerman B, Mattiroli F, Song J-Y, van der Poel H, Ponz OB, Pritchard C, Cornelissen-Steijger P, et al. 2012. Akt-mediated phosphorylation of Bmi1 modulates its oncogenic potential, E3 ligase activity, and DNA damage repair activity in mouse prostate cancer. *J Clin Invest* **122**: 1920–1932.

Nakagawa T, Kajitani T, Togo S, Masuko N, Ohdan H, Hishikawa Y, Koji T, Matsuyama T, Ikura T, Muramatsu M, et al. 2008. Deubiquitylation of histone H2A activates transcriptional initiation via trans-histone cross-talk with H3K4 di- and trimethylation. *Genes Dev* **22**: 37–49.

Nakamura S, Oshima M, Yuan J, Saraya A, Miyagi S, Konuma T, Yamazaki S, Osawa M, Nakauchi H, Koseki H, et al. 2012. Bmi1 Confers Resistance to Oxidative Stress on Hematopoietic Stem Cells. *PLoS ONE* **7**: e36209.

Nowak K. 2006. BMI1 is a target gene of E2F-1 and is strongly expressed in primary neuroblastomas. *Nucleic Acids Res* **34**: 1745–1754.

O'Loghlen A, Muñoz-Cabello AM, Gaspar-Maia A, Wu H-A, Banito A, Kunowska N, Racek T, Pemberton HN, Beolchi P, Lavial F, et al. 2012. MicroRNA regulation of Cbx7 mediates a switch of Polycomb orthologs during ESC differentiation. **10**: 33–46.

Ogawa H, Ishiguro K-I, Gaubatz S, Livingston DM, Nakatani Y. 2002. A Complex with Chromatin Modifiers That Occupies E2F- and Myc-Responsive Genes in G0 Cells. *Science* **296**: 1132–1136.

Oguro H, Yuan J, Ichikawa H, Ikawa T, Yamazaki S, Kawamoto H, Nakauchi H, Iwama A. 2010. Poised lineage specification in multipotential hematopoietic stem and progenitor cells by the polycomb protein Bmi1. **6**: 279–286.

Oliver TG, Mercer KL, Sayles LC, Burke JR, Mendus D, Lovejoy KS, Cheng MH, Subramanian A, Mu D, Powers S, et al. 2010. Chronic cisplatin treatment promotes enhanced damage repair and tumor progression in a mouse model of lung cancer. *Genes Dev* **24**: 837–852.

Pao W, Wang TY, Riely GJ, Miller VA, Pan Q, Ladanyi M, Zakowski MF, Heelan RT, Kris MG, Varmus HE. 2005. KRAS Mutations and Primary Resistance of Lung Adenocarcinomas to Gefitinib or Erlotinib ed. R. Herbst. *PLoS Med* **2**: e17.

Park I-K, Morrison SJ, Clarke MF. 2004. Bmi1, stem cells, and senescence regulation. *J Clin Invest* **113**: 175–179.

Patricelli MP, Janes MR, Li L-S, Hansen R, Peters U, Kessler LV, Chen Y, Kucharski JM, Feng J, Ely T, et al. 2016. Selective Inhibition of Oncogenic

KRAS Output with Small Molecules Targeting the Inactive State. *Cancer Discov* **6**: CD-15-1105-329.

Pengelly AR, Kalb R, Finkl K, Müller J. 2015. Transcriptional repression by PRC1 in the absence of H2A monoubiquitylation. - PubMed - NCBI. *Genes Dev* **29**: 1487–1492.

Persson K. 1976. Modification of the eye colour mutant zeste by Suppressor, Enhancer and Minute genes in Drosophila melanogaster. **82**: 111–120.

Piotrowska Z, Niederst MJ, Karlovich CA, Wakelee HA, Neal JW, Mino-Kenudson M, Fulton L, Hata AN, Lockerman EL, Kalsy A, et al. 2015. Heterogeneity Underlies the Emergence of EGFRT790 Wild-Type Clones Following Treatment of T790M-Positive Cancers with a Third-Generation EGFR Inhibitor. *Cancer Discov* **5**: 713–722.

Pollack Y, Stein R, Razin A, Cedar H. 1980. Methylation of foreign DNA sequences in eukaryotic cells. *Proc Natl Acad Sci USA* **77**: 6463–6467.

Pomerantz J, Schreiber-Agus N, Liégeois NJ, Silverman A, Alland L, Chin L, Potes J, Chen K, Orlow I, Lee H-W, et al. 1998. The Ink4a Tumor Suppressor Gene Product, p19Arf, Interacts with MDM2 and Neutralizes MDM2's Inhibition of p53. *Cell* **92**: 713–723.

Prendergast GC, Lawe D, Ziff EB. 1991. Association of Myn, the murine homolog of Max, with c-Myc stimulates methylation-sensitive DNA binding and ras cotransformation. *Cell* **65**: 395–407.

Qian T, Lee J-Y, Park J-H, Kim H-J, Kong G. 2010. Id1 enhances RING1b E3 ubiquitin ligase activity through the Mel-18/Bmi-1 polycomb group complex. *Oncogene* **29**: 5818–5827.

Rackley CR, Stripp BR. 2012. Building and maintaining the epithelium of the lung. *J Clin Invest* **122**: 2724–2730.

Ragunathan K, Jih G, Moazed D. 2015. Epigenetic inheritance uncoupled from sequence-specific recruitment. *Science* **348**: 1258699–1258699.

Rahl PB, Lin CY, Seila AC, Flynn RA, McCuine S, Burge CB, Sharp PA, Young RA. 2010. c-Myc regulates transcriptional pause release. *Cell* **141**: 432–445.

Rajalingam K, Schreck R, Rapp UR, Albert Š. 2007. Ras oncogenes and their downstream targets. *Biochimica et Biophysica Acta (BBA) - Molecular Cell Research* **1773**: 1177–1195.

Ramalingam SS, Maitland ML, Frankel P, Argiris AE, Koczywas M, Gitlitz B, Thomas S, Espinoza-Delgado I, Vokes EE, Gandara DR, et al. 2010. Carboplatin and Paclitaxel in combination with either vorinostat or placebo

for first-line therapy of advanced non-small-cell lung cancer. *J Clin Oncol* **28**: 56–62.

Rawlins EL, Okubo T, Xue Y, Brass DM, Auten RL, Hasegawa H, Wang F, Hogan BLM. 2009. The Role of Scgb1a1+ Clara Cells in the Long-Term Maintenance and Repair of Lung Airway, but Not Alveolar, Epithelium. **4**: 525–534.

Reck M, Heigener DF, Mok T, Soria J-C, Rabe KF. 2013. Management of non-small-cell lung cancer: recent developments. *The Lancet* **382**: 709–719.

Reddy EP, Reynolds RK, Santos E, Barbacid M. 1982. A point mutation is responsible for the acquisition of transforming properties by the T24 human bladder carcinoma oncogene. *Nature* **300**: 149.

Rehm S, Ward JM, Have-Opbroek ten AA, Anderson LM, Singh G, Katyal SL, Rice JM. 1988. Mouse papillary lung tumors transplacentally induced by N-nitrosoethylurea: evidence for alveolar type II cell origin by comparative light microscopic, ultrastructural, and immunohistochemical studies. **48**: 148–160.

Richly H, Rocha-Viegas L, Ribeiro JD, Demajo S, Gundem G, Lopez-Bigas N, Nakagawa T, Rospert S, Ito T, Di Croce L. 2010. Transcriptional activation of polycomb-repressed genes by ZRF1. *Nature* **468**: 1124–1128.

Robertson KD. 2005. DNA methylation and human disease. *Nat Rev Genet* **6**: 597–610.

Roulois D, Loo Yau H, Singhania R, Wang Y, Danesh A, Shen SY, Han H, Liang G, Jones PA, Pugh TJ, et al. 2015. DNA-Demethylating Agents Target Colorectal Cancer Cells by Inducing Viral Mimicry by Endogenous Transcripts. *Cell* **162**: 961–973.

Rowbotham SP, Kim CF. 2014. Diverse cells at the origin of lung adenocarcinoma. *Proc Natl Acad Sci USA* **111**: 4745–4746.

Sahu A, Singhal U, Chinnaiyan AM. 2015. Long noncoding RNAs in cancer: from function to translation. *Trends in cancer* **1**: 93.

Sakai T, Toguchida J, Ohtani N, Yandell DW, Rapaport JM, Dryja TP. 1991. Allele-specific hypermethylation of the retinoblastoma tumor-suppressor gene. *American Journal of Human Genetics* **48**: 880–888.

Sarhadi VK, Wikman H, Salmenkivi K, Kuosma E, Sioris T, Salo J, Karjalainen A, Knuutila S, Anttila S. 2006. Increased expression of high mobility group A proteins in lung cancer. **209**: 206–212.

Sato T, Denell RE. 1985. Homoeosis in Drosophila: Anterior and posterior transformations of Polycomb lethal embryos. *Dev Biol* **110**: 53–64.

Sato T, Kauffman SL. 1980. A scanning electron microscopic study of the Type II and Clara cell adenoma of the mouse lung. *Lab Invest* **43**: 28–36.

Schiller JH, Harrington D, Belani CP, Langer C, Sandler A, Krook J, Zhu J, Johnson DH, Eastern Cooperative Oncology Group. 2002. Comparison of four chemotherapy regimens for advanced non-small-cell lung cancer. *N Engl J Med* **346**: 92–98.

Schrump DS. 2013. Clinical Implications of Epigenetic Alterations in Lung Cancer. In *Epigenetic Therapy of Cancer* (eds. M. Lübbert and P.A. Jones), pp. 257–282, Springer Berlin Heidelberg, Berlin, Heidelberg.

Serresi M, Gargiulo G, Proost N, Siteur B, Cesaroni M, Koppens M, Xie H, Sutherland KD, Hulsman D, Citterio E, et al. 2016. Polycomb Repressive Complex 2 Is a Barrier to KRAS-Driven Inflammation and Epithelial-Mesenchymal Transition in Non-Small-Cell Lung Cancer. **29**: 17–31.

Sherr CJ. 2006. Divorcing ARF and p53: an unsettled case. *Nat Rev Cancer* **6**: 663–673.

Shinjo K, Okamoto Y, An B, Yokoyama T, Takeuchi I, Fujii M, Osada H, Usami N, Hasegawa Y, Ito H, et al. 2012. Integrated analysis of genetic and epigenetic alterations reveals CpG island methylator phenotype associated with distinct clinical characters of lung adenocarcinoma. *Carcinogenesis* **33**: 1277–1285.

Siegel RL, Miller KD, Jemal A. 2015. Cancer statistics, 2015. *CA: A Cancer Journal for Clinicians* **65**: 5–29.

Simon JA, Kingston RE. 2013. Occupying Chromatin: Polycomb Mechanisms for Getting to Genomic Targets, Stopping Transcriptional Traffic, and Staying Put. *Mol Cell* **49**: 808–824.

Singh M, Lima A, Molina R, Hamilton P, Clermont AC, Devasthali V, Thompson JD, Cheng JH, Reslan HB, Ho CCK, et al. 2010. Assessing therapeutic responses in Kras mutant cancers using genetically engineered mouse models. *Nat Biotechnol* **28**: 585–593.

Snyder EL, Watanabe H, Magendantz M, Hoersch S, Chen TA, Wang DG, Crowley D, Whittaker CA, Meyerson M, Kimura S, et al. 2013. Nkx2-1 represses a latent gastric differentiation program in lung adenocarcinoma. *Mol Cell* **50**: 185–199.

Sousa-Victor P, Gutarra S, García-Prat L, Rodriguez-Ubreva J, Ortet L, Ruiz-Bonilla V, Jardí M, Ballestar E, González S, Serrano AL, et al. 2014. Geriatric muscle stem cells switch reversible quiescence into senescence. *Nature* **506**: 316–321.

Spiegel J, Cromm PM, Zimmermann G, Grossmann TN, Waldmann H. 2014. Small-molecule modulation of Ras signaling. *Nat Chem Biol* **10**: 613–622.

Stehelin D, Varmus HE, Bishop JM, Vogt PK. 1976. DNA related to the transforming gene (s) of avian sarcoma viruses is present in normal avian DNA. *Nature* **260**: 170.

Stock JK, Giadrossi S, Casanova M, Brookes E, Vidal M, Koseki H, Brockdorff N, Fisher AG, Pombo A. 2007. Ring1-mediated ubiquitination of H2A restrains poised RNA polymerase II at bivalent genes in mouse ES cells. *Nat Cell Biol* **9**: 1428–1435.

Struhl G. 1981. A gene product required for correct initiation of segmental determination in Drosophila. *Nature* **293**: 36–41.

Subkhankulova T, Zhang X, Leung C, Marino S. 2010. Bmi1 directly represses p21Waf1/Cip1 in Shh-induced proliferation of cerebellar granule cell progenitors. *Mol Cell Neurosci* **45**: 151–162.

Sutherland KD, Song J-Y, Kwon M-C, Proost N, Zevenhoven J, Berns A. 2014. Multiple cells-of-origin of mutant K-Ras-induced mouse lung adenocarcinoma. *Proc Natl Acad Sci USA* **111**: 4952–4957.

Taherbhoy AM, Huang OW, Cochran AG. 2015. BMI1-RING1B is an autoinhibited RING E3 ubiquitin ligase. *Nature Communications* **6**: 7621.

Taparowsky E, Suard Y, Fasano O, Shimizu K. 1982. Activation of the T24 bladder carcinoma transforming gene is linked to a single amino acid change. *Nature* **300**:762-765

Tavares L, Dimitrova E, Oxley D, Webster J, Poot R, Demmers J, Bezstarosti K, Taylor S, Ura H, Koide H, et al. 2012. RYBP-PRC1 complexes mediate H2A ubiquitylation at polycomb target sites independently of PRC2 and H3K27me3. *Cell* **148**: 664–678.

Taverna SD, Li H, Ruthenburg AJ, Allis CD, Patel DJ. 2007. How chromatin-binding modules interpret histone modifications: lessons from professional pocket pickers. - PubMed - NCBI. *Nat Struct Mol Biol* **14**: 1025–1040.

Thaete LG, Malkinson AM. 1991. Cells of origin of primary pulmonary neoplasms in mice: morphologic and histochemical studies. *Exp Lung Res* **17**: 219–228.

Travis WD, Brambilla E, Nicholson AG, Yatabe Y, Austin JHM, Beasley MB, Chirieac LR, Dacic S, Duhig E, Flieder DB, et al. 2015. The 2015 World Health

Organization Classification of Lung Tumors. *Journal of Thoracic Oncology* **10**: 1243–1260.

Travis WD, Brambilla E, Noguchi M. 2011. International association for the study of lung cancer/american thoracic society/european respiratory society international multidisciplinary classification of .... *Journal of Thoracic* **6**: 244.

Trimarchi JM, Fairchild B, Wen J, Lees JA. 2001. The E2F6 transcription factor is a component of the mammalian Bmi1-containing polycomb complex. *Proc Natl Acad Sci USA* **98**: 1519–1524.

Vafa O, Wade M, Kern S, Beeche M, Pandita TK, Hampton GM, Wahl GM. 2002. c-Myc Can Induce DNA Damage, Increase Reactive Oxygen Species, and Mitigate p53 Function. *Mol Cell* **9**: 1031–1044.

van der Lugt NM, Alkema M, Berns A, Deschamps J. 1996. The Polycomb-group homolog Bmi-1 is a regulator of murine Hox gene expression. *Mech Dev* **58**: 153–164.

van der Lugt NM, Domen J, Linders K, van Roon M, Robanus-Maandag E, Riele te H, van der Valk M, Deschamps J, Sofroniew M, van Lohuizen M. 1994. Posterior transformation, neurological abnormalities, and severe hematopoietic defects in mice with a targeted deletion of the bmi-1 proto-oncogene. *Genes Dev* **8**: 757–769.

van Lohuizen M, Frasch M, Wientjens E, Berns A. 1991a. Sequence similarity between the mammalian bmi-1 proto-oncogene and the Drosophila regulatory genes Psc and Su(z)2. *Nature* **353**: 353–355.

van Lohuizen M, Verbeek S, Scheijen B, Wientjens E, van der Gulden H, Berns A. 1991b. Identification of cooperating oncogenes in E mu-myc transgenic mice by provirus tagging. *Cell* **65**: 737–752.

Varambally S, Cao Q, Mani R-S, Shankar S, Wang X, Ateeq B, Laxman B, Cao X, Jing X, Ramnarayanan K, et al. 2008. Genomic loss of microRNA-101 leads to overexpression of histone methyltransferase EZH2 in cancer. *Science* **322**: 1695–1699.

Varambally S, Dhanasekaran SM, Zhou M, Barrette TR, Kumar-Sinha C, Sanda MG, Ghosh D, Pienta KJ, Sewalt RGAB, Otte AP, et al. 2002. The polycomb group protein EZH2 is involved in progression of prostate cancer. *Nature* **419**: 624–629.

Visvader JE, Lindeman GJ. 2008. Cancer stem cells in solid tumours: accumulating evidence and unresolved questions. *Nat Rev Cancer* **8**: 755–768.

Vogelstein B, Lane D, Levine AJ. 2000. Surfing the p53 network. *Nature* **408**: 307–310.

Voncken JW, Niessen H, Neufeld B, Rennefahrt U, Dahlmans V, Kubben N, Holzer B, Ludwig S, Rapp UR. 2005. MAPKAP kinase 3pK phosphorylates and regulates chromatin association of the polycomb group protein Bmi1. *J Biol Chem* **280**: 5178–5187.

Voncken JW, Roelen BAJ, Roefs M, de Vries S, Verhoeven E, Marino S, Deschamps J, van Lohuizen M. 2003. Rnf2 (Ring1b) deficiency causes gastrulation arrest and cell cycle inhibition. *Proc Natl Acad Sci USA* **100**: 2468–2473.

Voncken JW, Schweizer D, Aagaard L, Sattler L, Jantsch MF, van Lohuizen M. 1999. Chromatin-association of the Polycomb group protein BMI1 is cell cycle-regulated and correlates with its phosphorylation status. *J Cell Sci* **112**: 4627–4639.

Vonlanthen S, Heighway J, Altermatt HJ, Gugger M, Kappeler A, Borner MM, van Lohuizen M, Betticher DC. 2001. The bmi-1 oncoprotein is differentially expressed in non-small cell lung cancer and correlates with INK4A-ARF locus expression. *Br J Cancer* **84**: 1372–1376.

Vrzalikova K, Skarda J, Ehrmann J, Murray PG, Fridman E, Kopolovic J, Knizetova P, Hajduch M, Klein J, Kolek V, et al. 2008. Prognostic value of Bmi-1 oncoprotein expression in NSCLC patients: a tissue microarray study. *J Cancer Res Clin Oncol* **134**: 1037–1042.

Waddington CH. 1953. Waddington: Epigenetics and evolution *Symp. Soc. Exp. Biol.*

Walsh CP, Chaillet JR, Bestor TH. 1998. Transcription of IAP endogenous retroviruses is constrained by cytosine methylation. *Nat Genet* **20**: 116–117.

Wang H, Pan K, Zhang H-K, Weng D-S, Zhou J, Li J-J, Huang W, Song H-F, Chen M-S, Xia J-C. 2008. Increased polycomb-group oncogene Bmi-1 expression correlates with poor prognosis in hepatocellular carcinoma. *J Cancer Res Clin Oncol* **134**: 535–541.

Wang H, Wang L, Erdjument-Bromage H, Vidal M, Tempst P, Jones RS, Zhang Y. 2004a. Role of histone H2A ubiquitination in Polycomb silencing. *Nature* **431**: 873–878.

Wang L, Brown JL, Cao R, Zhang Y, Kassis JA, Jones RS. 2004b. Hierarchical recruitment of polycomb group silencing complexes. *Mol Cell* **14**: 637–646.

Weber JD, Jeffers JR, Rehg JE, Randle DH, Lozano G, Roussel MF, Sherr CJ, Zambetti GP. 2000. p53-independent functions of the p19(ARF) tumor suppressor. *Genes Dev* **14**: 2358–2365.

Wei J, Zhai L, Xu J, Wang H. 2006. Role of Bmi1 in H2A ubiquitylation and Hox gene silencing. *J Biol Chem* **281**: 22537–22544.

West AC, Johnstone RW. 2014. New and emerging HDAC inhibitors for cancer treatment. *J Clin Invest* **124**: 30–39.

Westerman BA, Blom M, Tanger E, van der Valk M, Song J-Y, van Santen M, Gadiot J, Cornelissen-Steijger P, Zevenhoven J, Prosser HM, et al. 2012. GFAP-Cre-Mediated Transgenic Activation of Bmi1 Results in Pituitary Tumors. *PLoS ONE* **7**: e35943.

Widschwendter M, Fiegl H, Egle D, Mueller-Holzner E, Spizzo G, Marth C, Weisenberger DJ, Campan M, Young J, Jacobs I, et al. 2007. Epigenetic stem cell signature in cancer. *Nat Genet* **39**: 157–158.

Wienken M, Dickmanns A, Nemajerova A, Kramer D, Najafova Z, Weiss M, Karpiuk O, Kassem M, Zhang Y, Lozano G, et al. 2016. MDM2 Associates with Polycomb Repressor Complex 2 and Enhances Stemness-Promoting Chromatin Modifications Independent of p53. *Mol Cell* **61**: 68–83.

Winslow MM, Dayton TL, Verhaak RGW, Kim-Kiselak C, Snyder EL, Feldser DM, Hubbard DD, DuPage MJ, Whittaker CA, Hoersch S, et al. 2011. Suppression of lung adenocarcinoma progression by Nkx2-1. *Nature* **473**: 101–104.

Wu CT, Jones RS, Lasko PF, Gelbart WM. 1989. Homeosis and the interaction of zeste and white in Drosophila. *Mol Gen Genet* **218**: 559–564.

Xu F, Li X, Wu L, Zhang Q, Yang R, Yang Y, Zhang Z, He Q, Chang C. 2011. Overexpression of the EZH2, RING1 and BMI1 genes is common in myelodysplastic syndromes: relation to adverse epigenetic alteration and poor prognostic scoring. *Ann Hematol* **90**: 643–653.

Xu X, Rock JR, Lu Y, Futtner C, Schwab B, Guinney J, Hogan BLM, Onaitis MW. 2012. Evidence for type II cells as cells of origin of K-Ras-induced distal lung adenocarcinoma. *Proc Natl Acad Sci USA* **109**: 4910–4915.

Yi J-M, Kim H-S. 2007. Molecular Phylogenetic Analysis of the Human Endogenous Retrovirus E (HERV-E) Family in Human Tissues and Human Cancers. *Genes & Genetic Systems* **82**: 89–98.

Young NP, Jacks T. 2010. Tissue-specific p19Arf regulation dictates the response to oncogenic K-ras. *Proc Natl Acad Sci USA* **107**: 10184–10189.

Yu M, Mazor T, Huang H, Huang H-T, Kathrein KL, Woo AJ, Chouinard CR, Labadorf A, Akie TE, Moran TB, et al. 2012. Direct recruitment of polycomb repressive complex 1 to chromatin by core binding transcription factors. *Mol Cell* **45**: 330–343.

Zacharek SJ, Fillmore CM, Lau AN, Gludish DW, Chou A, Ho JWK, Zamponi R, Gazit R, Bock C, Jäger N, et al. 2011. Lung Stem Cell Self-Renewal Relies on BMI1-Dependent Control of Expression at Imprinted Loci. **9**: 272–281.

Zhang J-G, Guo J-F, Liu D-L, Liu Q, Wang J-J. 2011. MicroRNA-101 exerts tumor-suppressive functions in non-small cell lung cancer through directly targeting enhancer of zeste homolog 2. *Journal of Thoracic Oncology* **6**: 671–678.

Zhang Y. 2003. Transcriptional regulation by histone ubiquitination and deubiquitination. *Genes Dev* **17**: 2733–2740.

Zhang Y, Xiong Y, Yarbrough WG. 1998. ARF promotes MDM2 degradation and stabilizes p53: ARF-INK4a locus deletion impairs both the Rb and p53 tumor suppression pathways. *Cell* **92**: 725–734.

Zhou W, Zhu P, Wang J, Pascual G, Ohgi KA, Lozach J, Glass CK, Rosenfeld MG. 2008. Histone H2A Monoubiquitination Represses Transcription by Inhibiting RNA Polymerase II Transcriptional Elongation. *Mol Cell* **29**: 69–80.

Zhou Y, Wang L, Vaseghi HR, Liu Z, Lu R, Alimohamadi S, Yin C, Fu J-D, Wang GG, Liu J, et al. 2016. Bmi1 Is a Key Epigenetic Barrier to Direct Cardiac Reprogramming. *Cell Stem Cell* **18**: 382–395.

Zink B, Paro R. 1989. In vivo binding pattern of a trans-regulator of homoeotic genes in Drosophila melanogaster. *Nature* **337**: 468–471.

Zuber J, Shi J, Wang E, Rappaport AR, Herrmann H, Sison EA, Magoon D, Qi J, Blatt K, Wunderlich M, et al. 2011. RNAi screen identifies Brd4 as a therapeutic target in acute myeloid leukaemia. *Nature* **478**: 524–528.

Zuo W, Zhang T, Wu DZ, Guan SP, Liew A-A, Yamamoto Y, Wang X, Lim SJ, Vincent M, Lessard M, et al. 2015. p63(+)Krt5(+) distal airway stem cells are essential for lung regeneration. *Nature* **517**: 616–620.

CHAPTER 2: BMI1 PROMOTES LUNG ADENOCARCINOMA PROGRESSION

Daniel L Karl, Paul S Danielian, Arjun Bhutkar, Jenny Tadros, Rodrick Bronson, Jacqueline A Lees

D.L.K. and P.S.D. conducted all mouse experiments. J.T. contributed to Figures 1C and 2A. R.B. contributed to tumor grading analyses. D.L.K conducted the gene expression experiments. D.L.K and A.B analyzed the gene expression data. D.L.K, P.S.D, and J.A.L designed the study, analyzed the data. D.L.K and J.A.L. wrote the chapter.

ABSTRACT

Bmi1 is implicated as an oncogene in a variety of human cancers. Previous reports indicated that Bmi1 acts largely by restraining the canonical target $p19^{ARF}$ to promote tumorigenesis in the lung. However, these studies were unable to critically examine a role for Bmi1 in the context of a developmentally wild-type adult. In this study, we use mouse models of adult Kras driven lung adenocarcinoma to assess the consequences of deleting Bmi1 at the time of tumor initiation. Our data demonstrate that Bmi1 is oncogenic independent of its capacity to repress the canonical $p19^{ARF}$-p53 tumor suppressive axis. Furthermore, we find that Bmi1 is dispensable for tumor initiation but impacts survival by mediating the transition from low grade lesions to advanced disease. This is due, in part, to a critical role for Bmi1 in sustaining the proliferative capacity of adenomas. Gene expression analyses reveals that Bmi1 restrains developmental regulators and may contribute to the atypical presentation of tumor differentiation markers in response to Bmi1 loss. Together, this work advances our understanding of Bmi1's role during lung tumor initiation and progression, and highlights potential tumor dependencies that may be exploited for therapeutic purposes.

INTRODUCTION

Accumulating evidence suggests that epigenetic events play a critical role during tumorigenesis and are viable targets for therapeutic intervention (Brien et al. 2016). In lung adenocarcinoma, one of the deadliest and more prevalent forms of cancer, epigenetic events such as DNA methylation are frequently deregulated (Collisson et al. 2014; Lin et al. 2010). The promise of epigenetic therapy is to globally alter these reversible events (Dawson and Kouzarides 2012). DNA Methyl Transferase (DNMT) inhibitors, for instance, can lead to the re-expression of tumor suppressors and mediate tumor regression in some forms of leukemia (Issa and Kantarjian 2009; Baylin and Jones 2011; Chiappinelli et al. 2015).

Polycomb Group proteins (PcGs) largely suppress transcription at target loci by maintaining repressive chromatin in part through modifying histones (Laugesen and Helin 2014). PcGs play a prominent role in lineage commitment during development and can be coopted during tumorigenesis to enforce self-renewal and differentiation status (Laugesen and Helin 2014; Bracken et al. 2006; Boyer et al. 2006; Chiacchiera et al. 2016). Small molecule inhibitors have been developed to target PcG components, including some that are in clinical trials for other types of cancer (Brien et al. 2016). Inhibitors of Polycomb Repressive Complex 2 (PRC2) protein Ezh2 have proven effective in preclinical trials of lymphoma and are moving into the clinic (Knutson et al. 2013; 2014). Recent studies have also suggested that modulation of PcGs may prove to be beneficial for a subset of lung adenocarcinoma patients based on their underlying genetic landscape (Fillmore et al. 2015; Serresi et al. 2016).

Bmi1 is a core member of the Polycomb Repressive Complex 1 (PCR1) and has been implicated as an oncogene in many types of cancer, including in the lung (Glinsky et al. 2005; Siddique and Saleem 2012; 2001). Traditionally, it was shown to maintain the repression of two tumor suppressors encoded at the *Cdkn2a* locus - $p16^{INK4A}$ and $p14^{ARF}$ ($p19^{ARF}$ in mice), which mediate the self-renewal capacity of stem and progenitor cells (Park et al. 2004). Previous studies using mice with germ line deficiency of Bmi1 have implicated the derepression of *Cdkn2a,* as well as other cell cycle inhibitors such as p57, as a critical events leading to stem cell exhaustion and tumor suppression in the lung (Dovey et al. 2008; Becker et al. 2009; Zacharek et al. 2011). However, there has been little examination of potential roles for Bmi1 in mediating tumorigenesis in the adult lung, and, for several reasons, it remains unclear whether loss or inhibition of BM1 in this setting would have the same effect on lung cancer. First, mice lacking Bmi1 throughout embryogenesis also display a number of abnormalities including a defective immune compartment and a short lifespan that could influence lung cancer progression in a non-cell autonomous manner (van der Lugt et al. 1994). Second, oncogenic roles independent of *Cdkn2a* have been identified for Bmi1 that are both tissue and tumor type specific (Bruggeman et al. 2007; Nacerddine et al. 2012). Third, Bmi1 loss in adult tissues can intersect with a different set of pathways compared with the absence of Bmi1 through embryogenesis. This was demonstrated in various tissue compartments in which *Cdkn2a* was critically deregulated in tumors arising in Bmi1 germline deficient animals (Bruggeman et al. 2005; Jacobs et al. 1999a; Maynard et al. 2014; Kreso et al. 2014). Inhibition of Bmi1 in the gliomas, for instance, uncovered novel interactions

between Bmi1 and differentiation networks independent of *Cdkn2a* (Bruggeman et al. 2007; Gargiulo et al. 2013).

Tissue and context specificity is a critical determinant for Bmi1's role in mediating normal stem cell self renewal, but little is known about underlying contextual factors in lung tumors and how they impact the target specificity of Bmi1 (Gil and O'Loghlen 2014; Koppens and van Lohuizen 2015). Tumor initiating cells and established tumor cells may be sustained by different mechanisms that are still not well understood. Indeed, modulating Bmi1 in tumors results in variable consequences depending on the tissue of origin (Hsu and Lawlor 2011; Lukacs et al. 2010; Lopez-Arribillaga et al. 2014; Gargiulo et al. 2013; Liu 2006). Furthermore, it is also clear that there is phenotypic and genetic diversity in established lung tumors that might lead to differential Bmi1 targets in any given tumor (Chen et al. 2014; Collisson et al. 2014; Travis et al. 2015). Elucidating Bmi1's lung specific genetic dependencies remains an unmet need in the field.

In lung adenocarcinoma, Kras is the most commonly mutated oncogenic driver - occurring in a third of tumors (Collisson et al. 2014). Despite progress in developing targeted therapies for other drivers, oncogenic Kras has been notoriously difficult to target (Chen et al. 2014; Patricelli et al. 2016). Identifying potential cooperating pathways may uncover novel sensitivities and inform therapeutic strategies. Importantly, since *p53* is mutated in half of all lung adenocarcinomas, any effective treatment of Kras mutant lung cancer would ideally be irrespective of p53 status (Collisson et al. 2014). In this study, we set out to determine whether the acute deletion of *Bmi1* could affect the initiation and/or progression of Kras driven lung tumors. We

have done so in the context of p53 proficiency and deficiency to understand if Bmi1 function depends on the $p19^{ARF}$-p53 tumor suppressive axis. This allowed us to identify a critical role for Bmi1 in mediating the transition from low grade tumors to advanced disease. Furthermore, we demonstrate that Bmi1 is critical for maintaining the proliferative capacity of lung adenomas independent of the $p19^{ARF}$-53 axis. Importantly, we also show that Bmi1 loss modulates the differentiation state of advanced adenocarcinoma, and it may do so by altering developmental regulators. Overall, our work clarifies essential roles for Bmi1 in lung adenomagenesis and identifies a therapeutic window for the targeted intervention of patients that present with this deadly disease.

RESULTS

Loss of Bmi1 enhances overall survival in Kras driven lung cancer

Genetically engineered mouse models of lung adenocarcinoma recapitulate human tumor progression and have proven useful in the identification of molecular determinants of the disease (Kwon and Berns 2013; Westcott et al. 2014). To determine whether and how Bmi1 contributes to tumorigenesis in the adult lung, we generated lung adenomas in mice and ablated Bmi1 at the time of oncogenic Kras activation. This model dissociates potential oncogenic roles for Bmi1 in the lung from confounding consequences of global germ-line Bmi1 deficiency. Specifically, we crossed mice conditional for Bmi1 (*Bmi1*$^{fl/fl}$) with mice harboring an inducible oncogenic form of Kras (*K-ras*$^{LSL\text{-}G12D/+}$) (Maynard et al. 2014; Jackson et al. 2001). Delivery of a lentivirus constitutively expressing Cre-recombinase inactivated Bmi1 coincident with the activation of oncogenic Kras in tumor initiating cells (Dupage et al. 2009). We used lentivirus that integrates into the mouse genome to ensure Bmi1 recombination. Immuno-histochemical analysis of BMI1 protein levels confirmed that tumor cells in Bmi1 conditional mice lacked detectable BMI1 protein (Figure 1A). Importantly, the stromal compartment within Bmi1 conditional tumors retained expression, as did almost all lesions from *Bmi1*$^{+/+}$;*Kras*$^{LSL\text{-}G12D/+}$ infected mice (Figure 1A,B). Therefore we have established a robust system in which to test the role of Bmi1 during lung adenomagenesis.

We first determined whether loss of Bmi1 in lung tumors of adult mice conferred an overall survival advantage. Previous studies assessing roles for Bmi1 were

hampered by an inability to examine long term consequences since the *Bmi1*$^{-/-}$ mouse is short lived (Dovey et al. 2008; Becker et al. 2009; van der Lugt et al. 1994). To test whether loss specifically in lung tumors confers a survival benefit, we infected a large cohort of *Bmi1*$^{fl/fl}$; *Kras*$^{LSL\text{-}G12D/+}$ mice harboring an inducible Luciferase (*R26*$^{LSL\text{-}Luciferase}$), along with wild-type and heterozygous littermates, with a virus that constitutively expresses Cre. Strikingly, we observed that loss of Bmi1 significantly enhances overall survival, and extends median survival by almost 50% (Figure 1C). *Bmi1*$^{+/fl}$ mice displayed an intermediate response, perhaps suggesting that dosage of Bmi1 may impact tumor growth (Figure 1C). These data indicate that Bmi1 supports lung adenomagenesis over an extended time in a tumor cell intrinsic manner in adult mice.

Bmi1 cooperates with Kras to drive tumor growth in the lung

We wished to determine whether loss of Bmi1 extends survival by diminishing the capacity of tumors to initiate, directly impacting tumor growth, or both. To do this, we infected additional cohorts of *Bmi1*$^{+/+}$; *Kras*$^{LSL\text{-}G12D/+}$ and *Bmi1*$^{fl/fl}$; *Kras*$^{LSL\text{-}G12D/+}$ mice and examined tumor bearing lungs at early and late time points (8 and 20 weeks post infection, respectively). When we examined lungs from animals collected at 8 weeks we did not observe reduced tumor number in *Bmi1*$^{fl/fl}$ mice compared to *Bmi1*$^{+/+}$ litter-mates (Figure 1D). In fact, we observed that some *Bmi1*$^{fl/fl}$ mice tended to have a greater number of lesions, though this did not reach significance for the cohort. We then analyzed the size distribution of individual lesions from these mice 8 weeks after infection (Figure 1E). Since each adenoma represents an independent initiating event, we considered all the tumors from several mice by genotype. At this early time point,

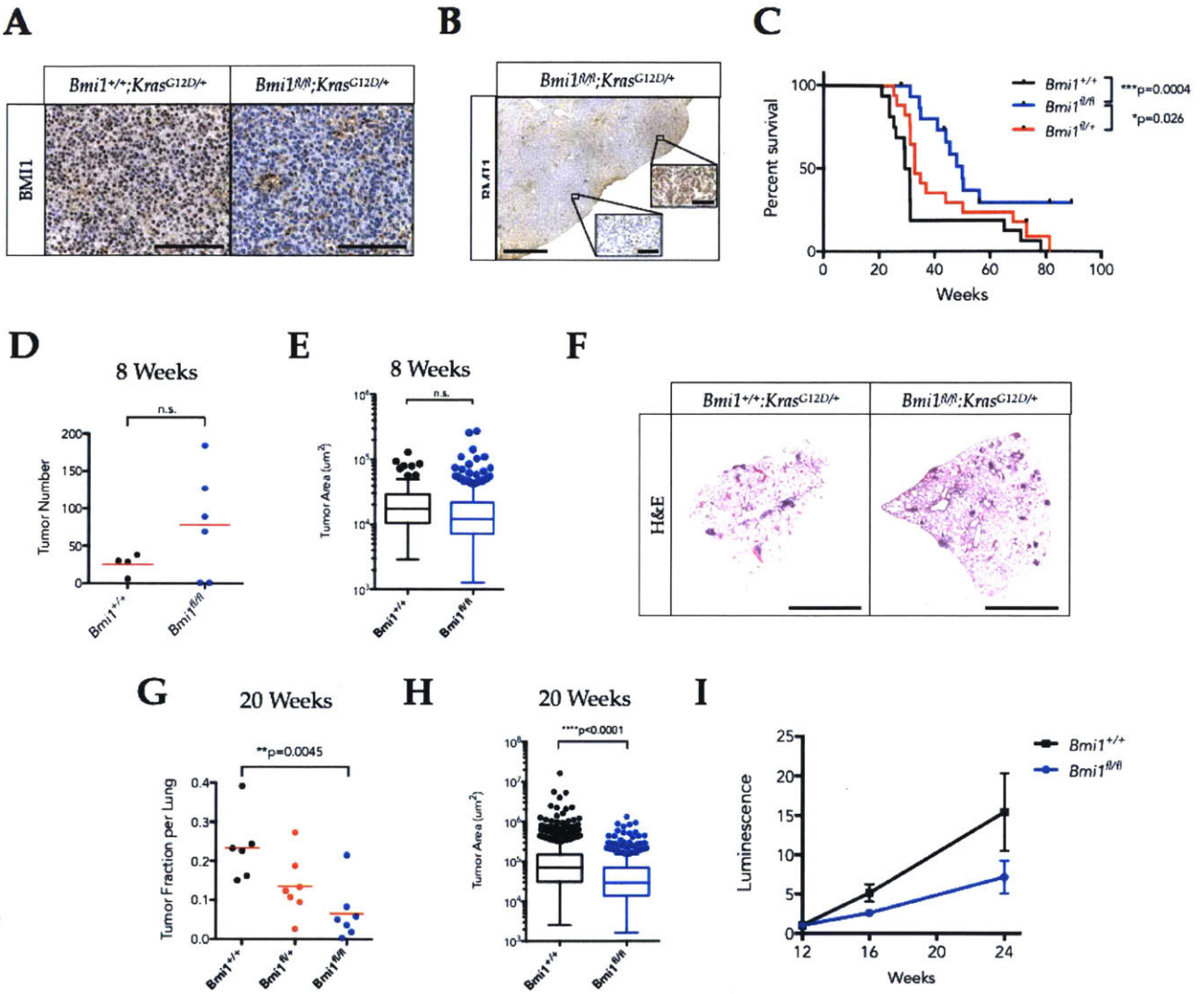

Figure 1. Bmi1 cooperates with Kras to drive lung tumor growth
(A) Representative immunohistochemical (IHC) staining for Bmi1 in tumors from $Kras^{G12D/+}$ and $Kras^{G12D/+}$;$Bmi1^{fl/fl}$ mice. Bar = 100μm **(B)** IHC for Bmi1 in lungs from a terminal $Bmi1^{fl/fl}$ mouse. Most tumors lack BMI1 expression. Bars = 1mm, 50μm **(C)** Overall Survival of Lenti-PGK-Cre activated $Kras^{G12D/+}$;$Bmi1^{+/+}$ (n=16), $Kras^{G12D/+}$;$Bmi1^{fl/+}$ (n=17), $Kras^{G12D/+}$;$Bmi1^{fl/fl}$ (n=16). p values determined by Wilxocon tests and are significant by log rank tests. **(D)** Tumor number from mice euthanized 8 weeks after infection. **(E)** Individual tumor areas from H&E sections of mice euthanized 8 weeks post infection from $Bmi1^{+/+}$ (4 mice, n=103) and $Bmi1^{fl/fl}$ (6 mice, n=471). **(F)** Representative H&E sections of mouse lung lobes 8 weeks post-infection. Bar = 2mm **(G)** Fraction of tumor tissue per lung area 20 weeks post infection. p value by one way ANOVA. **(H)** Tumor areas 20 weeks post infection from $Bmi1^{+/+}$ (6 mice, n=1156) and $Bmi1^{fl/fl}$ (7 mice, n=698) animals. **(I)** IVIS luminescent detection of tumor burden. Each mouse (n=11 per group) was normalized to luminescence at 12 weeks.
Box plots were generated according to the Tukey method.

we did not observe large differences between the genotypes (Figure 1F). Indeed, the two largest adenomas developed in *Bmi1*$^{fl/fl}$ lungs. Thus, Bmi1 appears dispensable for Kras driven tumor initiation.

We next examined tumor bearing lungs from mice at 20 weeks, a late time point before *Bmi1*$^{+/+}$ mice begin to succumb due to disease. First we assessed tumor burden by calculating the fraction of tumor tissue to total lung tissue. Strikingly, tumor burden was dramatically reduced in *Bmi1*$^{fl/fl}$ lungs compared to *Bmi1*$^{+/+}$ controls (Figure 1G). Furthermore, heterozygous ablation of Bmi1 trended toward an intermediate effect reminiscent of *Bmi1*$^{fl/+}$ mouse survival (Figure 1C). Bmi1 dosage, then, may be important for sustaining Kras driven tumors. To assess the contribution of Bmi1 on tumor growth more directly, we quantified individual tumor areas from these mice (Figure 1H). In contrast to our observations at 8 weeks post infection, tumors from *Bmi1*$^{fl/fl}$ mice were significantly smaller than those from *Bmi1*$^{+/+}$ controls, indicating that the tumor suppressive effect of Bmi1 loss is exaggerated over time. Together, this data suggests that Bmi1 promotes lung cancer by sustaining tumor growth after initiation. To test this, we infected another set of mice that also harbored a Cre inducible Luciferase expressed from the ubiquitous Rosa26 locus (*R26*$^{LSL\text{-}Luciferase}$) and monitored the change in bioluminescence per mouse over time (Figure 1I). Indeed, bioluminescence from *Bmi1*$^{+/+}$ mice increased more rapidly over time than it did for *Bmi1*$^{fl/fl}$ mice. We conclude that BMI1 promotes the continued growth of tumors throughout tumor progression.

Bmi1 promotes lung tumorigenesis independent of 19^{ARF}-p53 suppression.

In other tumor types, particularly among the hematological malignancies, Bmi1 promotes tumorigenesis in part by restraining the *Cdkn2a* locus that encodes two distinct tumor suppressors - $p16^{INK4A}$ and $p19^{ARF}$ (Park et al. 2004). In lymphomas, for instance, repression of $p19^{ARF}$ by Bmi1 is critical for inhibiting p53 dependent tumor suppressive networks during tumorigenesis (Jacobs et al. 1999b). Previous studies using different models of lung adenomagenesis implicated $p19^{ARF}$ deregulation as a major mediator of tumor suppression in the context of Bmi1 germline deficiency (Dovey et al. 2008; Becker et al. 2009; Young and Jacks 2010). Therefore, we decided to test whether Bmi1 promotes Kras driven lung cancer through sustained targeting of the $p19^{ARF}$-p53 axis by ablating p53 with Bmi1 at the time of tumor initiation. Assessing tumorigenesis in the context of p53 deficiency is also relevant for the human disease where its network disrupted in almost two thirds of patients (Collisson et al. 2014). If Bmi1 loss acts through $p19^{ARF}$, we would expect to see little survival benefit in $Kras^{G12D/+};p53^{fl/fl}$ mice. Instead, we observed that Bmi1 ablation dramatically prolonged the lifespan, indicating that the $p19^{ARF}$-p53 axis is not a critical determinant for Bmi1 in Kras driven lung adenocarcinoma (Figure 2A). Moreover, the roughly 50% median survival benefit in $Bmi1^{fl/fl}$ animals mirrors what we observe in p53 sufficient mice (Figure 1C). These data suggest that Bmi1 promotes lung tumorigenesis independent of its capacity to restrain the p53 pathway and thus the canonical Bmi1 target $p19^{ARF}$.

Since p53 deficiency in Kras driven lung adenomagenesis changes the tumor spectrum, we set out to determine whether the loss of Bmi1 similarly inhibits tumorigenesis with or without functional p53. Compared to p53 proficient mice,

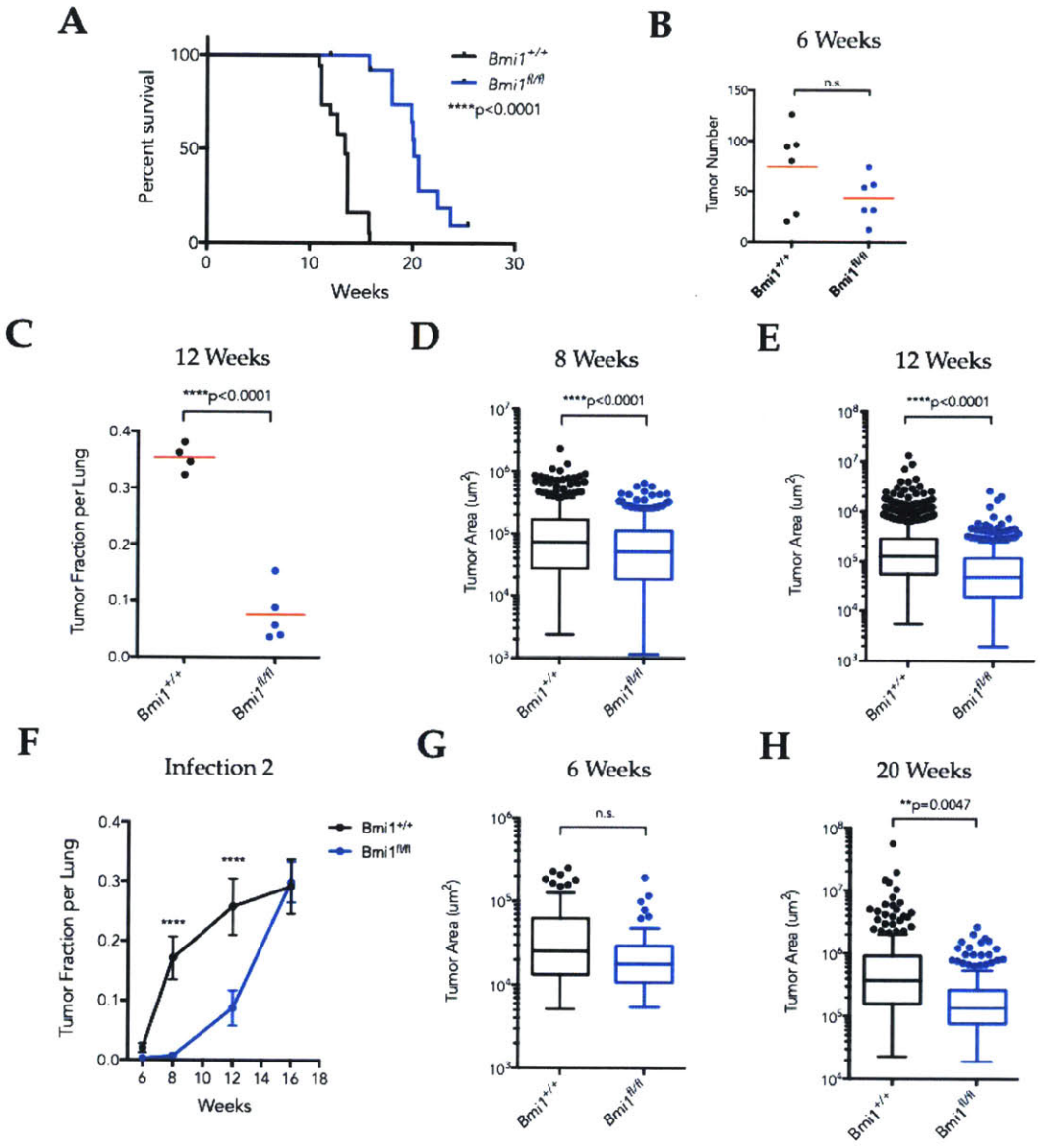

Figure 2. Bmi1 promotes Kras driven lung cancer independent of p19^{ARF}-p53
(A) Overall Survival of Lenti-PGK-Cre activated *Kras$^{G12D/+}$;p53$^{fl/fl}$;Bmi1$^{+/+}$* (n=19), *Kras$^{G12D/+}$;p53$^{fl/fl}$;Bmi1$^{fl/fl}$* (n=14). p value determined by Wilxocon and log rank tests. **(B)** Tumor number from *p53$^{fl/fl}$;Bmi1$^{+/+}$* and *p53$^{fl/fl}$;Bmi1$^{fl/fl}$* mice 6 weeks post infection. **(C)** Fraction of tumor tissue per lung 12 weeks post infection. **(D)** Tumor areas 8 weeks post infection from *Bmi1$^{+/+}$* (4 mice, n=493) and *Bmi1$^{fl/fl}$* (5 mice, n=514) *p53$^{fl/fl}$* mice. **(E)** Tumor areas 12 weeks post infection from Bmi1$^{+/+}$ (4 mice, n=1029) and *Bmi1$^{fl/fl}$* (5 mice, n=382) *p53$^{fl/fl}$* mice. **(F)** Tumor burden over time from second infection. **(G)** Tumor areas 6 weeks post second infection from *Bmi1$^{+/+}$* (3 mice, n=151) and *Bmi1$^{fl/fl}$* (5 mice, n=110) *p53$^{fl/fl}$* mice. **(H)** Tumor areas 20 weeks post low titer infection from *Bmi1$^{+/+}$* (5 mice, n=216) and *Bmi1$^{fl/fl}$* (5 mice, n=141) *p53$^{fl/fl}$* mice.

tumors arising in *Kras*^{G12D};*p53*$^{fl/fl}$ lungs progress to advance disease more rapidly, display early onset nuclear atypia, proliferate more rapidly (Meylan et al. 2009; Feldser et al. 2010; Winslow et al. 2011; Dupage et al. 2009). We therefore infected mice to assess the number of initiating events after 6 weeks and did not observe a dramatic reduction in tumor number (Figure 2B). Next, we infected a cohort of mice and collected their lungs for histological examination 8 and 12 weeks after infection. By 12 weeks we observed a dramatic reduction of tumor burden in *Kras*^{G12D};*p53*$^{fl/fl}$ lungs in *Bmi1*$^{fl/fl}$ mice compared to *Bmi1*$^{+/+}$ mice, consistent with the hypothesis that their extended survival results from decreased tumor burden (Figure 2C). We analyzed the distribution of sizes of individual tumors from these mice at both 8 and 12 weeks after infection and observed a pronounced exaggeration over time of the tumor suppressive effects of Bmi1 loss. We noted a similar trend in *Kras*$^{G12D/+}$ mice (Figure 2D,E). Taken together, this argues that Bmi1 exerts its oncogenic effect largely through comparable mechanisms with or without p53.

Kinetics of BMI1 deficient tumor growth reveal a biphasic adaptive response.

Since Kras driven lung tumors display a time dependent response to loss of Bmi1, we set out to more closely examine the kinetics of tumor growth in *Bmi1*$^{fl/fl}$;*Kras*^{G12D};*p53*$^{fl/fl}$ mice. We chose to use the *Kras*^{G12D};*p53*$^{fl/fl}$ background due the consistency of the tumor onset in this model. We infected roughly 20 mice per genotype and collected mice at 4 stages of tumor development. Critically, the last time point, 16 weeks after infection, was when wild type animals began to succumb to disease at this viral titer in our survival analysis. Confirming our previous results, we observed a

sustained tumor suppressive window through 12 weeks as measured by overall tumor burden (Figure 2F). We also did not observe a significant difference in tumor initiation per mouse after 6 weeks, nor did we observe differences in the sizes of individual tumors (data not shown and Figure 2G). However, between 12 and 16 weeks after infection we noticed an exponential increase in the tumor burden in Bmi1 conditional mice, whereas Bmi1 competent lungs launch at an exponential rate. These data suggest an adaptive response by tumor bearing animals to the loss of Bmi1.

We next wanted to determine whether the bulk of *Bmi1*$^{fl/fl}$;*Kras*^{G12D};*p53*$^{fl/fl}$ tumors exhibited an adaptive response, or whether the exponential growth phase was driven by a small subset of tumors indifferent to Bmi1 status. Upon histological examination of *Bmi1*$^{fl/fl}$ lungs collected after 16 weeks, we detected very large and aggressive Bmi1 deficient tumors, though we were unable to accurately quantitate the distribution of tumors sizes owing to the inability to globally distinguish individual tumors. Therefore, we infected a new cohort of mice at a low viral titer and assessed tumor sizes after 20 weeks (Figure 2H). We observed that the bulk of Bmi1 conditional tumors remained significantly smaller in size. We attribute the plateauing of wild-type tumor burden at 16 weeks to be the result of steric hindrance of individual tumors, which begins prior to succumbing to disease (Figure 2F). This data suggests, then, that in a majority of tumors, the loss of Bmi1 remains tumor suppressive over and extended timeframe.

Bmi1 is a critical regulator of tumor progression to advanced disease

We next set out to identify how Bmi1 regulates the progression of individual tumors over time. Our first insight that this may be a critical function for Bmi1 in this model came after inspecting histological sections from $Kras^{G12D/+}$ mice 20 weeks after infection (Figure 3A). We noticed a striking absence of large advanced grade 3 lesions in $Bmi1^{fl/fl}$ lungs compared to $Bmi1^{+/+}$ lungs. We therefore quantified the spectrum of graded tumors at different times after infection. Indeed, $Bmi1^{fl/fl}$ mice display a reduced propensity to advance to higher grades (Figure 3B). This became more prominent over time and culminated in the absence of Bmi1 deficient grade 3 tumors after 20 weeks. By comparison, grade 3 adenocarcinomas represented an average of 12% of tumors in $Bmi1^{+/+}$ mice. We did see a single grade 3 lesion in $Bmi1^{fl/fl}$ lungs, but found that this represented a rare escaper that still expressed BMI1, highlighting a prominent role of Bmi1 in this grade transition (Figure 3D,E). This led us to assess whether Bmi1 is required for the progression to grade 3 adenocarcinomas. Grade 3 tumors develop more frequently in $Kras^{G12D};p53^{fl/fl}$ mice, so we graded $Bmi1^{fl/fl}$ and $Bmi1^{+/+}$ tumors in this background at 8 and 12 weeks after infection (Figure 3F,G). In this model, we observed $Bmi1^{fl/fl}$ grade 3 tumors with documented loss of BMI1 protein, but these occurred at much lower frequency at both time points. Therefore, Bmi1 is not absolutely required for progression to advanced disease, but it does dramatically impact the propensity of tumors to make this transition.

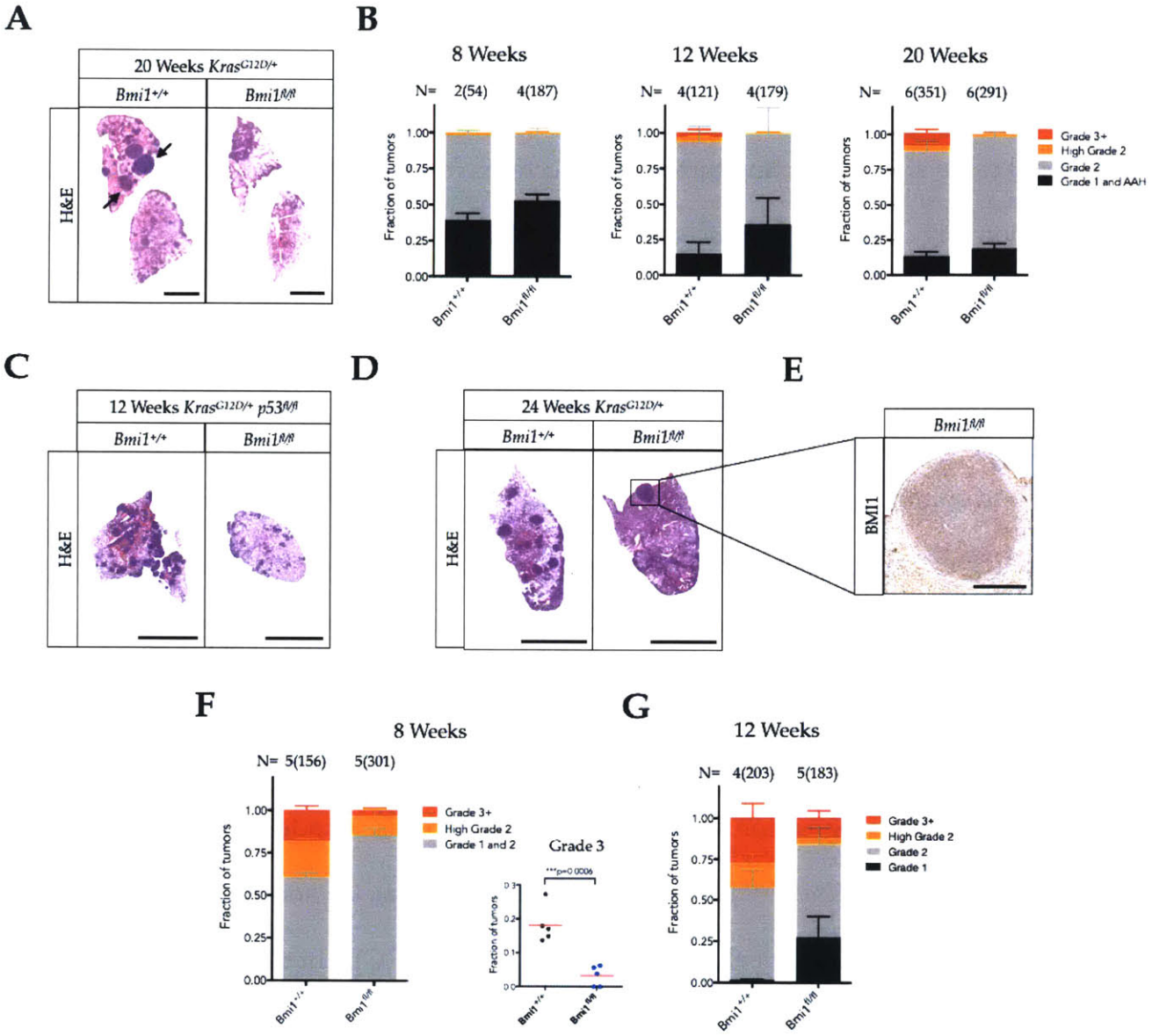

Figure 3. Bmi1 promotes lung adenoma progression to advanced disease
(A) H&E stain of representative lobes from *Kras*$^{G12D/+}$;*Bmi1*$^{+/+}$ or *Kras*$^{G12D/+}$;*Bmi1*$^{fl/fl}$ mice 20 weeks post infection. *Bmi1*$^{+/+}$ lungs have large advanced tumors as indicated. **(B)** Fraction of tumors by grade from *Kras*$^{G12D/+}$ mice at specified weeks after infection. **(C)** H&E stain of representative lobes from *Kras*$^{G12D/+}$;*p53*$^{fl/fl}$;*Bmi1*$^{+/+}$ or *Kras*$^{G12D/+}$;*p53*$^{fl/fl}$;*Bmi1*$^{fl/fl}$ mice 12 weeks post infection. Bar = 4mm **(D)** Representative lung 24 weeks *Kras*$^{G12D/+}$. Bar = 5mm **(E)** IHC for Bmi1 in 24 week *Kras*$^{G12D/+}$;*Bmi1*$^{fl/fl}$ tumor that retained Bmi1 expression. Bar = 600 μm **(F)** Fraction of tumors by grade from *Kras*$^{G12D/+}$;*p53*$^{fl/fl}$ mice after 8 weeks. Inset: Fraction grade 3 tumors per mouse. **(G)** Fraction of tumors by grade from *Kras*$^{G12D/+}$;*p53*$^{fl/fl}$ mice after 12 weeks.
For grading: N reflects number of mice and tumor number per group.

BMI1 contributes to the development of papillary-like lung adenocarcinoma.

While examining individual tumors by grade, we noticed that Bmi1 conditional lungs were depleted of a common histological subtype: papillary-like adenocarcinomas. Whereas cells in papillary-like lesions appear to line up in cuboidal elongated patterns, solid-like tumors - the other major subtype in this model - are largely comprised of polygonal cells forming unorganized scaly sheets (Figure 4A) (Travis et al. 2015). After scoring lung tumors for papillary-like characteristics, we observed a sharp reduction of this subtype in $Bmi1^{fl/fl};Kras^{G12D/+}$ mice at 20 weeks compared to $Bmi1^{+/+};Kras^{G12D/+}$ controls (Figure 4B). Furthermore, the only papillary-like tumors we observed in these mice retained Bmi1 expression. We then assessed the frequency of papillary-like tumors in $Bmi1^{fl/fl}$ and $Bmi1^{+/+}$ mice in $Kras^{G12D};p53^{fl/fl}$ backgrounds 12 weeks after initiation and also found a reduction in the frequency of papillary-like tumors in $Bmi1^{fl/fl}$ mice (Figure 4C). We confirmed that the papillary-like tumors that arose in these mice did not express BMI1, suggesting that Bmi1 is not critically required for their emergence.

Previous studies have implicated a differential propensity of various tumor cells of origin in the lung to give rise to papillary tumors (Kim et al. 2005; Mainardi et al. 2014; Xu et al. 2014; Sutherland et al. 2014). It has been argued that club cells are largely responsible for the initiation of the subtype in this model, while Alveolar Type II (ATII) cells initiate solid tumors (Sutherland et al. 2014). Tumors that arise after viral infection of an SPC promoter driven Cre-recombinase are thought to develop mostly from ATII cells. Therefore, we infected $Kras^{G12D};p53^{fl/fl}$ mice with adenovirus packaging SPC-Cre and assessed the distribution of papillary-like tumors in $Bmi1^{+/+}$, $Bmi1^{fl/+}$, and $Bmi1^{fl/fl}$ mice 12 weeks after infection (Figure 4D). Although we were only able to score one

SPC-Cre infected *Bmi1*$^{fl/fl}$ mouse, we saw a reduction in the frequency of advanced lesions in the absence of Bmi1, consistent with previous results. However, when we assessed the fraction of grade 3 tumors that were papillary-like, we found them to be comparable across genotypes (Figure 4D). Moreover, the fraction of papillary-like tumors in grade 3 adenocarcinomas was comparable in *Bmi1*$^{fl/fl}$ and *Bmi1*$^{+/+}$ *Kras*^{G12D};*p53*$^{fl/fl}$ mice 12 weeks after being initiated by a constitutive Lenti-Cre (Figure 4E). Indeed, all infections from both SPC-Cre and Lenti-Cre cohorts resulted in a similar percentage of papillary-like tumors in grade 3 lesions 12 weeks after tumor initiation in *Kras*^{G12D};*p53*$^{fl/fl}$ mice. This argues that tumor cell of origin may not influence the appearance of papillary-like tumors in this model. It also provides further evidence that Bmi1 is not differentially required by tumor initiating cell populations for the development of papillary-like adenocarcinomas.

Papillary-like tumors arise during progression to advanced disease.

These data suggest that papillary-like tumors arise as a consequence of tumor progression in lungs that are wild-type for Bmi1. We therefore decided to interrogate this more closely in our model of Kras driven lung cancer independent of Bmi1. Twenty weeks after viral infection, we observed a sharp increase in the frequency of papillary-like tumors in higher grade lesions from *Kras*$^{G12D/+}$ mice (Figure 4F). Furthermore, as grade 2 adenomas increase in size, the incidence of papillary-like features increases, hinting at an enrichment in this subtype during progression (Figure 4G). Since this phenotype appears to exist along a spectrum, we characterized individual tumors on a papillary-like scale from solid to very papillary (P3) with the assistance of a veterinary

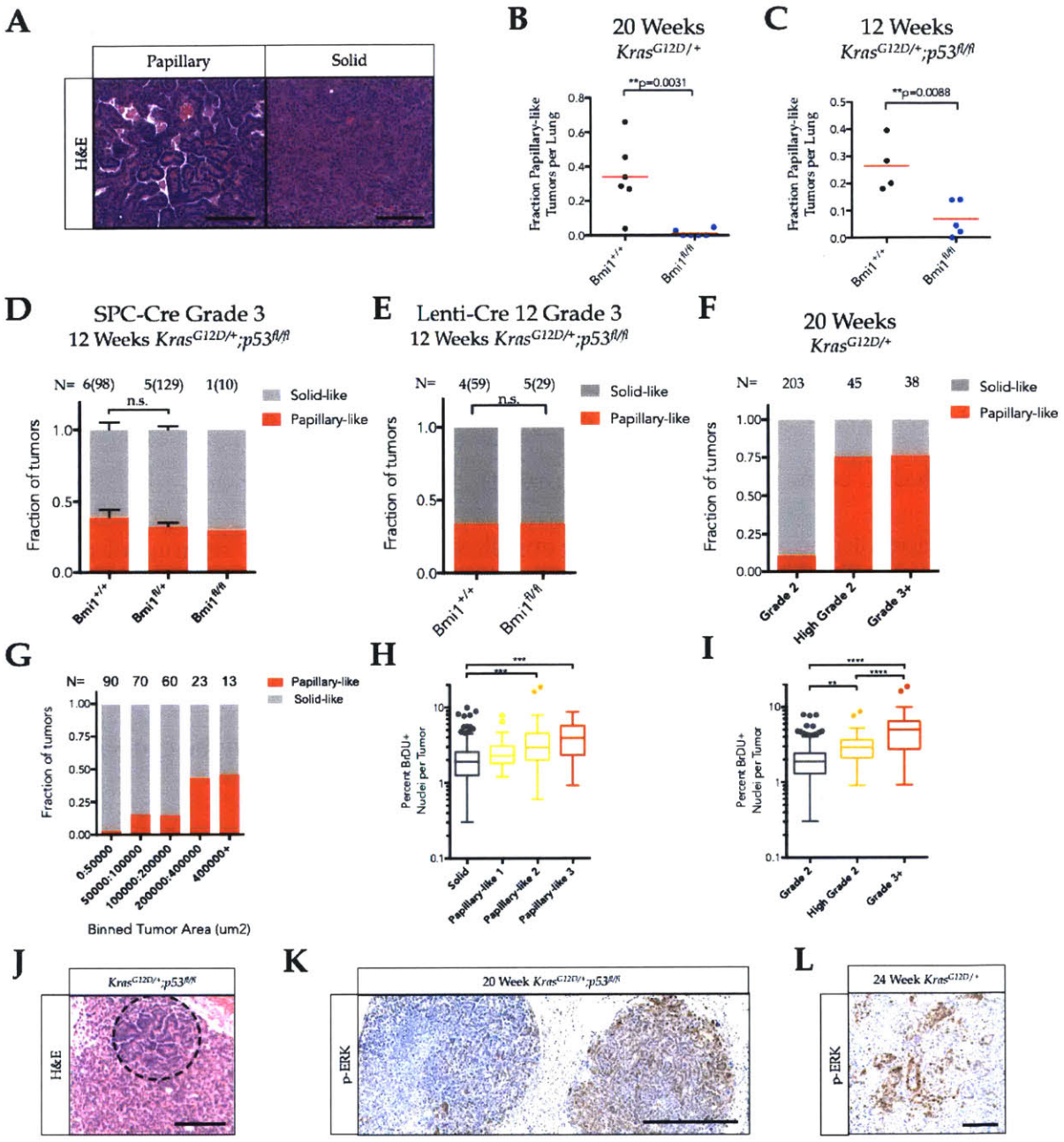

Figure 4. Bmi1 contributes to papillary-like adenocarcinomas by sustaining tumor progression
(A) Representative images of very papillary-like and solid-like tumors. **(B)** Fraction of papillary-like tumors per lung at 20 weeks. **(C)** Fraction of papillary-like tumors per lung at 12 weeks. **(D)** Fraction of grade 3 papillary-like or solid-like tumors per lung in 12 weeks after SPC-Cre infection. **(E)** Fraction of total grade 3 papillary-like or solid-like lesions 12 weeks after Lenti-Cre infection. **(F)** Fraction of total papillary-like and solid-like lesions binned by grade. **(G)** Fraction of papillary-like or solid-like grade 2 adenomas binned by size from 20 week $Kras^{G12D/+}$ mice. **(H)** Percent BrDU positive nuclei per tumor by IHC from 20 week $Kras^{G12D/+}$ mice binned by papillary features. **(I)** Percent BrDU positive nuclei per tumor determined by IHC from 6 20 week $Kras^{G12D/+}$ mice binned by grade.**(J)** Representative image of a mixed tumor. The more advanced papillary-like area is circled. **(K)** Representative p-ERK IHC from 20 week $Kras^{G12D/+};p53^{fl/fl}$ lungs. Bar =4000um **(L)** Representative image of p-ERK IHC of a mixed 24 week $Kras^{G12D/+}$ tumor. Bar=100um.
P value determined by t test or one-way ANOVA (**p<0.01, ****p<0.0001).

pathologist. P3 tumors displayed highly developed papillary structures with fibro-vascular cores. Intermediate types are characterized by the extent to which they display papillary architecture. Based on these categories, we determined the proliferative index of individual tumors by BrdU incorporation and found that highly papillary features correlate with high proliferative index (Figure 4H). Importantly, we also found that increased proliferative index is a key marker of progression to advanced disease (Figure 4I). Also, in tumors with mixed solid and papillary morphologies, the papillary-like regions tended to be more advanced (Figure 4J). Interestingly, immuno-histochemical (IHC) detection of phophorylated ERK is enriched in papillary-like regions of mixed tumors (Figure 4K,L). Together, these data reinforce the hypothesis that papillary-like tumors are a consequence of progression and not initiation in this model of lung adenocarcinoma. Furthermore, deregulation of Mapk signaling may be crucial for the emergence of this subtype.

Bmi1 is a critical regulator of proliferation in grade 2 lung adenomas

A hallmark of adenoma progression to advanced adenocarcinoma is the increased rate of tumor cell proliferation. It remains unclear to what extent accelerated proliferation drives progression as opposed to being the result of acquired pro-tumorigenic changes. Since we previously observed that $Bmi1^{fl/fl};Kras^{G12D/+}$ mice with our without $p53^{fl/fl}$ presented with smaller lung tumors compared to $Bmi1^{+/+}$ controls, we set out to determine whether this was due to a decreased rate of tumor proliferation. Indeed, lesions from $Bmi1^{fl/fl};Kras^{G12D/+}$ lungs 20 and 24 weeks after infection maintained a reduced capacity to proliferate compared with $Bmi1^{+/+};Kras^{G12D/+}$ lungs (Figure 5A,B).

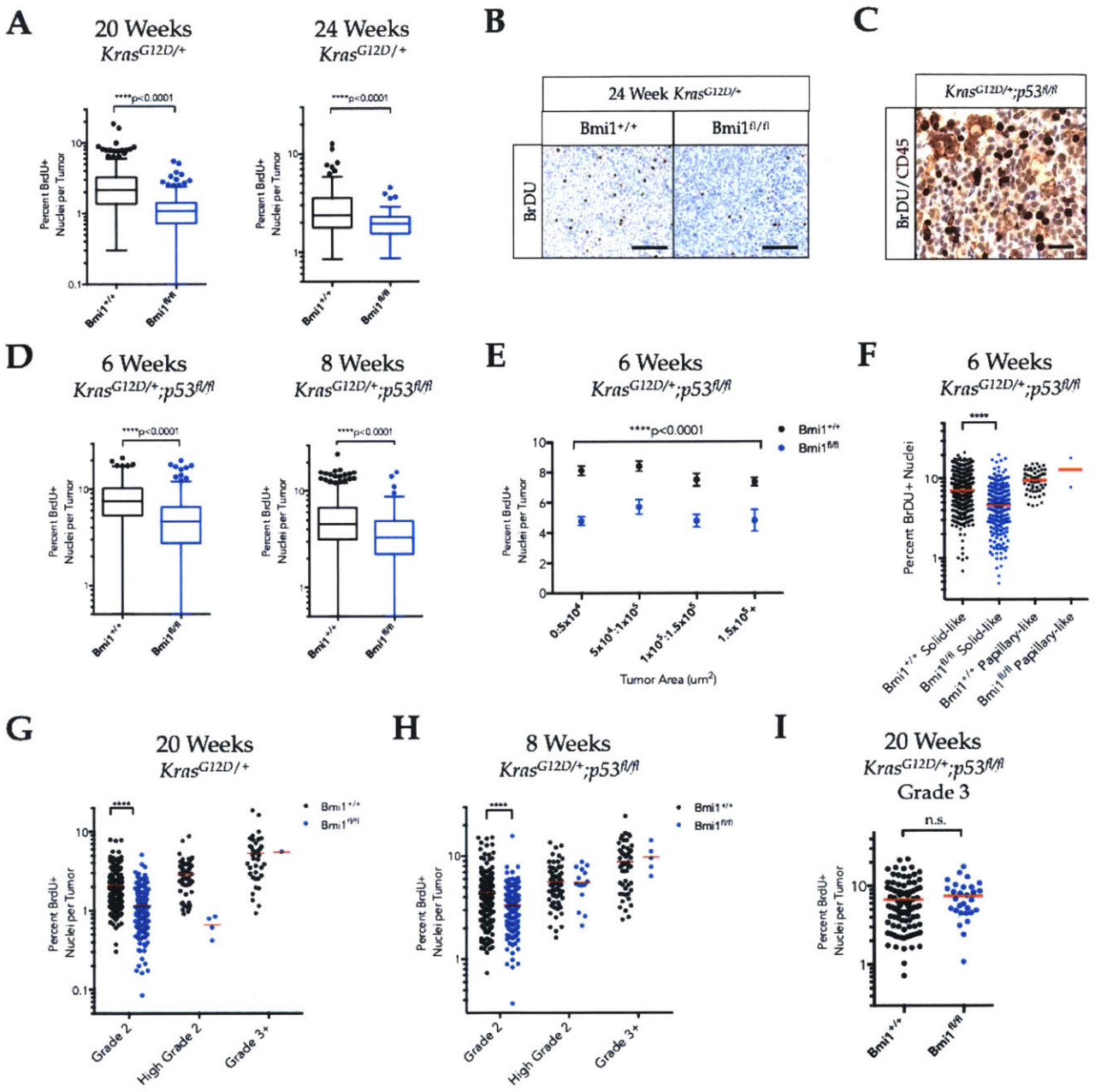

Figure 5. Bmi1 regulates the proliferation of grade 2 lung adenomas

(A) Percent BrdU positive nuclei per tumor (%BrdU) by IHC from 20 and 24 week $Kras^{G12D/+}$ mice. **(B)** Representative images of BrdU IHC. Bar = 100um. **(C)** Representative image of dual IHC for BrdU and CD45 on a tumor section. Very few immune cells display nuclear BrdU. **(D)** %BrdU of $Kras^{G12D/+};p53^{fl/fl}$ mice 6 and 8 week after infection. **(E)** Average %BrdU of 6 week $Bmi1^{+/+}$ and $Bmi1^{fl/fl}$ $Kras^{G12D/+};p53^{fl/fl}$ tumors binned by tumor area. **(F)** %BrdU of 6 week $Kras^{G12D/+};p53^{fl/fl}$ tumors binned by papillary-like and solid-like features. **(G)** %BrdU of 20 week $Kras^{G12D/+}$ tumors separated by grade. **(H)** %BrdU of 8 week $Kras^{G12D/+};p53^{fl/fl}$ tumors separated by grade. **(I)** %BrdU of grade 3 adenocarcinomas from $Kras^{G12D/+};p53^{fl/fl}$ 20 weeks after infection.

****p<0.0001.

We confirmed that immune infiltration was not biasing our BrdU scoring by co-detecting BrdU and CD45, a pan immune marker, by immuno-histochemistry (Figure 5C). We also observed a decrease in the proliferative capacity of $Bmi1^{fl/fl}$ tumors in the context of p53 deficiency at 6 and 8 weeks after initiation (Figure 5D). This affect was independent of tumor size after 6 weeks, indicating that Bmi1 is an important regulator of tumor proliferation at at early stages post initiation (Figure 5E). Furthermore, when we segregate lesions by histological subtype, we see that as an aggregate, Bmi1 deficient solid-like tumors do not proliferate as well as controls (Figure 5F). Lastly, we wanted to determine the impact of Bmi1 loss on proliferation by grade in both $Kras^{G12D/+}$ and $Kras^{G12D/+};p53^{fl/fl}$ backgrounds. Bmi1 deficient grade 2 $Kras^{G12D/+}$ lesions retained a proliferative disadvantage compared with controls (Figure 5G). We observed a similar trend in $Kras^{G12D/+};p53^{fl/fl}$ mice (Figure 5H). This supports a model whereby Bmi1 is required to sustain the proliferation of early lesions to affect progression.

BMI1 deficient tumors may adapt in order to progress to high grade.

When we separated $Kras^{G12D/+};p53^{fl/fl}$ lung tumors by genotype and grade we noticed that higher grade tumors proliferated at similar rates regardless of Bmi1 status (Figure 5H). This led us to speculate that a rare subset of tumors may adapt to Bmi1 loss to progress to adenocarcinoma. Since there were few $Bmi1^{fl/fl}$ grade 3 tumors 8 weeks after infection, we determined the proliferative index of $Bmi1^{fl/fl}$ grade 3 tumors 20 weeks post infection (Figure 5H). This shows that once Bmi1 deficient tumors advanced to high grade adenocarcinomas, they proliferate as well as Bmi1 proficient controls. Bmi1 is only required by grade 2 adenomas to maintain a high proliferative

index. We then tested whether Bmi1 deficient adenocarcinomas expressed known markers of tumor progression 16 weeks after infecting $Kras^{G12D/+};p53^{fl/fl}$ mice. Hmga2 is an embryonal marker that correlates with a dedifferentiated, highly advanced disease and has been associated with the metastatic cascade in this model (Fusco and Fedele 2007; Winslow et al. 2011). Surprisingly, we observed a striking increase in tumors with high HMGA2 positivity in $Bmi1^{fl/fl}$ lungs compared to $Bmi1^{+/+}$ controls (Figure 6A,B,C). We also observed a significant increase in the percent HMGA2 positive nuclei per tumor in $Bmi1^{fl/fl}$ lungs compared to $Bmi1^{+/+}$ litter-mates, which is largely driven by a smaller set of tumors with very high HMGA2 positivity (Figure 6C). When we stained $Kras^{G12D/+};p53^{fl/fl}$ lungs 12 weeks after initiation, we were unable to detect HMGA2 positive tumors in $Bmi1^{+/+}$. However, we detected rare small lesions that expressed Hmga2 in 3 out of 4 $Bmi1^{fl/fl}$ lungs 12 weeks after infection (Figure 6C). Hmga2 expression, then, is a specific adaptive response to Bmi1 loss in a subset of lung adenocarcinomas.

We next wanted to determine the extent that Hmga2 expressing $Bmi1^{fl/fl}$ lung adenocarcinomas activate other markers of tumor progression and differentiation programs. First we decided to assesses the expression of Nkx2.1 in these mice. Nkx2.1 is a lung specific transcription factor widely expressed in early lesions, and may act as a tumor suppressor by restraining latent progenitor and embryonal networks critical involved in progression (Snyder et al. 2013). HMGA2 positive $Bmi1^{+/+}$ adenocarcinomas typically lose NKX2.1 staining. To our surprise, we observed robust NKX2.1 staining in all the HMGA2 positive $Bmi1^{fl/fl}$ lesions (Figure 6E). We did not detect any expression of Cdx2, a marker of progression indicative of a latent gastric program, in Bmi1 deficient tumors even though we can detect this in tumors from $Bmi1^{+/+}$ mice. Therefore, we

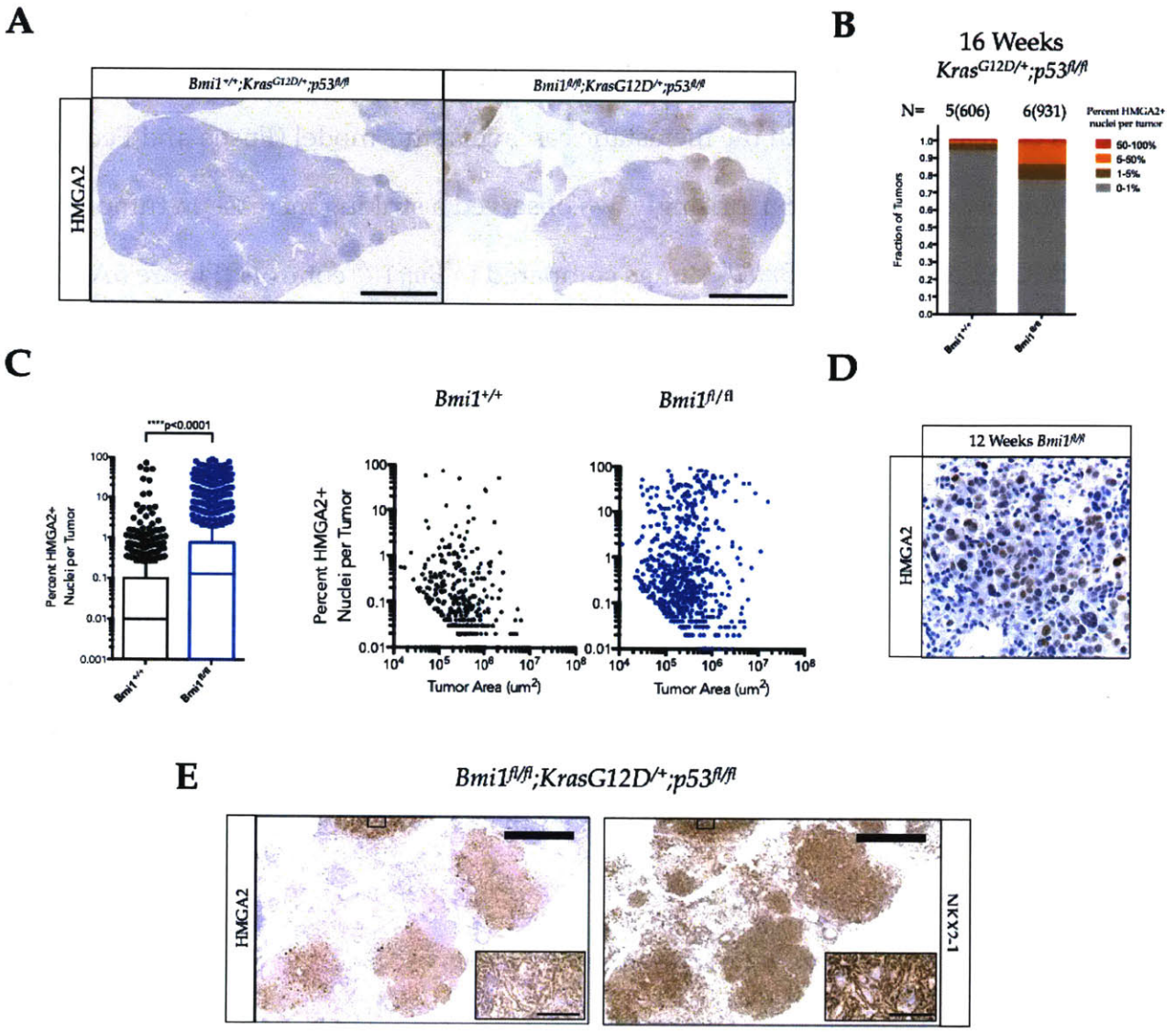

Figure 6. Loss of Bmi1 results in atypical Hmga2 expression during tumor progression
(A) Representative IHC for HMGA2 in lungs 16 weeks after infection. Bar = 3mm. **(B)** Fraction of tumors binned by percent of nuclei staining positive for HMGA2. N represents mice and total tumor number. **(C)** Percent positive HMGA2 nuclei per tumor 16 weeks after infection of *Kras*$^{G12D/+}$;*p53*$^{fl/fl}$ mice. Graphs on the right plot tumor sizes with HMGA2 positivity. These exclude 286 and 264 tumors from *Bmi1*$^{+/+}$ and *Bmi1*$^{fl/fl}$, respectively, due to the absence of HMGA2+ nuclei. **(D)** A tumor staining positive for HMGA2 in a *Bmi1*$^{fl/fl}$;*Kras*$^{G12D/+}$;*p53*$^{fl/fl}$ animal 12 weeks after tumor initiation. **(E)** Representative images from HMGA2 and NKX2.1 IHC from lung adjacent sections. Bars = 900um or 200um.

conclude that advanced lung adenocarcinomas compensate for Bmi1 loss by altering the state of differentiation during tumor progression.

BMI1 does not sustain the repression of classic cell cycle regulators.

BMI1 has been implicated as an oncogene in several tumor types in part by restraining the activity of cell cycle inhibitors (Park et al. 2004). When we began our investigation of the potential roles for Bmi1 in lung adenocarcinoma, we hypothesized that Bmi1 might similarly enforce the sustained repression of these factors. We

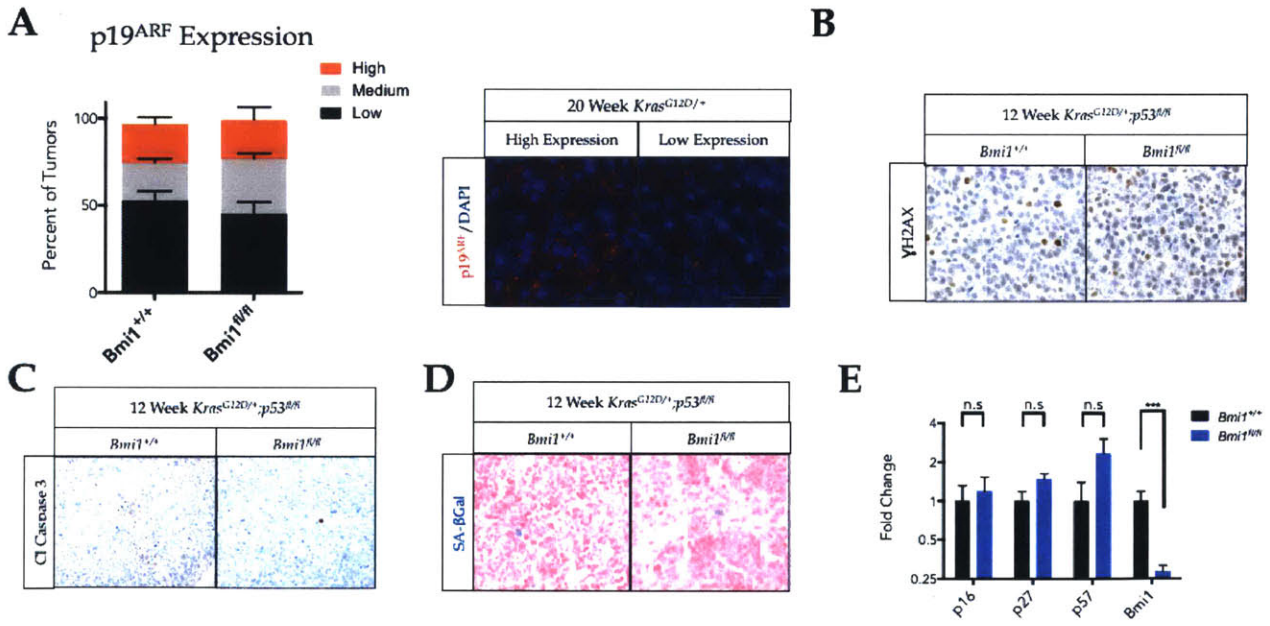

Figure 7. Bmi1 is not required in lung adenocarcinomas to suppress apoptosis or senescence
(A) Percent tumors binned by p19^{ARF} expression 20 weeks after infecting *Kras*$^{G12D/+}$ mice as detected by immune-fluorescence; and representative images. Bar = 38μm. **(B)** Representative images from γH2AX IHC. **(C)** Representative images from cleaved caspase 3 IHC. **(D)** Representative images from histochemical detection of Senescence Associated β-Galactosdase. **(E)** R qRT-PCR detection of cell cycle transcripts from 6-8 grade 2 *Kras*$^{G12D/+}$;*p53*$^{fl/fl}$ adenomas. ***p<0.001.

therefore interrogated whether Bmi1 loss deregulated these tumor suppressors in lung adenomas. Kras driven lung tumors frequently express $p19^{ARF}$ (Young and Jacks 2010). Immunofluorescent detection in $Kras^{G12D/+}$ lung sections did not reveal a shift in the spectrum of $p19^{ARF}$ expression in $Bmi1^{fl/fl}$ adenomas compared to $Bmi1^{+/+}$ controls (Figure 7A). Furthermore, we did not observe noticeable differences in the expression of p21 by immuno-histochemistry between genotypes (data not shown). Markers of DNA damage, apoptosis, senescence and were similarly unchanged following loss of Bmi1 (Figure 7B,C,D). Finally, we isolated RNA from grade 2 tumors isolated from $Bmi1^{fl/fl}$ and $Bmi1^{+/+}$ mice and found no significant differences in $p16^{INK4A}$, p27, or p57 transcript levels (Figure 7E). These data indicate that Bmi1 does not sustain lung adenoma proliferation and progression by directly repressing known cell cycle or apoptotic inhibitors.

High-Throughput Digital Gene Expression sequencing provides a robust methodology for extracting biological meaning from heterogenous tumors.

Collectively, our data show that Bmi1 promotes tumor proliferation and progression independent of canonical Bmi1 targets. In an effort to gain insight into the mechanisms by which Bmi1 regulates tumorigenesis, we isolated and graded 48 tumors for high throughput transcriptional analysis using a Digital Gene Expression (HT-DGE) strategy (Figure 8A) (Soumillon et al. 2014). In total, we sequenced 24 $Bmi1^{fl/fl}$ and 24 $Bmi1^{+/+}$ tumors split equally between grade 2 and grade 3 from $Kras^{G12D/+};p53^{fl/fl}$ mice. We confirmed loss of BMI1 by immuno-histochemistry for all but one $Bmi1^{fl/fl}$ tumor that retained partial expression, and screened for tumors with minimal immune and tissue contamination. HT-DGE enriches for mature transcripts, negates amplification biases,

and captures unique transcripts with high fidelity. Anticipating inter-tumoral heterogeneity, we chose this strategy for transcriptomic analysis in order to prioritize replicate power over sequencing depth. Briefly, we added unique molecular identifiers

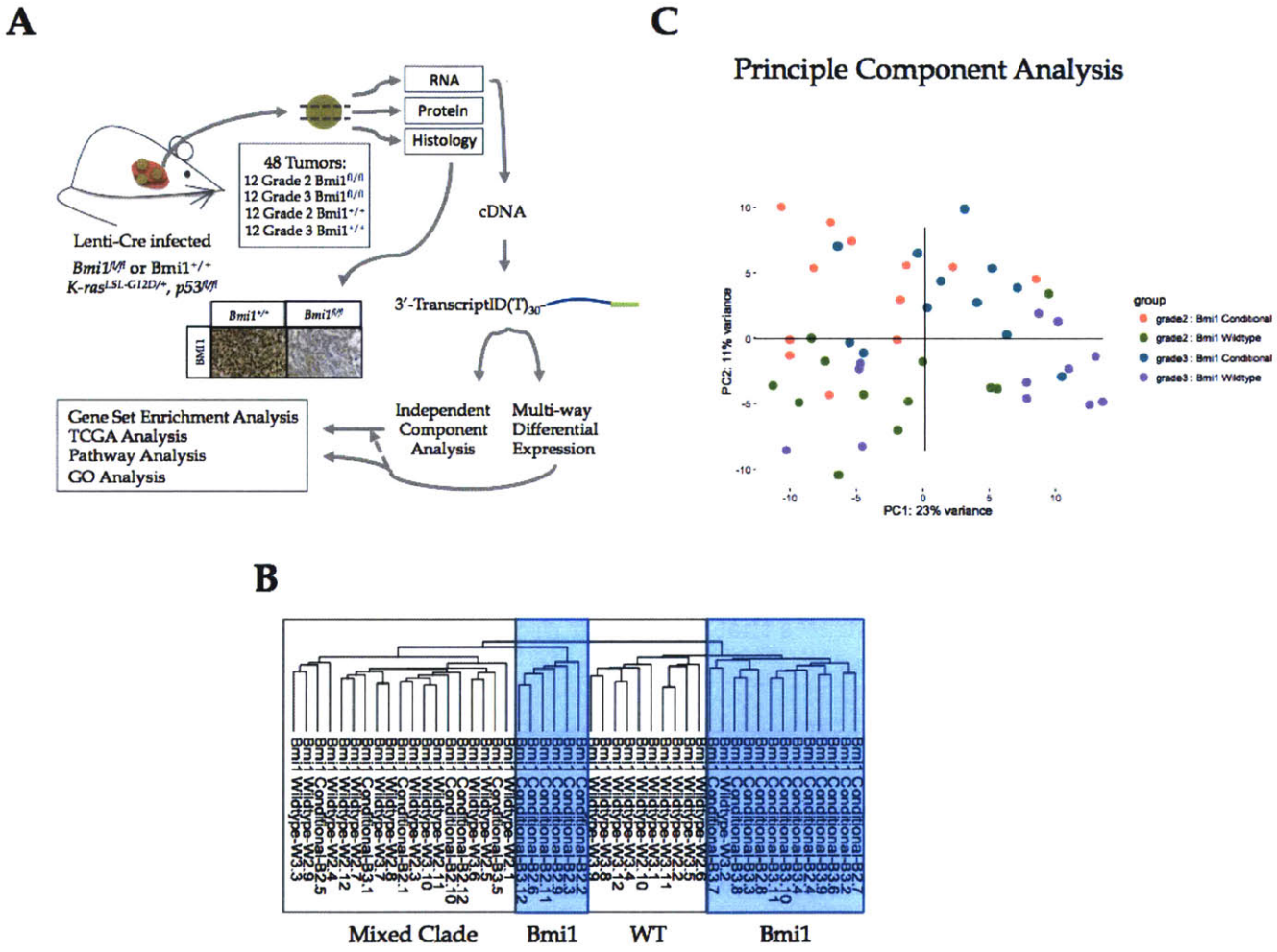

Figure 8. Identification of Grade and Bmi1 gene signatures from heterogenous lung tumors **(A)** Scheme illustrating our Bmi1 signature generation and downstream applications. Briefly, individual tumors were bi- or trisected for RNA, paraffin embedding, or protein extraction. Histological examination confirmed grade and BMI1 status of all tumors. cDNA was generated from RNA and enriched for 3' fragments for sequencing. Single transcripts were counted and sent for downstream computational analyses. Multi-way Differential Expression (DE) analysis **(B)** Unbiased clustering of samples by euclidean distance. **(C)** Principle component analysis from differential expression analysis identified a primary axes corresponding to grade and Bmi1 status.

to each transcript, barcoded by sample, and transposase tagged the cDNA. Subsequent poly-A capture effectively limited transcriptome sequencing space and enriched for 3' sequencing reads. We used stringent criteria for calling uniquely mapped transcripts and recovered reads from roughly 60% of annotated genome features, regardless of initial read number per sample (data not shown). As expected, inter-tumoral heterogeneity was a predominant factor when we clustered samples in an unbiased dendogram (Figure 8B). Nevertheless, most major clades represent biologically meaningful groups, largely distinguishing tumors by grade or genotype. Principle component analysis also identified axes that separated tumors based on these features (Figure 8C). Together, this strategy provided us with confidence that we sequenced with sufficient depth and replicate power to extract biologically meaningful data from our heterogenous population of tumors.

RNA profiling demonstrates that the tumor progression in the mouse reflects human grade transitions

In order to capture the major molecular determinants underlying our dataset, we performed unbiased Independent Component Analysis to extract the statistically independent gene expression signatures from all 48 samples (Figure 9A) (Rutledge and Jouan-Rimbaud Bouveresse 2013). Reassuringly, the first two predominant components significantly represented tumor grade and Bmi1 status, respectively (Figure 9A). We then generated an ICA Grade Signature reflecting higher grade tumors, based on genes most significantly determining ICA component 1 (Figure 9B). We then employed pathway analysis to reveal potential upstream regulators of this grade transition and identified well characterized pathways previously implicated in mouse models of lung

adenocarcinoma progression - Hnf1a/4a, Foxa2/1 (Figure 9C) (Snyder et al. 2013; Sugano et al. 2013). Indeed, we also find a strong enrichment of liver specific genes that are driven by these transcription factors using Gene Set Enrichment Analysis (GSEA)

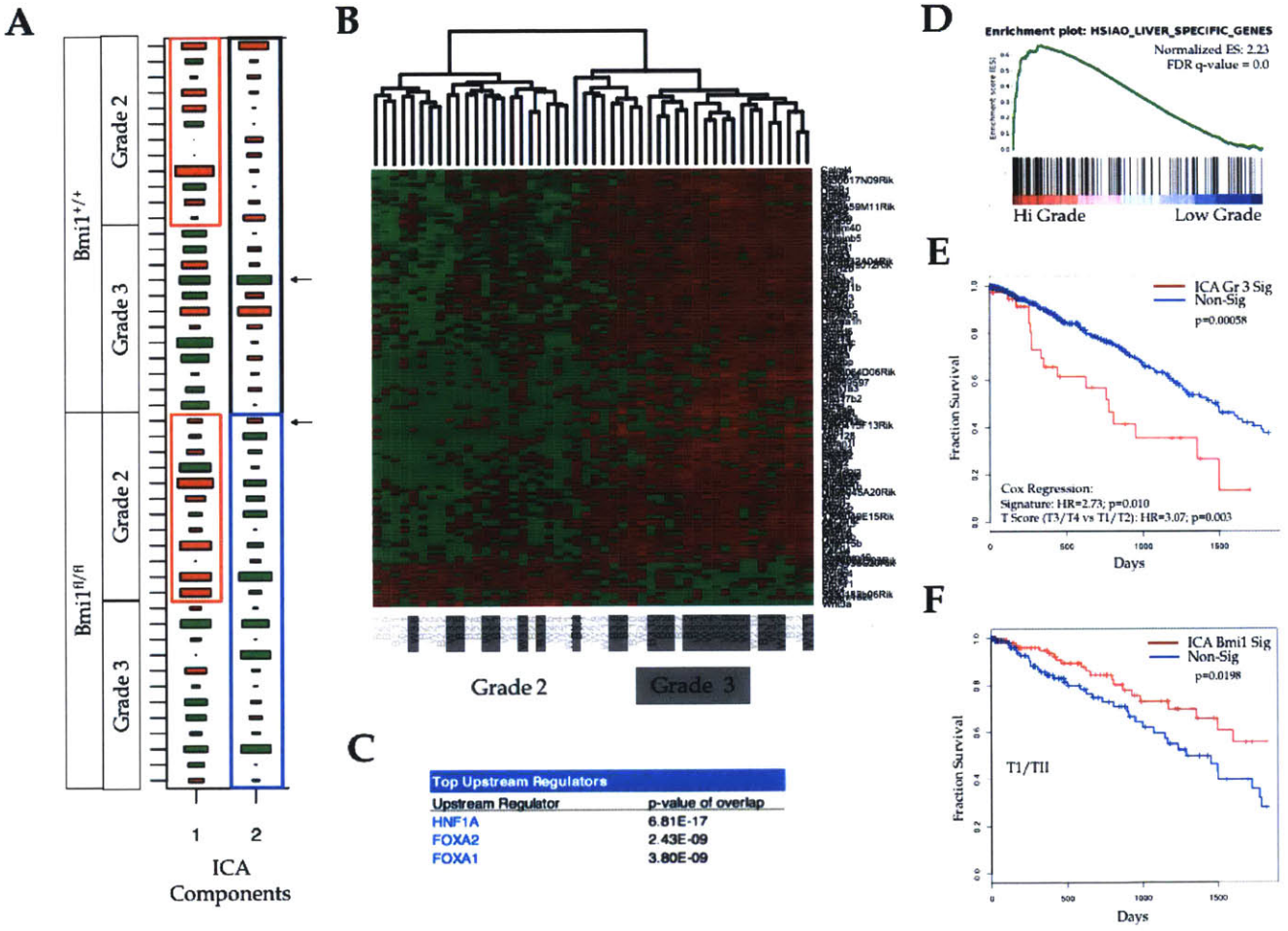

Figure 9. Lung tumor grade transitions in mice correspond with grade changes in the human disease **(A)** The first two component axes generated from unbiased Independent Component Analysis correspond with grade and Bmi1 status. Arrows identify a *Bmi1*$^{+/+}$ tumor with little Bmi1 expression; and a *Bmi1*$^{fl/fl}$ tumor that retained Bmi1 expression. **(B)** Heatmap developed from the grade gene signature. Samples highlighted in: Dark Grey = Grade 3; Light Grey = Grade 2. **(C)** Top upstream regulators enriched in grade 3 tumors as identified by Independent Pathway Analysis from the grade signature. **(D)** Gene Set Enrichment Analysis on grade signature identified an enrichment in liver specific genes in advanced grade lesions. **(E)** Decreased overall survival of TCGA patients whose tumor transcriptomes best correlates with the grade signature. Top 10% correlations vs all remaining tumors. **(F)** Improved overall survival of TCGA patients with T1/TII grade tumors correlating with the ICA Bmi1 deficiency signature.

(Figure 9D) (Wederell et al. 2008; Subramanian et al. 2005; Mootha et al. 2003). To determine whether this grade signature corresponds to human grade transitions, we ranked 457 lung adenocarcinoma transcriptomes from the Tumor Cancer Genome Atlas (TCGA) network according to their correlation with the ICA Grade Signature. The odds of having a low grade T1 tumor is 1.8x higher in human patients not correlated with our high grade ICA signature compared to the top 10% that do (p=0.054). Furthermore, the interaction between the ICA Grade signature and human tumor grade covariates is borderline significant (p=0.061, Wald test). Importantly, this signature was prognostic for patient survival, even after adjusting for covariants (Figure 9E). Together, this analysis confirms that we can extract biologically meaningful data from HT-DGE based on isolated mouse lung tumors. More importantly, it establishes that the mouse adenoma (grade 2) to adenocarcinoma (grade 3) transition reflects grade differences in the human disease.

Transcriptomic analysis identifies a cell cycle role for Bmi1 in grade 2 adenomas

Next we focused our transcriptomic analysis toward identifying potential tumor suppressive mechanisms resulting from loss of Bmi1. Our unbiased ICA component 2 significantly binned tumors by Bmi1 status (Figure 9A). We developed an ICA Bmi1 deficiency gene signature based on this component that largely distinguishes tumors by genotype (Figure 10A). Of note, this gene signature clusters all Bmi1 deficient grade 2 *Bmi1*$^{fl/fl}$ tumors, except one, away from *Bmi1*$^{+/+}$ tumors. It further clustered one *Bmi1*$^{+/+}$ tumor with low Bmi1 expression with *Bmi1*$^{fl/fl}$ lesions. Interestingly, the signature does not robustly segregate grade 3 *Bmi1*$^{fl/fl}$ adenocarcinomas, indicating that the signature is

driven largely by grade 2 *Bmi1*$^{fl/fl}$ transcriptomes. We next wanted to determine whether ICA Bmi1 deficiency signature, reflects a survival benefit in human patients. To do this we ranked TCGA tumor transcriptomes according to our signature. Since Bmi1 loss strongly impacts the progression of adenomas, we narrowed our analysis to early grade human tumors. We find that the ICA Bmi1 deficiency signature predicts improved outcome (Figure 9F). Together, our transcriptomic analysis indicates that a critical molecular analysis of our mouse tumors reflects human tumor biology and that interrogating roles for Bmi1 in our model is applicable for human disease.

Next, we ran GSEA on the ICA Bmi1 deficiency component and observed a striking enrichment for transcripts associated with the G2/M phase of the cell cycle (Figure 10B). These transcripts also intersect with E2F1 targets (data not shown). Since our previous data identified a proliferative disadvantage in grade 2 *Bmi1*$^{fl/fl}$ adenomas, we suspect that this result is indicative of cell cycle delays rather than an increased number of proliferating cells. We used differential expression analysis comparing grade 2 *Bmi1*$^{fl/fl}$ and *Bmi1*$^{+/+}$ tumors to confirm that this result is specific for grade 2 lesions (Figure 10B and data not shown) (Love et al. 2014). Notably, loss of Bmi1 did not derepress canonical Bmi1 target cell cycle inhibitors in these tumors, although we observed a modest but significant increase in p57 transcript levels (Figure 10D). Together, these data argue that loss of Bmi1 in adenomagenesis is tumor suppressive in part by impacting the cell cycle.

If loss of Bmi1 delays or arrests cycling cells, we would expect that cell cycle transcripts decouple from the proliferative index of tumors as measured by BrdU incorporation during DNA replication. Therefore, we stained *Bmi1*$^{fl/fl}$ and *Bmi1*$^{+/+}$

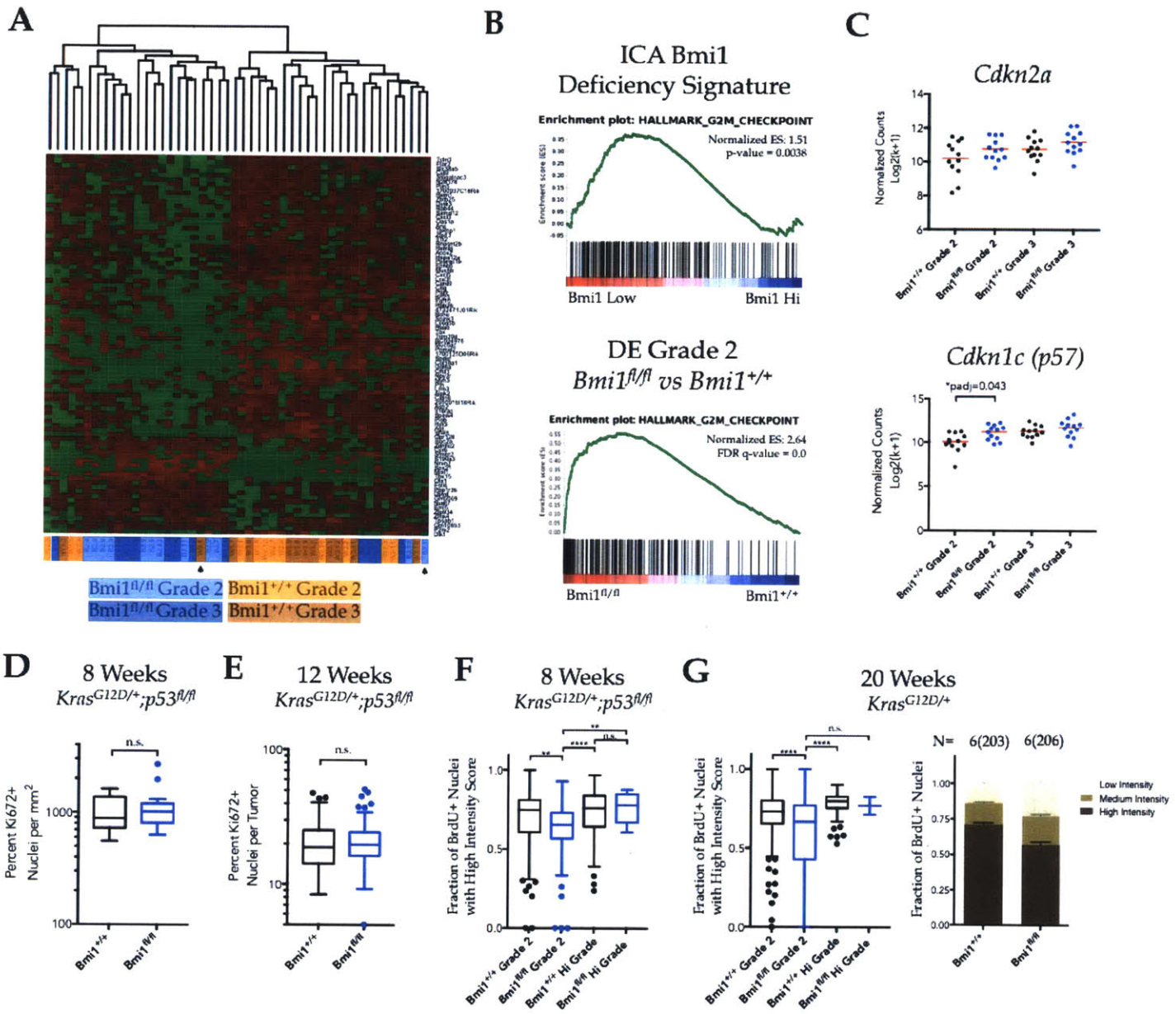

Figure 10. Bmi1 loss affects progression through the cell cycle
(A) Heatmap developed from the ICA Bmi1 deficiency gene signature. **(B)** Gene Set Enrichment Analysis on genes ranked by ICA Bmi1 deficiency signature or fold change comparing grade 2 *Bmi1*$^{fl/fl}$ and *Bmi1*$^{+/+}$ for differential expression using DESeq2. **(C)** Log2 transformed IQR 20 normalized counts from HT-DGEseq. padj reflects BH FDR correction. **(D)** Percent Ki67 positive cells per mm^2 in grade 2 adenomas as detected by IHC. **(E)** Percent Ki67 positive cells per tumor by IHC. **(F,G)** Fraction of BrdU positive nuclei binned as high intensity. p=values represent one-way ANOVA. ****p<0.0001, **p<0.01. N represents number of mice and tumors analyzed.

Kras$^{G12D/+}$;*p53*$^{fl/fl}$ lungs 8 weeks after initiation for the cell cycle marker KI67 and found comparable levels of KI67 positive cells between genotypes (Figure 10D). Critically, we previously showed that *Bmi1*$^{fl/fl}$ grade 2 tumors in these lungs had lower proliferative indices than *Bmi1*$^{+/+}$ controls (Figure 5H). We also detected Ki67 in all lung tumors 12 weeks after initiation and observed a slight increase in Bmi1 deficient tumors overall (Figure 10E). Together, this indicates that while fewer cells are undergoing replication at a given time in Bmi1 deficient adenomas, they spend more time in the cell cycle. We next wanted to determine whether Bmi1 loss impacts the rate of DNA synthesis. To do this, we examined only cells in tumors that incorporated BrdU over a one hour pulse prior to euthanasia. We then quantified the fraction of BrdU positive nuclei per tumor in groups of high, intermediate or low BrdU intensities using an unbiased algorithm with set thresholds. Unexpectedly, we found that grade 2 Bmi1 deficient adenomas uniquely and significantly displayed a smaller fraction of high intensity BrdU nuclei (Figure 10E). This suggests that there is a defect in DNA replication in Bmi1 deficient grade 2 adenomas. Lastly, we extended these findings to our *Kras*$^{G12D/+}$ cohorts 20 weeks after infection, indicating that this is a global response to Bmi1 loss in adenomas (Figure 10F). Together this data demonstrates that Bmi1 loss impairs proliferation of grade 2 lesions in part by delaying progression through the cell cycle.

Bmi1 represses a core set of differentiation factors in lung adenomas.

We demonstrated previously that Bmi1 loss induces changes in the differentiation state of advanced adenocarcimas (Figure 6). Therefore, we hypothesized that Bmi1 is involved in repressing a set of the developmental regulators. Indeed, the

top altered developmental systems identified by pathways analysis using the ICA Bmi1 deficiency signature have been previously implicated in lung adenocarcinoma progression (Figure 11A) (Snyder et al. 2013). In order to extract potential tumor suppressor genes targeted by Bmi1 in lung adenomas, we buttressed our ICA Bmi1 deficiency gene signature by overlapping it with differential expression signatures generated on grade 2 adenomas (Figure 11B). To home in on potential direct targets, we filtered our list based on publicly available ChIP and RNA sequencing data sets (Gargiulo et al. 2013; Kallin et al. 2009; Zhou et al. 2016). From this list, we identified 20 transcription factors that are typically repressed in the lung (Figure 11C,D). Several high confidence genes are implicated as tumor suppressors in various human cancers, including in lung adenocarcinoma (Yuan et al. 2011; Collisson et al. 2014; Chudnovsky et al. 2014). Furthermore, one of the most significantly differentially expressed genes in our grade 2 *Bmi1*$^{fl/fl}$ adenomas compared with grade 2 *Bmi1*$^{+/+}$ adenomas was Porcn, a general Wnt activator that has been shown to induce Hmga2 in other contexts (Figure 11E) (Cheng et al. 2015). Together, this data show that Bmi1 loss leads to the re-expression of developmental factors that can impact tumorigenesis.

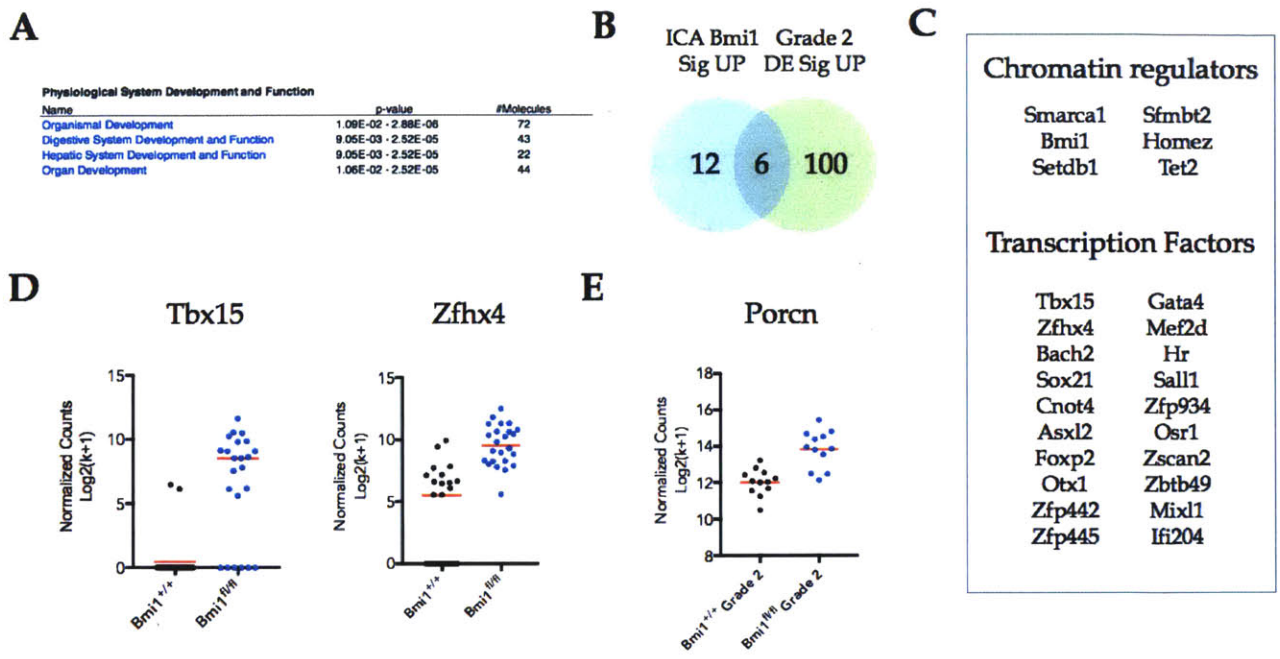

Figure 11. Bmi1 sustains the repression of developmental regulators in grade 2 adenomas
(A) Pathway analysis showing top developmental pathways altered in tumors correlating with ICA Bmi1 deficiency signature. **(B)** Venn Diagram showing overlap of unregulated genes in ICA Bmi1 deficiency signature and Bmi1 grade 2 adenomas by differential expression analysis using DESeq2. **(C)** List of top chromatin regulators and transcription factors unregulated in Bmi1 deficient grade 2 tumors. **(D)** Log2 transformed IQR 20 normalized counts of the two most differentially regulated genes in ICA Signature 2 by genotype. **(E)** Log2 transformed IQR 20 normalized counts of the most differentially expressed gene by differential expression analysis of only grade 2 adenomas.

DISCUSSION

The polycomb group proteins (PcGs) maintain an extensively chronicled and complex link to human cancer (Koppens and van Lohuizen 2015). They often act in a context dependent manner based on the underlying genetic landscape (Fillmore et al. 2015; Serresi et al. 2016). The mammalian Polycomb Repressive Complex 1 has evolved into a dynamic compilation of interchangeable subunits, each contributing to differential target specification (Gil and O'Loghlen 2014). Bmi1 appears to target tumor suppressive pathways that impinge on self-renewal in both stem cell biology and tumorigenesis. However, it regulates differential pathways depending on the tissue of origins (Hsu and Lawlor 2011; Lukacs et al. 2010; Lopez-Arribillaga et al. 2014; Gargiulo et al. 2013; Liu 2006). In the context of Kras driven lung adenocarcinoma, we demonstrate that Bmi1 is oncogenic independent of its capacity to repress the canonical $p19^{ARF}$-p53 tumor suppressive axis; that Bmi1 deficiency is broadly tumor suppressive in early lesions by impacting proliferation and differentiation status; and that it is a critical regulator of tumor progression to advanced disease.

Our data largely contrasts with other studies, including our own, that assess Bmi1 deficiency in the lung using mouse models. In particular, previous work implicated a critical role for Bmi1 in repressing the *Cdkn2a* locus that encodes the tumor suppressors $p16^{INK4A}$ and $p19^{ARF}$ (Dovey et al. 2008; Becker et al. 2009; Zacharek et al. 2011; Young and Jacks 2010). One of these studies further demonstrated that Bmi1 regulates stem cell self-renewal through maintenance of imprinted loci (Zacharek et al. 2011). We did not identify these phenotypes in our work and attribute these differences to specific requirements for Bmi1 during lung development. Indeed, much of the

evidence linking Bmi1 to *Cdkn2a* in mice was generated using animals with germ line Bmi1 deficiency, suggesting a role for Bmi1 in marking this locus in embryogenesis. For instance, Bmi1 critically inhibits *Cdkn2a* in neuronal stem cells and glioblastoma in Bmi1 deficient animals; however the locus is not affected by Bmi1 knockdown in established gliomas (Bruggeman et al. 2005; Jacobs et al. 1999a). Furthermore, $p19^{ARF}$ partially rescued intestinal tumorigenesis in *Bmi1*$^{-/-}$ mice, however Bmi1 knockout or inhibition later in embryogenesis or after development ameliorates these effects (Maynard et al. 2014; Kreso et al. 2014). We also do not find *Cdkn2a* mutations enriched in human cancers that display a gene signature of Bmi1 deficiency. By conditionally ablating Bmi1 in adult mice, we dissociated potentially confounding factors such as Bmi1 activity during lung development and demonstrated that targeting Bmi1 may be beneficial in lung tumors carrying p53 mutations.

Our work establishes that Bmi1 affects the rate of cell proliferation through grade 2 lesions. Thus, it must, in part, influence entry or progression through the cell cycle, though it remains unclear how it impacts distinct cell cycle phases. Our transcriptomic analysis identifies a strong enrichment of cell cycle related transcripts in Bmi1 deficient adenomas, which is striking given the dramatic reduction of cells undergoing DNA synthesis at a any time. Since we do not see increased apoptosis or DNA damage, we do not believe that Bmi1 loss is inducing a strict cell cycle block. Recent reports suggests that PRC1 directly modulates the rate of DNA replication origin firing and fork progression in addition to S phase entry (Piunti et al. 2014; Bravo et al. 2015). Our BrdU pulse experiment is consistent with these roles and may identify Bmi1 as a critical component of PRC1 in regulating this function in lung adenomas. However, it does not

entirely explain the overall decrease in proliferation. We favor the view that Bmi1 may regulate both the rate of cell cycle entry as well as the efficiency of progression through the cell cycle, warranting closer examination.

Our data make clear that Bmi1 mediates the transition of Kras driven lung adenomas to advanced grade adenocarcinoma. We speculate that the proliferative impairment of Bmi1 deficient tumors contributes to the delay in tumor progression. Accordingly, reduced cell divisions results in the decreased chance of acquiring pro-tumorigenic events during the cell cycle, such as copy number alterations due to mis-segregation. Interestingly, this lung cancer mouse model has been shown to rely on copy number alterations for tumor progression, further highlighted by nuclear atypia being a hallmark of advanced disease (Westcott et al. 2014). An alternative hypothesis is that Bmi1 may play a role in tolerating global increases in transcription - either due to overabundance of transcriptional activators such as Myc or copy number variation - that would result in the increase tumor suppressor activity. A CpG Island Methylator Phenotype (CIMP) has been described to have a comparable role in lung adenocarcinoma (Collisson et al. 2014). It would be informative to assess whether CIMP tumors are insensitive to Bmi1 inhibition, though we did not find a correlation between Bmi1 deficiency and CIMP status in human tumors. Thus, we favor the hypothesis that decrease cell divisions largely contributes to the delayed progression to advanced disease in the absence of Bmi1.

We envision several other potential mechanisms that may singly or in combination mediate tumor suppression in Bmi1 deficient lung adenomas. The Polycomb Repressive Complex 1 (PRC1) is involved in cell fate commitment in part by

repressing developmental factors involved in alternate lineage specification (Bracken et al. 2006; Oguro et al. 2010; Morey et al. 2015). This also appears to be the case in the context of cancer and where these factors may act as tumor suppressors (Chiacchiera et al. 2016). Our data suggest that Bmi1 may play a similar role in lung adenomas, since several of our highest confidence derepressed transcripts are factors involved in lineage specification. These transcripts are implicated in other contexts as direct Bmi1 targets that may also function as tumor suppressors (Yuan et al. 2011; Collisson et al. 2014; Chudnovsky et al. 2014). Strikingly, one of these genes Zfhx4, on which little is known, is found to be mutated in 27% of human lung adenocarcinomas, the seventh most frequently mutated gene in TCGA datasets. Furthermore, Gata4 has been reported as a putative tumor suppressor in lung adenocarcinoma and is a frequent target in CIMP high tumors (Collisson et al. 2014). It would be of particular interest to determine whether these factors can directly modulate the cell cycle, or whether they represent distinct tumor suppressive phenotypes governed by Bmi1. Collectively, these genes deserve further examination for potential tumor suppressive roles in lung adenocarcinoma.

While proliferative impairment may impede tumor progression in Bmi1 deficient adenomas, it may also lead to a selective pressure resulting in an adaptive response. The embryonal protein Hmga2 is a well-known chromatin repressor and marker of advanced disease in both mice and humans (Fusco and Fedele 2007; Winslow et al. 2011). How it acts in lung adenocarcinoma remains an active topic of research. Surprisingly, we find rapid onset of Hmga2 expression in a subset of Bmi1 deficient lesions such that it now overlaps with expression of a lung differentiation maker

Nkx2.1. This could be the result of several possibilities. Hmga2 may have no functional consequences, but may be indicative of the deregulation of differentiation networks in Bmi1 deficient tumors. An alternate hypothesis, which we favor, is that Hmga2 and Bmi1 have overlapping roles. Hmga2, for instance, enforces heterochromatin and may have similar genetic targets as PcGs (Nishino et al. 2008). Interestingly, we observe decreasing Bmi1 transcripts and increasing Hmga2 transcripts as tumor progress from grade 2 to grade 3. Furthermore, where Hmga2 is thought to be expressed after stages of dedifferentiation in tumors, Bmi1 deficient Hmga2 expressing tumors retain lung markers and do not exhibit other latent lineage programs (Winslow et al. 2011; Snyder et al. 2013). Nevertheless, not all grade 3 Bmi1 deficient adenocarcinomas express Hmga2, which might implicate genetic context as a potential determinant for this apparent adaptive response.

Due in part to its widely described oncogenic roles, there is broad interest in assessing the therapeutic benefit of targeting Bmi1. Indeed, there are now small molecules reported to specifically inhibit Bmi1 in humans (Kreso et al. 2014). Our work identifies a therapeutic window in which targeting Bmi1 may be efficacious. Understanding the genetic dependencies of Bmi1, both in terms of inter-tumor heterogeneity as well as in the context of the adult lung, has the potential to broaden that window.

MATERIALS AND METHODS

Lentiviral Production

Lentiviral backbone PGK-Cre plasmid was a gift from Tyler Jacks (MIT) (modified from Addgene plasmid 17408). Lentiviral particles were generated by transfection of 293T cells using TransIT-LT1 (Mirus) with lentiviral backbone plasmid and packaging vectors Δ8.9 (gag/pol) and CMV-VSV-G (Dupage et al. 2009). Supernatant was collected at 48 and 72 hours after transfection, concentrated at 25,000 r.p.m with an Optima L-100 XP ultra-centrifuge (Beckman Coulter), and resuspended in Opti-Mem (Gibco). Viral titer was determined using 3TZ cells (Dupage et al. 2009).

Mice and Tumor Initiation

Mice harboring *Kras*^{G12D} (Jackson et al. 2001), *p53*^{fl} (Jonkers et al. 2001), *R26*$^{LSL\text{-}Luciferase}$ (Safran et al. 2003), and *Bmi1*^{fl} (Maynard et al. 2014) alleles have been previously described. Mice were intubated intratracheally with lentivirus (described above) or adenovirus (University of Iowa Vector Core) as described in (Dupage et al. 2009). *Kras*$^{G12D/+}$;*R26*$^{LSL\text{-}Luciferase}$ mice were infected with $5x10^4$ lentiviral particles per mouse. *Kras*$^{G12D/+}$;*p53*$^{fl/fl}$ mice were infected with 10^5 or 10^4 lentiviral particles or $6x10^7$ adenoviral particles per mouse. Littermates were invariably used as controls. Animal studies were approved by the Committee for Animal Care, and conducted in compliance with the Animal Welfare Act Regulations and other federal statutes relating to animals and experiments involving animals and adheres to the principles set forth in the Guide for the Care and Use of Laboratory Animals, 8th ed. National Research

Council, 2011 (institutional animal welfare assurance no. A-3125-01). All animals were maintained on a mixed C57BL/6J x 129SvJ x Balb/c background.

Histology and Immunohistochemistry

Where indicated, BrdU in sterile PBS was dosed at 30mg/kg and injected 1 hour before euthanasia. Lungs were perfused with 10% formalin and fixed overnight. Tissue was transferred to 70% ethanol, embedded in paraffin, and 4 micron sections were cut. Immuno-histochemistry (IHC) or Immunofluorescence (IF) was performed using the following antibodies: BMI1(1:100, Millipore F6(05-637)), phospho-ERK (1:400, Cell Signaling 4370), BrdU (1:100, Abcam ab6326), CD45 (1:100, Abcam ab10558), HMGA2 (1:2000, Biocheck 59170AP), NKX2.1 (1:200, Epitomics 2044-1), Cleaved Caspase 3 (1:200, Cell Signaling 9661), γH2AX (1:200, Cell Signaling 9718), phospho-CHK2 (1:100, Cell Signaling 2661), CDX2 (1:200, Bethyl IHC-00126), p57 (1:400, Sigma M20), p19 (1:100, Novus 5-C3-1), Ki67 (1:100, BD 550609) Images were captured using a Leica Aperio AT2 Digital Slide Scanner and Aperio ImageScope Software v12.3.0.5056 or on a Nikon Eclipse microscope with a DS Ri2 camera and NIS Elements Software.

IHC was performed on Thermo Autostainer 360 machine for the following antibodies: BrdU, CD45, NKX2.1, and Ki67. Heat induced epitope retrieval procedure using Thermo citrate buffer pH6.0 was performed on the pre-treatment module and slides subsequently treated with Biocare rodent block, primary antibody, and anti-mouse (Biocare), anti-rat (Vector Labs), or anti-rabbit (Vector Labs) HRP-polymer and

developed with Thermo Ultra DAB. Slides were counterstained with haematoxylin in a Thermo Gemini stainer and coverslips added using the Thermo Consul cover slipper.

IHC for all other antibodies was performed as follows: Rehydrated slides were washed in PBS 0.15% Triton X-100 followed by inactivation of endogenous peroxidases by incubation with 3% H_2O_2 in PBS. Antigen retrieval was performed by heating in an 800 W microwave for 6.5 min at full power followed by three rounds of 5 min at 60% power using a solution 8.2 mM sodium citrate, 1.8 mM citric acid, pH 6.0. Slides were blocked with PBS containing 5% of the appropriate serum and incubated overnight with the primary antibody diluted in PBS 0.15% Triton X-100 or this buffer alone or a non-specific antiserum as controls. Secondary antibodies (Vectastain ABC kits, Vector laboratories) were diluted 1:200 in PBS containing 0.4% of the appropriate blocking serum and detected using a DAB substrate following the manufacturers instructions (Vector Laboratories). For BMI1 staining, a MOM kit (Vector Laboratories) was used according to the manufacturers instructions and an UltraVision LP Detection System (Thermo) for staining. Slides were counterstained with haematoxylin in a Thermo Gemini stainer and coverslips added using the Thermo Consul cover slipper.

IF of $p19^{ARF}$ was performed as described above except detected with an anti-Rat-APC (Invitrogen 10540) and mounted using SlowFade Gold with DAPI (Invitrogen). Images were obtained using a Zeiss Axioplan II.

Senescence Detection

Individual mouse lobes were perfused with 1:1 PBS/O.C.T Compound (Tissue-Tek, Sakura Finetek), embedded in O.C.T Compound, frozen over dry ice, and sectioned into 5 to 10 micron sections. A modified protocol was used on sections obtained within 1 hour of euthanasia based on Senescence β-Galactosidase Staining Kit (Cell Signaling 9860). After washing with PBS, sections were incubated with Fixative Solution for 10 min, washed with PBS and stained using β-Galactosidase Staining Solution overnight at 37C. After washing, slides were counterstained with Nuclear Fast Red (Thermo) in a Thermo Gemini stainer and coverslips added using the Thermo Consul cover slipper.

Histological grading and quantification

Lung sections were stained with haematoxylin and eosin. Images were captured using Leica Aperio AT2 Digital Slide Scanner and Aperio ImageScope Software. Tumor burden was measured as the fraction of tumor tissue per total lung area in a section. Tumor and lung areas were determined using Aperio ImageScope Software v12.3.0.5056.

Tumors arising in mice were classified into 3 grades with the assistance of a board certified veterinary pathologist (R.B.). Grade 1 tumors displayed minimal pleomorphism and include atypcial adenomatous hyperplasias or small adenomas. Grade 2 adenomas were larger and exhibited uniform nuclei that are sometime slightly enlarged. Hi Grade 2 was classified based on prominent nucleoli formation and larger nuclei with some pleomorphism. Grade 3 tumors were identified as adenocarcinomas with severe nuclear atypia and cellular pleomorphism.

Tumors assessed for papillary-like features were classified with the assistance of a board certified veterinary pathologist (R.B.). At low magnification, tumors were classified for papillary-like features as: Solid morphology without papillary-like architecture; P1 representing minimal glandular architecture and cellular alignment; P2 encompassing overt and widespread glandular or papillary structures; and P3 including highly papillary-like tumors with fibro-vascular cores. After determination of papillary-like status, high magnification was used to determine grade.

Quantification of Immunohistochemistry

Quantification of positive nuclei and intensity scoring for BrdU, HMGA2 and Ki67 (12 week *Kras*$^{G12D/+}$;*p53*$^{fl/fl}$) was performed on tumors using Aperio ImageScope Software v12.3.0.5056 analysis algorithm Nuclear v9 with the following algorithm inputs:

Version	9.1
View Width	1000
View Height	1000
Overlap Size	100
Image Zoom	1
Classifier	None
Class List	
Classifier Neighborhood	0
Pixel Size (um)	0.504
Averaging Radius (um)	1
Averaging Radius (Pixels)	2
Curvature Threshold	2
Segmentation Type	0

Threshold Type	2
Lower Intensity Threshold	0
Upper Intensity Threshold	214
Min Nuclear Size (um^2)	10
Min Nuclear Size (Pixels)	39
Max Nuclear Size (um^2)	1.00E+06
Max Nuclear Size (Pixels)	3.94E+06
Min Roundness	0.2
Min Compactness	0
Min Elongation	5E-02
Remove Light Objects	0
Weak(1+) Threshold	210
Moderate(2+) Threshold	188
Strong(3+) Threshold	162
Black Threshold	0
Edge Trim	Weighted
Markup Image Type	Analysis
Nuclear Red OD	0.696858
Nuclear Green OD	0.643073
Nuclear Blue OD	0.317563
Positive Red OD	0.244583
Positive Green OD	0.509334
Positive Blue OD	0.825081
Color(3) Red OD	0
Color(3) Green OD	0
Color(3) Blue OD	0
Clear Area Intensity	233
Use Mode	Analysis/Tuning
Classifier Type	IHCNuclear
Classifier Definition File	IHCNuclearTraining
Display Plots	Yes

Quantification of Ki67 on grade 2 $Kras^{G12D/+};p53^{fl/fl}$ mice at 8 weeks was calculated by visually counting positive nuclei and measuring tumor area by Aperio ImageScope Software as described above. Images could not be analyzed as described above due to high non-specific background staining on this sections.

Live Animal Imaging

Live animal imaging experiments were performed using a Caliper IVIS Spectrum-bioluminescent and fluorescent imaging system (Xenogen Corporation). Shaved mice were anesthetized and injected with D-Luciferin (Perkin Elmer) at 165mg/kg mouse body weight for 10 minutes before imaging. Bioluminescent output was calculated with identical regions of interest as flux (photons/second/cm^2) using Living Image v4.3.1.0.15880.

qRT-PCR

Isolated tumors from mouse lungs were bisected. Half the tumor was fixed for histology as described above, and half snap frozen in liquid nitrogen and stored in -80C. Grade 2 tumors were pulverized using Geno/Grinder 2010 (SPEX SamplePrep) and RNA was extracted from frozen powder using TRIZOL Reagent (Invitrogen) and spun to remove non-soluble fraction. Following addition of chloroform and centrifugation per manufacturer's protocol, RNA was purified from the aqueous phase using an RNeasy Mini Kit (Qiagen) including an on column DNAse I incubation step (Qiagen).

cDNA was generated using Superscript III RT (Invitrogen) per manufacturer. Real-Time quantitative PCR reactions were performed using SYBR Green PCR Master Mix (Applied Biosystem) and a Step One Plus Real-Time PCR System (Applied Biosystem). All gene expression was shown relative to 18S and normalized to the average value of $Bmi1^{+/+}$ tumors. Primers qPCR were: 18S forward (5'-CGT CTG CCC TAT CAA CTT TGC-3'), 18S reverse (5'-CTT GGA TGT GGT AGC CGT TTC-3'), Bmi1 forward (5'-CAA AAC CAG AAC ACT CCT GAA-3'), Bmi1 reverse (5'-TCT TCT TCT CTT CAT CTC ATT TTT GA-3'), $p16^{INK4A}$ forward (5'-GCG GGC ACT GCT GGA AG-3'), $p16^{INK4A}$ reverse (5'-CGT TGC CCA TCA TCA TCA CC-3'); p57 forward (5'-CGA ACG ACT TCT TCG CCA A-3'); p57 reverse (5'-ACG CCT TGT TCT CCT GCG-3'); p27 forward (5'-TTG GTG GAC CAA ATG CCT GAC T-3'); p27 reverse (5'-AAT CTT CTG CAG CAG GTC GCT T-3').

High-Throughput Digital Gene Expression Sequencing

RNA from individual tumors were isolated as described above and checked for quality and purity using a 2100 BioAnalyzer (Agilent). 48 tumors were selected for Digital Gene Expression (DGE) based on purity of sample as measured by histology and RNA quality. RNA was processed for DGE as described (Soumillon et al. 2014). Briefly, 20ng of RNA was converted to cDNA, and enriched for polyA. Individual transcripts marked with unique molecular identifiers (UMI) and barcoded by tumor. cDNA was then tagmented using Nextera XT (Illumina) to enrich for 3' fragments for sequencing. Samples were sequenced in 40 nucleotide reads with paired ends using a HiSeq 2000 (Illumina). After sequencing, samples were de-convoluted by barcode and collapsed by

UMI+40 nucleotide stranded read. Reads were aligned to mm9 version of the mouse genome using tophat 2.0.4 with segment length of 16 and filtered for Q30 quality mapping. Mapped reads were annotated to UCSC mm9 annotated genes and counted using HTseq. Raw expression counts were upper-quartile normalized to a count of 2000 (Bullard et al. 2010).

Independent Component Analysis

For signature analysis, an unsupervised blind source separation strategy using Independent Component Analysis (ICA) was applied to elucidate statistically independent gene expression signatures (Bhutkar et al. in prep.; Hyvärinen and Oja, 2000; Rutledge and Jouan-Rimbaud Bouveresse, 2013). ICA is a general-purpose signal processing and multivariate data analysis technique in the category of unsupervised matrix factorization methods. Based on input data consisting of a hairpins-samples matrix, ICA uses higher order moments to characterize the dataset as a linear combination of statistically independent latent variables. These latent variables represent independent components based on maximizing non-gaussianity, and can be interpreted as independent source signals that have been mixed together to form the dataset under consideration. Each component includes a weight assignment to each gene that quantifies its contribution to that component. Additionally, ICA derives a mixing matrix that describes the contribution of each sample towards the signal embodied in each component. This mixing matrix can be used to select signatures among components with distinct expression profiles across the set of samples. All computations were done in the R Statistical Programming Language. The R

implementation of the core JADE algorithm (Joint Approximate Diagonalization of Eigenmatrices) (Biton et al., 2013; Nordhausen et al., 2012; Rutledge and Jouan-Rimbaud Bouveresse, 2013) was used along with custom R utilities.

Gene signatures were developed by filtering ICA components by z-score gene correlation to the component (+/- 4) and fold 2 change based on relevant identified tumor samples: Grade for ICA component 1 and Bmi1 genotype for ICA component 2. Heatmaps were generated using Heatplus 2.16.0 on R v3.2.3, clustered by Pearson correlation.

Differential Expression (DE) Analysis

Differential expression analysis was performed in a biased manner to directly compare gene expression between two subgroups of the HT-DGEseq samples as indicated. Specifically, raw counts were processed for differential expression and principal component analysis using DEseq2 v1.10.1 (Love et al. 2014). Gene signature was developed by filtering for fold 1.5 change and Benjamini Hochberg adjusted p value of 0.05.

Gene Set Enrichment Analysis and Pathway Analysis

Preranked gene set enrichment analysis (GSEA) using Hallmark gene sets was performed on ICA signatures sorted by z-score or on DE signatures sorted by fold change as described in (Subramanian et al. 2005; Mootha et al. 2003). Data were

analyzed through the use of QIAGEN's Ingenuity® Pathway Analysis (IPA®, QIAGEN Redwood City, www.qiagen.com/ingenuity).

Clinical Analyses

For clinical analyses, expression data from RNAseq transcriptome alignments from 457 lung adenocarcinoma patients openly available from the The Cancer Genome Atlas project (http://cancergenome.nih.gov/) were ranked according to their correlation an ICA gene signature. Five-year survival were analyzed by Kaplan-Meier curves and log-rank test. Using all tumors, survival was determined by comparing the 10% (n=45) of patients with tumors that correlate best with the ICA grade signature to the remainder of patients (n=412). Using only T1 and T2 staged tumors, survival analysis compared the 35% of patients with tumors with the best (n=138) or worst (n=138) correlations to the ICA Bmi1 signature. Multivariate analysis by the Cox proportional hazard model (adjusted by age, gender, tumor stage, smoking history, and mutational status). Significance called with an alpha of 0.05.

AKNOWLEDGMENTS

We thank Eric Snider for providing the Cre expressing lentiviral vector used for tumor initiation. We also thank members of the Lees Lab for input during the study and manuscript preparation. We thank the Koch Institute Swanson Biotechnology Center for technical support, specifically the Tang Histology Facility, Animal Imaging and Preclinical Testing Facility, and the BioMicro Center. This work was supported by a Janssen Transcend Grant to J.A.L. who is a Ludwig Scholar at MIT. D.L.K. was supported by an NSF pre-doctoral fellowship.

REFERENCES

Baylin SB, Jones PA. 2011. A decade of exploring the cancer epigenome — biological and translational implications. *Nat Rev Cancer* **11**: 726–734.

Becker M, Korn C, Sienerth AR, Voswinckel R, Luetkenhaus K, Ceteci F, Rapp UR. 2009. Polycomb group protein Bmi1 is required for growth of RAF driven non-small-cell lung cancer. *PLoS ONE* **4**: e4230.

Bhutkar, A., Blat, I., Boutz, P.L., Cameron, E.R., Chen, P.Y., Chen, S., Ferretti, R., Gurtan, A.M., Ianari, A., Muzumdar, M.D., et al. High-resolution signature discovery in NGS expression datasets using Blind Source Separation (In Submission).

Biton, A., Zinovyev, A., Barillot, E., and Radvanyi, F. 2013. MineICA: Independent component analysis of transcriptomic data.

Boyer LA, Plath K, Zeitlinger J, Brambrink T, Medeiros LA, Lee TI, Levine SS, Wernig M, Tajonar A, Ray MK, et al. 2006. Polycomb complexes repress developmental regulators in murine embryonic stem cells. *Nature* **441**: 349–353.

Bracken AP, Dietrich N, Pasini D, Hansen KH, Helin K. 2006. Genome-wide mapping of Polycomb target genes unravels their roles in cell fate transitions. *Genes Dev* **20**: 1123–1136.

Bravo M, Nicolini F, Starowicz K, Barroso S, Calés C, Aguilera A, Vidal M. 2015. Polycomb RING1A- and RING1B-dependent histone H2A monoubiquitylation at pericentromeric regions promotes S-phase progression. *J Cell Sci* **128**: 3660–3671.

Brien GL, Valerio DG, Armstrong SA. 2016. Exploiting the Epigenome to Control Cancer-Promoting Gene-Expression Programs. *Cancer Cell* **29**: 464–476.

Bruggeman SWM, Hulsman D, Tanger E, Buckle T, Blom M, Zevenhoven J, van Tellingen O, van Lohuizen M. 2007. Bmi1 Controls Tumor Development in an Ink4a/Arf-Independent Manner in a Mouse Model for Glioma. **12**: 328–341.

Bruggeman SWM, Valk-Lingbeek ME, van der Stoop PPM, Jacobs JJL, Kieboom K, Tanger E, Hulsman D, Leung C, Arsenijevic Y, Marino S, et al. 2005. Ink4a and Arf differentially affect cell proliferation and neural stem cell self-renewal in Bmi1-deficient mice. *Genes Dev* **19**: 1438–1443.

Bullard JH, Purdom E, Hansen KD, Dudoit S. 2010. Evaluation of statistical methods for normalization and differential expression in mRNA-Seq experiments. *BMC Bioinformatics* **11**:1

Chen Z, Fillmore CM, Hammerman PS, Kim CF, Wong K-K. 2014. Non-small-cell lung cancers: a heterogeneous set of diseases. *Nat Rev Cancer* **14**: 535–546.

Cheng Y, Phoon YP, Jin X, Chong SYS, Ip JCY, Wong BWY, Lung ML. 2015. Wnt-C59 arrests stemness and suppresses growth of nasopharyngeal carcinoma in mice by inhibiting the Wnt pathway in the tumor microenvironment. *Oncotarget* **6**: 14428–14439.

Chiacchiera F, Rossi A, Jammula S, Piunti A, Scelfo A, Ordóñez-Morán P, Huelsken J, Koseki H, Pasini D. 2016. Polycomb Complex PRC1 Preserves Intestinal Stem Cell Identity by Sustaining Wnt/β-Catenin Transcriptional Activity. *Stem Cell* **18**: 91–103. http://www.cell.com/cell-stem-cell/abstract/S1934-5909(15)00457-9.

Chiappinelli KB, Strissel PL, Desrichard A, Li H, Henke C, Akman B, Hein A, Rote NS, Cope LM, Snyder A, et al. 2015. Inhibiting DNA Methylation Causes an Interferon Response in Cancer via dsRNA Including Endogenous Retroviruses. *Cell* **162**: 974–986.

Chudnovsky Y, Kim D, Zheng S, Whyte WA, Bansal M, Bray M-A, Gopal S, Theisen MA, Bilodeau S, Thiru P, et al. 2014. ZFHX4 Interacts with the NuRD Core Member CHD4 and Regulates the Glioblastoma Tumor-Initiating Cell State. *Cell Reports* **6**: 313–324.

Collisson EA, Network TCGAR, Campbell JD, Brooks AN, Berger AH, Lee W, Chmielecki J, Beer DG, Cope L, Creighton CJ, et al. 2014. Comprehensive molecular profiling of lung adenocarcinoma. *Nature* **511**: 543–550.

Dawson MA, Kouzarides T. 2012. Cancer Epigenetics: From Mechanism to Therapy. *Cell* **150**: 12–27.

Dovey JS, Zacharek SJ, Kim CF, Lees JA. 2008. Bmi1 is critical for lung tumorigenesis and bronchioalveolar stem cell expansion. *Proc Natl Acad Sci USA* **105**: 11857–11862.

Dupage M, Dooley AL, Jacks T. 2009. Conditional mouse lung cancer models using adenoviral or lentiviral delivery of Cre recombinase. *Nat Protoc* **4**: 1064–1072.

Feldser DM, Kostova KK, Winslow MM, Taylor SE, Cashman C, Whittaker CA, Sanchez-Rivera FJ, Resnick R, Bronson R, Hemann MT, et al. 2010. Stage-specific sensitivity to p53 restoration during lung cancer progression. *Nature* **468**: 572–575.

Fillmore CM, Xu C, Desai PT, Berry JM, Rowbotham SP, Lin Y-J, Zhang H, Marquez VE, Hammerman PS, Wong K-K, et al. 2015. EZH2 inhibition

sensitizes BRG1 and EGFR mutant lung tumours to TopoII inhibitors. *Nature* **520**: 239–242.

Fusco A, Fedele M. 2007. Roles of HMGA proteins in cancer. *Nat Rev Cancer* **7**: 899–910.

Gargiulo G, Cesaroni M, Serresi M, de Vries N, Hulsman D, Bruggeman SW, Lancini C, van Lohuizen M. 2013. In vivo RNAi screen for BMI1 targets identifies TGF-β/BMP-ER stress pathways as key regulators of neural- and malignant glioma-stem cell homeostasis. **23**: 660–676.

Gil J, O'Loghlen A. 2014. PRC1 complex diversity: where is it taking us? *Trends Cell Biol* **24**: 632–641.

Glinsky GV, Berezovska O, Glinskii AB. 2005. Microarray analysis identifies a death-from-cancer signature predicting therapy failure in patients with multiple types of cancer. *J Clin Invest* **115**: 1503–1521.

Hsu JH, Lawlor ER. 2011. BMI-1 suppresses contact inhibition and stabilizes YAP in Ewing sarcoma. *Oncogene* **30**: 2077–2085.

Hyvärinen A, Oja E. Independent component analysis: algorithms and applications. *Neural Netw.* **13**:411-30.

Issa J-PJ, Kantarjian HM. 2009. Targeting DNA methylation. *Clin Cancer Res* **15**: 3938–3946.

Jackson EL, Willis N, Mercer K, Bronson RT, Crowley D, Montoya R, Jacks T, Tuveson DA. 2001. Analysis of lung tumor initiation and progression using conditional expression of oncogenic K-ras. *Genes Dev* **15**: 3243–3248.

Jacobs JJ, Kieboom K, Marino S, DePinho RA, van Lohuizen M. 1999a. The oncogene and Polycomb-group gene bmi-1 regulates cell proliferation and senescence through the ink4a locus. *Nature* **397**: 164–168.

Jacobs JJ, Scheijen B, Voncken JW, Kieboom K, Berns A, van Lohuizen M. 1999b. Bmi-1 collaborates with c-Myc in tumorigenesis by inhibiting c-Myc-induced apoptosis via INK4a/ARF. *Genes Dev* **13**: 2678–2690.

Jonkers J, Meuwissen R, van der Gulden H, Peterse H, van der Valk M, Berns A. 2001. Synergistic tumor suppressor activity of BRCA2 and p53 in a conditional mouse model for breast cancer. *Nat Genet* **29**: 418–425.

Kallin EM, Cao R, Jothi R, Xia K, Cui K, Zhao K, Zhang Y. 2009. Genome-wide uH2A localization analysis highlights Bmi1-dependent deposition of the mark at repressed genes. *PLoS Genet* **5**: e1000506.

Kim CFB, Jackson EL, Woolfenden AE, Lawrence S, Babar I, Vogel S, Crowley D, Bronson RT, Jacks T. 2005. Identification of bronchioalveolar stem cells in normal lung and lung cancer. *Cell* **121**: 823–835.

Knutson SK, Kawano S, Minoshima Y, Warholic NM, Huang K-C, Xiao Y, Kadowaki T, Uesugi M, Kuznetsov G, Kumar N, et al. 2014. Selective inhibition of EZH2 by EPZ-6438 leads to potent antitumor activity in EZH2-mutant non-Hodgkin lymphoma. *Mol Cancer Ther* **13**: 842–854.

Knutson SK, Warholic NM, Wigle TJ, Klaus CR, Allain CJ, Raimondi A, Porter Scott M, Chesworth R, Moyer MP, Copeland RA, et al. 2013. Durable tumor regression in genetically altered malignant rhabdoid tumors by inhibition of methyltransferase EZH2. *Proc Natl Acad Sci USA* **110**: 7922–7927.

Koppens M, van Lohuizen M. 2016. Context-dependent actions of Polycomb repressors in cancer. *Oncogene* **35**: 1341-1352.

Kreso A, van Galen P, Pedley NM, Lima-Fernandes E, Frelin C, Davis T, Cao L, Baiazitov R, Du W, Sydorenko N, et al. 2014. Self-renewal as a therapeutic target in human colorectal cancer. *Nat Med* **20**: 29–36.

Kwon M-C, Berns A. 2013. Mouse models for lung cancer. *Molecular Oncology* **7**: 165–177.

Laugesen A, Helin K. 2014. Chromatin Repressive Complexes in Stem Cells, Development, and Cancer. **14**: 735–751.

Lin R-K, Hsieh Y-S, Lin P, Hsu H-S, Chen C-Y, Tang Y-A, Lee C-F, Wang Y-C. 2010. The tobacco-specific carcinogen NNK induces DNA methyltransferase 1 accumulation and tumor suppressor gene hypermethylation in mice and lung cancer patients. *J Clin Invest* **120**: 521–532.

Liu S. 2006. Hedgehog Signaling and Bmi-1 Regulate Self-renewal of Normal and Malignant Human Mammary Stem Cells. **66**: 6063–6071.

Lopez-Arribillaga E, Rodilla V, Pellegrinet L, Guiu J, Iglesias M, Roman AC, Gutarra S, Gonzalez S, Munoz-Canoves P, Fernandez-Salguero P, et al. 2014. Bmi1 regulates murine intestinal stem cell proliferation and self-renewal downstream of Notch. *Development* **142**: 41–50.

Love MI, Huber W, Anders S. 2014. Moderated estimation of fold change and dispersion for RNA-seq data with DESeq2. *Genome Biol* **15**: 1–21.

Lukacs RU, Memarzadeh S, Wu H, Witte ON. 2010. Bmi-1 Is a Crucial Regulator of Prostate Stem Cell Self-Renewal and Malignant Transformation. **7**: 682–693.

Mainardi S, Mijimolle N, Francoz S, Vicente-Duenas C, Sanchez-Garcia I, Barbacid M. 2014. Identification of cancer initiating cells in K-Ras driven lung adenocarcinoma. *Proc Natl Acad Sci USA* **111**: 255–260.

Maynard MA, Ferretti R, Hilgendorf KI, Perret C, Whyte P, Lees JA. 2014. Bmi1 is required for tumorigenesis in a mouse model of intestinal cancer. *Oncogene* **33**: 3742–3747.

Meylan E, Dooley AL, Feldser DM, Shen L, Turk E, Ouyang C, Jacks T. 2009. Requirement for NF-κB signalling in a mouse model of lung adenocarcinoma. *Nature* **462**: 104–107.

Mootha VK, Lindgren CM, Eriksson K-F, Subramanian A, Sihag S, Lehar J, Puigserver P, Carlsson E, Ridderstråle M, Laurila E, et al. 2003. PGC-1 | [alpha] | -responsive genes involved in oxidative phosphorylation are coordinately downregulated in human diabetes. *Nat Genet* **34**: 267–273.

Morey L, Santanach A, Blanco E, Aloia L, Nora EP, Bruneau BG, Di Croce L. 2015. Polycomb Regulates Mesoderm Cell Fate-Specification in Embryonic Stem Cells through Activation and Repression Mechanisms. *Stem Cell* **17**: 300–315.

Nacerddine K, Beaudry J-B, Ginjala V, Westerman B, Mattiroli F, Song J-Y, van der Poel H, Ponz OB, Pritchard C, Cornelissen-Steijger P, et al. 2012. Akt-mediated phosphorylation of Bmi1 modulates its oncogenic potential, E3 ligase activity, and DNA damage repair activity in mouse prostate cancer. *J Clin Invest* **122**: 1920–1932.

Nishino J, Kim I, Chada K, Morrison SJ. 2008. Hmga2 promotes neural stem cell self-renewal in young but not old mice by reducing p16Ink4a and p19Arf Expression. *Cell* **135**: 227–239.

Nordhausen, K., Cardoso, J.F., Miettinen, J., Oja, H., and Ollila, E. (2012). JADE: JADE and other BSS methods as well as some BSS performance criteria (R package version).

Oguro H, Yuan J, Ichikawa H, Ikawa T, Yamazaki S, Kawamoto H, Nakauchi H, Iwama A. 2010. Poised lineage specification in multipotential hematopoietic stem and progenitor cells by the polycomb protein Bmi1. **6**: 279–286.

Park I-K, Morrison SJ, Clarke MF. 2004. Bmi1, stem cells, and senescence regulation. *J Clin Invest* **113**: 175–179.

Patricelli MP, Janes MR, Li L-S, Hansen R, Peters U, Kessler LV, Chen Y, Kucharski JM, Feng J, Ely T, et al. 2016. Selective Inhibition of Oncogenic KRAS Output with Small Molecules Targeting the Inactive State. *Cancer Discov* **6**: CD–15–1105–329.

Piunti A, Rossi A, Cerutti A, Albert M, Jammula S, Scelfo A, Cedrone L, Fragola G, Olsson L, Koseki H, et al. 2014. Polycomb proteins control proliferation and transformation independently of cell cycle checkpoints by regulating DNA replication. *Nature Communications* **5**.

Rutledge DN, Jouan-Rimbaud Bouveresse D. 2013. Independent Components Analysis with the JADE algorithm. *TrAC Trends in Analytical Chemistry* **50**: 22–32.

Safran M, Kim WY, Kung AL, Horner JW, DePinho RA, Kaelin WG. 2003. Mouse reporter strain for noninvasive bioluminescent imaging of cells that have undergone Cre-mediated recombination. *Mol Imaging* **2**: 297–302.

Serresi M, Gargiulo G, Proost N, Siteur B, Cesaroni M, Koppens M, Xie H, Sutherland KD, Hulsman D, Citterio E, et al. 2016. Polycomb Repressive Complex 2 Is a Barrier to KRAS-Driven Inflammation and Epithelial-Mesenchymal Transition in Non-Small-Cell Lung Cancer. *Cancer Cell* **29**: 17–31.

Siddique HR, Saleem M. 2012. Role of BMI1, a stem cell factor, in cancer recurrence and chemoresistance: preclinical and clinical evidences. *Stem Cells* **30**: 372–378.

Snyder EL, Watanabe H, Magendantz M, Hoersch S, Chen TA, Wang DG, Crowley D, Whittaker CA, Meyerson M, Kimura S, et al. 2013. Nkx2-1 represses a latent gastric differentiation program in lung adenocarcinoma. *Mol Cell* **50**: 185–199.

Soumillon M, Cacchiarelli D, Semrau S, van Oudenaarden A, Mikkelsen TS. 2014. Characterization of directed differentiation by high-throughput single-cell RNA-Seq. *bioRxiv* 003236.

Subramanian A, Tamayo P, Mootha VK, Mukherjee S, Ebert BL, Gillette MA, Paulovich A, Pomeroy SL, Golub TR, Lander ES, et al. 2005. Gene set enrichment analysis: a knowledge-based approach for interpreting genome-wide expression profiles. *Proc Natl Acad Sci USA* **102**: 15545–15550.

Sugano M, Nagasaka T, Sasaki E, Murakami Y, Hosoda W, Hida T, Mitsudomi T, Yatabe Y. 2013. HNF4α as a marker for invasive mucinous adenocarcinoma of the lung. - PubMed - NCBI. *Am J Surg Pathol* **37**: 211–218.

Sutherland KD, Song J-Y, Kwon M-C, Proost N, Zevenhoven J, Berns A. 2014. Multiple cells-of-origin of mutant K-Ras-induced mouse lung adenocarcinoma. *Proc Natl Acad Sci USA* **111**: 4952–4957.

Travis WD, Brambilla E, Nicholson AG, Yatabe Y, Austin JHM, Beasley MB, Chirieac LR, Dacic S, Duhig E, Flieder DB, et al. 2015. The 2015 World Health

Organization Classification of Lung Tumors. *Journal of Thoracic Oncology* **10**: 1243–1260.

van der Lugt NM, Domen J, Linders K, van Roon M, Robanus-Maandag E, Riele te H, van der Valk M, Deschamps J, Sofroniew M, van Lohuizen M. 1994. Posterior transformation, neurological abnormalities, and severe hematopoietic defects in mice with a targeted deletion of the bmi-1 proto-oncogene. *Genes Dev* **8**: 757–769.

Vonlanthen S, Heighway J, Altermatt HJ, Gugger M, Kappeler A, Borner MM, van Lohuizen M, Betticher DC. 2001. The bmi-1 oncoprotein is differentially expressed in non-small cell lung cancer and correlates with INK4A-ARF locus expression. *Br J Cancer* **84**: 1372–1376.

Wederell ED, Bilenky M, Cullum R, Thiessen N, Dagpinar M, Delaney A, Varhol R, Zhao Y, Zeng T, Bernier B, et al. 2008. Global analysis of in vivo Foxa2-binding sites in mouse adult liver using massively parallel sequencing. *Nucleic Acids Res* **36**: 4549–4564.

Westcott PMK, Halliwill KD, To MD, Rashid M, Rust AG, Keane TM, Delrosario R, Jen K-Y, Gurley KE, Kemp CJ, et al. 2014. The mutational landscapes of genetic and chemical models of Kras-driven lung cancer. *Nature* **517**: 489–492.

Winslow MM, Dayton TL, Verhaak RGW, Kim-Kiselak C, Snyder EL, Feldser DM, Hubbard DD, DuPage MJ, Whittaker CA, Hoersch S, et al. 2011. Suppression of lung adenocarcinoma progression by Nkx2-1. *Nature* **473**: 101–104.

Xu X, Huang L, Futtner C, Schwab B, Rampersad RR, Lu Y, Sporn TA, Hogan BLM, Onaitis MW. 2014. The cell of origin and subtype of K-Ras-induced lung tumors are modified by Notch and Sox2. *Genes Dev* **28**: 1929–1939.

Young NP, Jacks T. 2010. Tissue-specific p19Arf regulation dictates the response to oncogenic K-ras. *Proc Natl Acad Sci USA* **107**: 10184–10189.

Yuan J, Takeuchi M, Negishi M, Oguro H, Ichikawa H, Iwama A. 2011. Bmi1 is essential for leukemic reprogramming of myeloid progenitor cells. *Leukemia* **25**: 1335–1343.

Zacharek SJ, Fillmore CM, Lau AN, Gludish DW, Chou A, Ho JWK, Zamponi R, Gazit R, Bock C, Jäger N, et al. 2011. Lung Stem Cell Self-Renewal Relies on BMI1-Dependent Control of Expression at Imprinted Loci. **9**: 272–281.

Zhou Y, Wang L, Vaseghi HR, Liu Z, Lu R, Alimohamadi S, Yin C, Fu J-D, Wang GG, Liu J, et al. 2016. Bmi1 Is a Key Epigenetic Barrier to Direct Cardiac Reprogramming. *Cell Stem Cell* **18**: 382–395.

CHAPTER 3: ASSESSING ROLES FOR BMI1 IN LUNG ADENOCARCINOMA MAINTENANCE

Daniel L Karl, Rachit Neupane, Stephanie Riocci, Paul S Danielian, Anna Kuperman, Jacqueline Lees

D.L.K. conducted all cell line and *in vivo* studies. R.N. contributed to Fiures 1F, and 3D,E. S.R. contributed to Figures 2F and 3J. P.S.D. contributed to Figure 1. A.K. contributed to 3D. D.L.K and J.A.L. designed the study, analyzed the data and wrote the chapter.

ABSTRACT

Bmi1 is a core member of the Polycomb Repressive Complex 1 that mediates transcriptional silencing of target loci by epigenetically modifying chromatin. Recent progress on identifying epigenetic drivers in lung cancer has led to and increasing interest in determining whether these reversible events can be modulated for the therapeutic benefit of cancer patients. In this study, we have begun to probe the requirement for Bmi1 in tumor maintenance. Specifically, we developed an autochthonous mouse model of lung adenocarcinoma with the potential to ablate Bmi1 in established lesions. We present evidence that Bmi1 loss may lead to a durable response which may be partially mediated by an immune interaction. We also generated cell lines to probe the effects of Bmi1 loss at a cellular level. Our data strongly suggest that acute Bmi1 loss has little or no impact on the proliferative capacity of the bulk of cancer cells *in vitro*. However, it suggests the possible existence of *in vivo* specific functions. Together, this work hints that targeting Bmi1 may be therapeutically beneficial in a subset of tumors, and identifies specific conditions that may reveal novel roles for Bmi1 in lung tumorigenesis.

INTRODUCTION

Cancers arising in the lung and bronchus are estimated to be the leading cause of cancer related deaths in 2016 and account for roughly a quarter of all new cases (Siegel et al. 2016). Among this group of cancers, Non-Small Cell Lung Cancer (NSCLC) is the most prevalent with the vast majority of cases presenting as lung adenocarcinoma (Chen et al. 2014). While targeted therapies have emerged over the last decade to specifically inhibit known drivers - such as mutated Epidermal Growth Factor Receptor (EGFR) or Anaplastic Lymphoma Kinase (ALK) - there remains a large unmet need in the treatment of this disease (Mok et al. 2009; Kwak et al. 2010). For instance, the most frequently mutated oncogenic driver in lung adenocarcinoma is Kras, for which there are no inhibitors in the clinic (Collisson et al. 2014). Furthermore, the high mutational background of this disease results in the rapid emergence of resistance to therapy (Kandoth et al. 2013; McGranahan et al. 2015; Piotrowska et al. 2015). Immune checkpoint modulators may overcome these limitations for a subset of patients (Brahmer et al. 2015; Kazandjian et al. 2016). Nevertheless, targeting epigenetic regulators in cancer may supplement the current arsenal by widely reversing epigenetic dependencies. In fact, histone deacetylase inhibitors (HDACs) are currently approved for the treatment of lung adenocarcinoma, and inhibitors of other regulators are now approved for use in other cancer types (DNMT) (Jakopovic et al. 2013; Ahuja et al. 2016).

Polycomb group proteins (PcGs) mediate the transcriptional repression of target loci largely by modifying histones (Kerppola 2009). These proteins have frequently been implicated in tumorigenesis and inhibitors for at least one PcG protein Ezh2 have entered clinical trials (Knutson et al. 2014; Ahuja et al. 2016). PcG proteins have been

described to impact tumor maintenance in various ways, particularly by sustaining the repression of tumor suppressors. This is particularly well described for the PcG protein Bmi1, a member of the Polycomb Repressive Complex 1, which is known to target the cell cycle and apoptotic regulators $p16^{INK4A}$ and $p14^{ARF}$ (known as $p19^{ARF}$ in humans) (Jacobs et al. 1999). Emerging evidence suggests that the role of PcGs in cancer is complicated and context dependent (Koppens and van Lohuizen 2015). Inhibition of Polycomb Repressive Complex 2 (PRC2) components, for instance, may have variable consequences based on the underlying genetic context (Serresi et al. 2016). Bmi1 can also impact tumorigenesis independent the *Cdkn2a* locus (Bruggeman et al. 2007).

Previous work identifies a critical role for Bmi1 in sustaining the proliferative capacity of lung adenomas as they progress to advanced adenocarcinomas. The question remains whether established tumors display sensitivity to Bmi1 loss. In this chapter, I describe various attempts to clarify the therapeutic implications of targeting Bmi1 in established tumors and lung adenocarcinoma cell lines. My data suggest that Bmi1 contributes to the maintenance of a subset of advanced cancer cells. This work highlights the need to better understand the molecular determinants intersecting with Bmi1 in lung cancer.

RESULTS

Assessing the response of Kras driven lung cancer to acute ablation of *Bmi1 in vivo*.

Loss of Bmi1 during Kras driven lung tumor initiation results in profound tumor suppressive effects. To determine whether Bmi1 may be a viable target for therapeutic intervention, we established a system in which we assessed potential roles for Bmi1 in lung tumor maintenance. Specifically, we crossed mice bearing a Cre recombinase dependent conditional allele for Bmi1 ($Bmi1^{fl}$) with animals carrying a FlpO recombinase inducible oncogenic form of Kras ($Kras^{FSF\text{-}G12D}$) at the endogenous locus. These mice also carried a Cre responsive Luciferase reporter ($R26^{LSL\text{-}Luciferase}$). Intra-tracheal intubation of these mice with lentivirus expressing a CreER and FlpO activated oncogenic $Kras^{G12D}$ without affecting Bmi1 (Figure 1A). In response to systemic delivery of tamoxifen, infected cells translocate CreER to the nucleus where it may induce loss of Bmi1. In order to determine the response of tumors to acute Bmi1 ablation over an extended period of time, we initiated tumors in $Bmi1^{fl/fl}$ or $Bmi1^{+/+}$ $Kras^{FSF\text{-}G12D}$;$R26^{LSL\text{-}Luciferase}$ mice with a low viral titer such that one to three tumors developed per lung. This allowed us to monitor individual tumors over time using x-ray micro-computed tomography (μCT) (Figure 1B,C). Importantly, tumors retain Bmi1 expression in the absence of tamoxifen (Figure 1D). After administration of tamoxifen over four consecutive days, we monitored individual tumor volumes for 20 weeks using μCT (Figure 1B,C). All lesions from $Bmi1^{+/+}$ mice increased in volume throughout the experiment. However, 3 of 9 lesions in $Bmi1^{fl/fl}$ mice regressed below detectable levels. This suggests that Bmi1 may play a role in the maintenance of a subset of tumors.

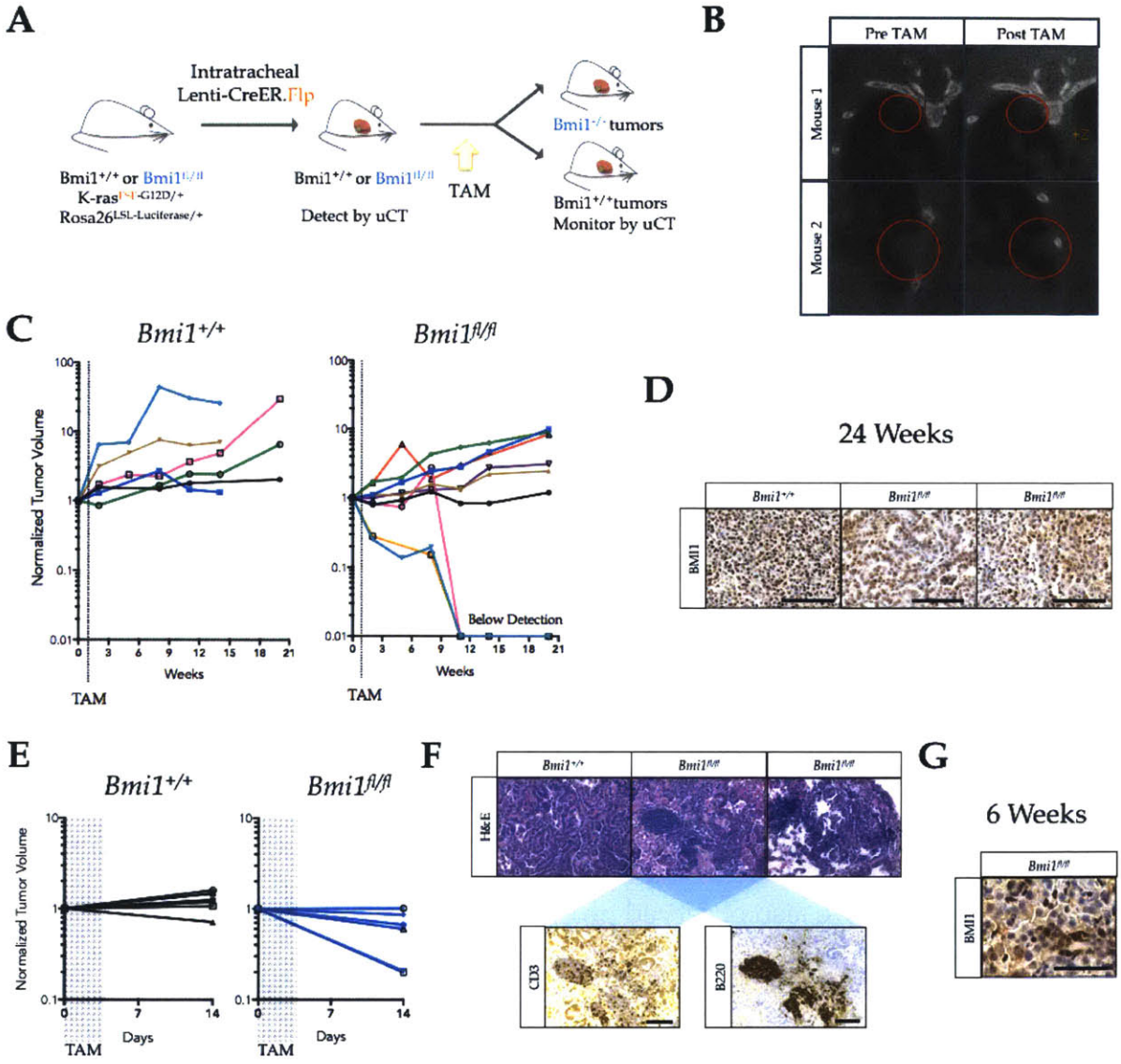

Figure 1. Ablating Bmi1 in established autochthonous Kras driven lung cancer
(A) Strategy to initiate, monitor and induce *Bmi1* recombination in lung tumors. **(B)** Representative scans illustrating increase in tumor size after tamoxifen (Mouse 1, red circle), or decreased size after tamoxifen (Mouse 2, red circle). **(C)** Tumor volumes as measured over time by µCT image analysis and normalized to the first day of tamoxifen (TAM) treatment. **(D)** Staining for BMI1 by immunohistochemistry (IHC) revealed partial ablation of Bmi1 in two tumors 24 weeks after TAM. Bar = 100µm **(E)** Tumor volumes as measured after 2 weeks by µCT image analysis and normalized to the first day of tamoxifen (TAM) treatment. **(F)** Histology showing 2 of 3 *Bmi1$^{fl/fl}$* tumors with immune infiltration 2 weeks after TAM. Bar = 100µm **(G)** Representative image of BMI1 staining in a *Bmi1$^{fl/fl}$* tumor 6 weeks after TAM as measured by IHC. Bar = 40µm

We next wanted to determine whether the failure to respond to tamoxifen treatment was due to retention of Bmi1. Therefore, we collected individual non-responding tumors 24 weeks after treatment and detected Bmi1 by immuno-histochemistry (IHC). We observed strong Bmi1 expression in both *Bmi1*$^{fl/fl}$ and *Bmi1*$^{+/+}$ tumors indicating that tamoxifen induction failed to completely ablate the conditional Bmi1 allele in a subset of the tumors. Only 2 of the 6 remaining *Bmi1*$^{fl/fl}$ tumors displayed a partial reduction of Bmi1 expression by IHC (Figure 1D). This observation could be explained either by widespread repression of the viral locus in all tumor cells or by a selective advantage conferred by retention of Bmi1. To address this question, we challenged a second cohort of animals with tamoxifen and collected tumors after two weeks for histological examination. Interestingly, we noticed that while most tumors from *Bmi1*$^{+/+}$ mice increased in volume, the majority of *Bmi1*$^{fl/fl}$ mice lost volume or displayed little change (Figure 1E). Most of these changes were modest, though, and potentially within the technical error μCT and volume calculations. When we assayed BMI1 expression two weeks after treatment, we detected BMI1 expression in all *Bmi1*$^{fl/fl}$ tumors. Intriguingly, we also observed gross immune infiltration in 2 of 3 *Bmi1*$^{fl/fl}$ tumors analyzed (Figure 1F). In contrast, we did not observe these responses in 3 of 3 *Bmi1*$^{+/+}$ tumors. Together, this data hints that tumors can respond to acute ablation of Bmi1.

To better understand the response of Kras driven lung tumors to acute Bmi1 deficiency, we assessed the kinetics of Bmi1 loss following tamoxifen administration in tumor bearing mice. We collected tumors or measured tumor volume at 1, 2, 4 and 6 weeks after tamoxifen. We found that tumors largely retained BMI1 expression up to 4

weeks post-tamoxifen. However, after 6 weeks we found that 3 out of 6 *Bmi1*$^{fl/fl}$ tumors display a checkered pattern of BMI1 deficient nuclei (Figure 1G). We cannot rule out the possibility that this reflects tumor to tumor variation in the heterogenous ability to inactivate Bmi1. However, this results hints at the possibility that a stable fraction of Bmi1 may persist for an extended period after recombination. Together, this data suggests that a durable response in a subset of tumors may occur if one can achieve efficient and extended loss of Bmi1.

Assessing the response of lung adenocarcinomas to acute Bmi1 ablation *in vitro*

We next wanted to assess the cellular responses to Bmi1 ablation in lung adenocarcinoma. We chose to do so *in vitro* by generating multiple cell lines isolated from individual lung tumors carrying the conditional or wild-type Bmi1 alleles (Figure 2A). Specifically, we crossed our inducible mouse model with mice carrying a heterozygous germ-line deletion of *p53*. We reasoned that loss of heterozygosity of the wild-type allele would be sufficient to propagate lung cancer cells *in vitro*. After initiating tumors with lentivirus packaging FlpO and CreER, we established multiple low passage cell lines from the resulting lesions. These cells did not appear to retain p53 activity as evidenced by their failure to induce p21 following irradiation (Figure 2B). Next, we assessed whether these cells could recombine the Bmi1 allele in response to 4-hydroxytamoxifen (TAM) (Figure 2C). Individual cell lines responded deferentially to TAM treatment. For instance, we identified cell lines that had recombined *Bmi1* without TAM exposure, lines that did not respond to TAM regardless of concentration, and lines that specifically recombined *Bmi1* in response to TAM. No cell line completely

ablated *Bmi1* in the entire population after TAM administration *in vitro*. This was further evidenced by the retention of BMI1 over multiple passages after TAM (Figure

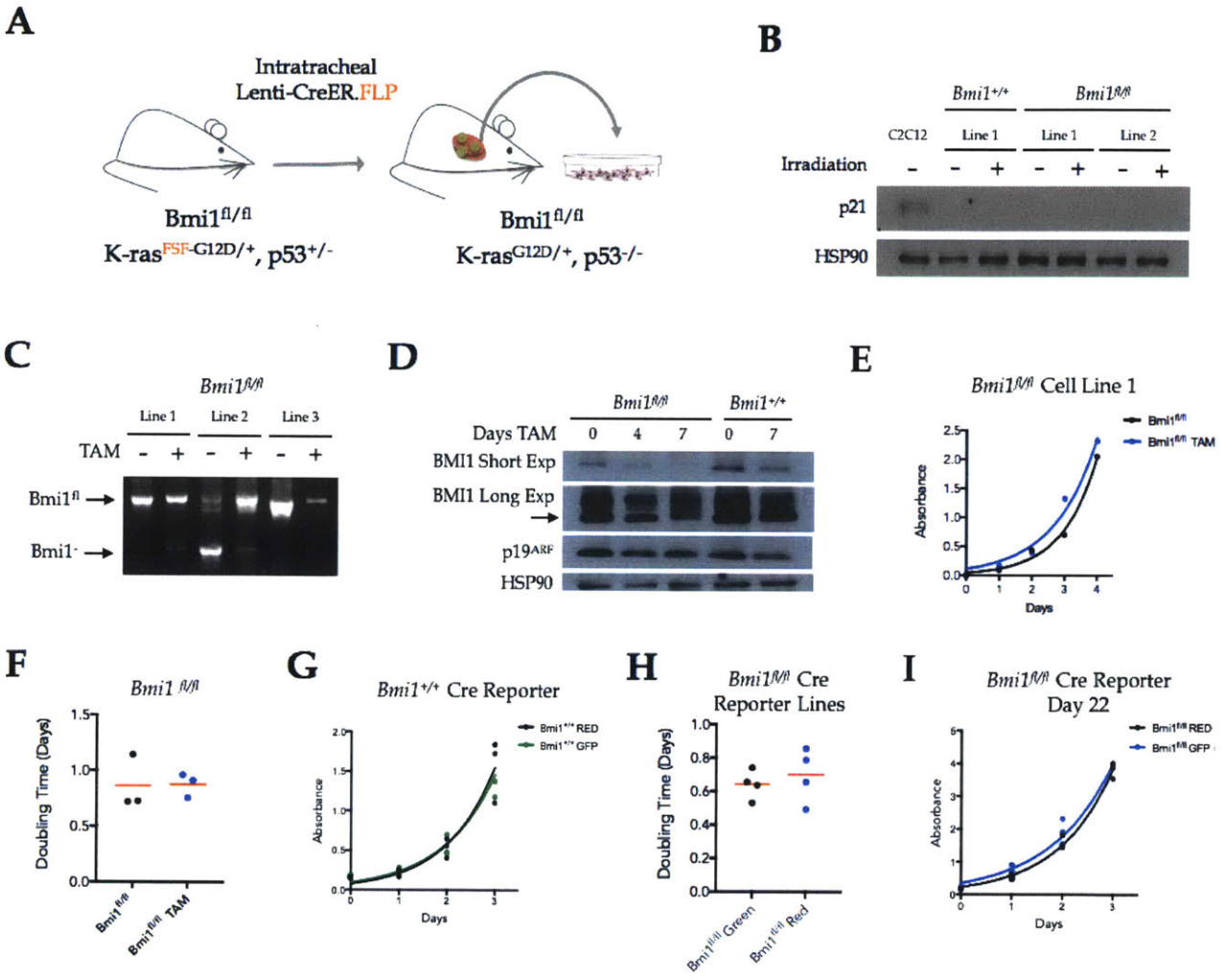

Figure 2. Bmi1 knockdown in isolated mouse lung adenocarcinoma cell lines
(A) Strategy for isolating cell lines in order to modulate Bmi1 *in vitro*. **(B)** Western blot demonstrating that cell lines are p53 deficient. **(C)** Agarose gel of a PCR reaction showing the variable responsiveness of cell lines to 4-OH-tamoxifen (TAM) by recombining the *Bmi1^{fl}* allele. **(D)** Western blot of a TAM responsive cell line several days after TAM treatment. **(E)** Representative growth assay of a *Bmi1$^{fl/fl}$* cell line following TAM or vehicle treatment. **(F)** Doubling times of three independently derived TAM responsive cell lines. Doubling time determined by exponential growth fit. **(G)** Growth curve of sorted *Bmi1$^{+/+}$* cell line with a Cre switchable dsRed/ eGFP reporter construct after TAM or vehicle. **(H)** Doubling times of as measured by growth assays from 4 matched *Bmi1$^{fl/fl}$* TAM responsive cell lines sorted after TAM or vehicle. **(I)** Growth assay of a sorted *Bmi1$^{fl/fl}$* cell line 22 days after TAM or vehicle treatment.

2D). Despite the inability to entirely ablate *Bmi1* in culture, dosing TAM responsive cells resulted in decreased protein levels of Bmi1 (Figure 2D). These cells also induced Luciferase after TAM, indicating latent CreER activity (data not shown). We decided to focus our efforts on TAM responsive cell lines that displayed minimal recombination without TAM and maximal recombination after treatment.

To determine whether Bmi1 deficiency conferred a growth disadvantage, we performed growth assays on TAM and vehicle treated cells from three independent $Bmi1^{fl/fl}$ cell lines (Figure 2E,F). We did not observe any differences in the doubling time of TAM treated cells compared with controls. However, we remained uncertain of the extent of Bmi1 recombination, which confounded our interpretation of the results. Moreover, it is unclear whether partial loss reflects the fact that some cells are wild type for Bmi1 and others are null, or whether these cells only recombine one allele. This led us to employ a Cre reporter strategy to enrich for Bmi1 depleted cells after TAM. Specifically, we infected early passage cell lines with a lentivirus packaging a Cre switchable dared to eGFP construct (Diego S. D'Astolfo et al. 2015). Cells infected with this lentivirus robustly and exclusively expressed dsRed. In the presence of nuclear Cre, the dsRed is excised and eGFP expresses constitutively (data not shown). We infected TAM responsive cell lines with a low multiplicity of infection and sorted for dsRed positive cells. Next, we exposed these cells to TAM or vehicle and sorted for eGFP or dsRed, respectively, to isolate a population of cells exposed to nuclear Cre and controls. Interestingly, we observed that even in TAM responsive cell lines, two thirds of all cells did not induce eGFP indicating that CreER was non-functional in a large percentage of tumor derived cells (data not shown). Five to seven days after sorting, we

assayed the proliferation eGFP positive cells from 4 independently derived TAM responsive cell lines and found no difference in the doubling times o dared versus eGFP positive cells (Figure 3H). We repeated growth curves three weeks after TAM and did not observe growth difference between treatment groups (Figure 3I). Accordingly, despite enriching for Cre activity, eGFP positive cells retained BMI1 protein expression after 3 weeks, indicating a failure to completely ablate Bmi1 in these cells after exposure to nuclear Cre (data not shown). Together, these data reinforce the difficulty of ablating the conditional Bmi1 allele *in vitro,* whether due to technical or biological challenges. They also indicate that partial depletion of Bmi1 does not grossly impact the proliferation of lung adenocarcinoma cell lines in culture.

Variable responses of lung adenocarcinoma cell lines after ablation of Bmi1

Owing to the difficulties of relying on a CreER driven by a tumor initiating lentivirus, we pursued alternative strategies to achieve robust ablation of Bmi1 in tumor cells *in vitro.* First we infected cell lines with various titers of an adenovirus delivering Cre (Figure 3A). High titer adenovirus infections largely depleted BMI1 from these cells. However many cells displayed evidence of senescence that appeared to correlate with infectivity as measured by GFP intensity (Figure 3B). This may indicate that the dose needed to ablate *Bmi1* results in an overwhelming viral response. We let cells recover from infection for several days and assessed their proliferative capacity. Both Cre infected cells and control virus infected cells exhibited decreased doubling time compared to pre infected cells, yet there was no difference in growth of infected cells with or without Cre (Figure 3C). This may indicate that Bmi1 loss does not grossly

impact these cell lines, but we were unable to assess this in the absence of the confounding viral response. We also could not rule out that a subset of Bmi1 responsive cells were selected against before we began our assay.

We wanted to determine whether strict ablation of Bmi1 was required for tumor cell maintenance or proliferation. Therefore, we decided to generate isogenic Bmi1 proficient and deficient cell lines lines using a single cell cloning strategy (Figure 3D). Specifically, we single cell cloned multiple lung adenocarcinoma cell lines from independent tumors and then subjected them to low dose TAM followed by another round of single cell cloning. Using this strategy, we generated isogenic paired Bmi1 proficient and deficient cell lines (Figure 3E). First we determined their doubling times from growth curves (Figure 3F). One of the 3 cell lines displayed a proliferative impairment *in vitro* (Figure 3G). We then tested the capacity of these cells to grow subcutaneously in the flanks of immunocompromised mice (Figure 3H,I,J). Unsurprisingly, the one Bmi1 null cell line that displayed an impairment in *in vitro* proliferation compared to Bmi1 proficient controls also developed xenograft tumors more slowly than its parental control (Figure 3H). Unexpectedly, though, one of the two cell lines that did not show *in vitro* growth impairment nevertheless displayed impaired xenograft growth *in vivo* (Figure 3J). We confirmed this result in a second cohort of mice (Figure 3J). We also observed differences in ability of these cells to colonize and expand in the lung (Figure 3K). However, these cells did not display a differential capacity to form spheroids in soft agar, suggesting that these phenotypes were the result of proliferative *in vivo* (Figure 3L). Thus, we conclude that Bmi1 may be important for the proliferative capacity of tumors depending on the tumor of origin, or the conditions

in which they expand. This may reflect differential requirements by tumor cells based on their underlying genetic landscape.

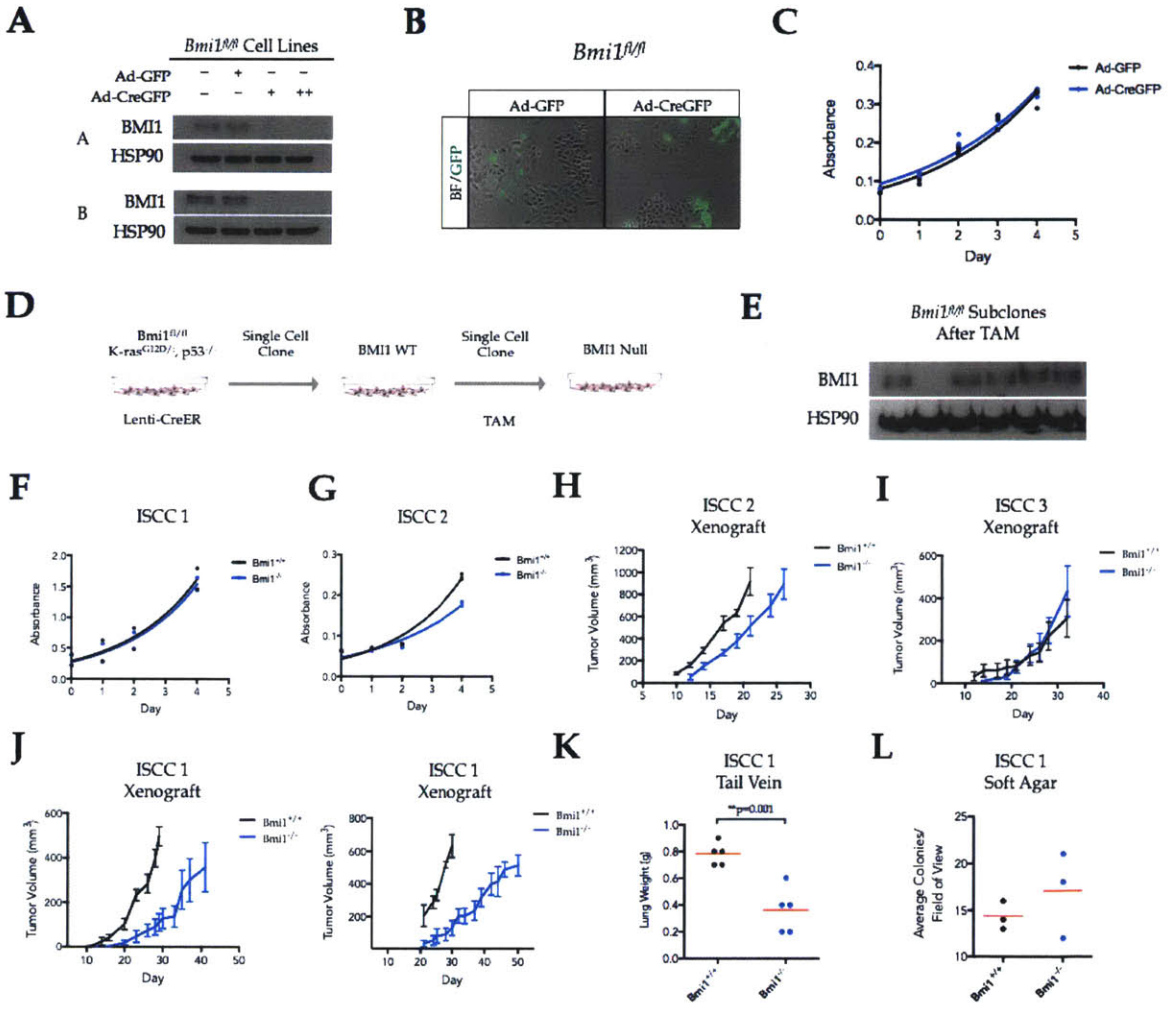

Figure 3. Differential growth responses after *Bmi1* ablation *in vitro*
(A) Western blot of two *Bmi1*$^{fl/fl}$ cell lines (A and B) after infection with adenovirus carrying CreGFP or GFP. **(B)** Merged Brightfield and GFP images of a *Bmi1*$^{fl/fl}$ cell line infected with either adenovirus packaging CreGFP or GFP. **(C)** Growth curve from a *Bmi1*$^{fl/fl}$ cell line after infection with adeno-GFP or adeno-CreGFP. **(D)** Strategy for generating Bmi1 null paired isogenic since cell clones (ISCC). **(E)** Western blot identifying a Bmi1 deficient ISCC. **(F,G)** *In vitro* growth curve of ISCC 1 and 2. **(H,I)** Growth of xenograft in immunocompromised mice from ISCC 2 or 3 injected subcutaneously. **(J)** Replicate experiments of ISCC1 growth subcutanesouly in immunocompromised mice. **(K)** Lung weight three weeks after tail vein injection with matched ISCC1 cell lines. **(L)** Soft agar colony formation of matched ISCC1 lines.

DISCUSSION

Lung adenocarcinomas are known to be heterogenous both in histological presentation as well as underlying mutational landscapes (Chen et al. 2014; Collisson et al. 2014). It is increasingly evident that Polycomb Group proteins (PcGs) play various roles in different tumor types (Koppens and van Lohuizen 2015). Recent studies are uncovering context dependent roles for PcGs based on tumor variability (Fillmore et al. 2015). This suggests that similar context dependent interactions exist for Bmi1 in advanced lung adenocarcinoma. Our previous work identified a crucial role for Bmi1 in sustaining the proliferative capacity of lung adenomas. Bmi1 deficient tumors could eventually progress to advanced grade and regain a high rate of proliferation. It remained unclear, though, whether all tumors are insensitive to Bmi1 loss after attaining advanced grade, or whether a fraction of these lesions maintain a critical dependency on Bmi1. Overall, our data suggest that a subset of lung adenocarcinoma are sensitive to Bmi1 depletion and thus further understanding the genetic interactions in these populations may broaden a therapeutic window.

In this study, we explored whether autochthonous tumors responded to Bmi1 ablation over time. We showed that a subset of *Bmi1*$^{fl/fl}$ lesions regressed when tracked over extended months. Though we were not able to isolate them after euthanasia, we believe that these represented tumor response. First we followed these individual masses by μCT for many weeks to monitor growth before dosing mice with tamoxifen. Second, pilot studies confirmed that we could detect differences between macrophage infiltration and adenoma growth by imaging. Although we cannot confirm that the regressing masses were responding to Bmi1 loss, we remain confident that we tracked

tumors. Therefore, we believer our data reflects that some tumors retain Bmi1 dependency after establishment.

We also present evidence that the immune system plays a role in determining whether or not a tumor responds in the short term. We observed 2 of 3 *Bmi1*$^{fl/fl}$ tumors with a dramatic tumor infiltration. One tumor displayed evidence of immune mediated regression. Bmi1 may impact this recruitment in several ways, including by maintaining the suppression of immune attractants such as chemokines. Interestingly, when we compared the gene expression of adenomas that lost Bmi1 at initiation to Bmi1 proficient tumors, we observed that Bmi1 proficient tumors are enriched for mediators of the immune system (unpublished observations). Indeed, previous studies suggest that inflammation may be critical for tumor growth in mouse models of lung cancer (Rowbotham and Kim 2014). These data may indicate that Bmi1 plays a role in balancing the immune system between pro- or anti-tumorigenic immune responses. This warrants further investigation, since immune checkpoint therapies now exist that might could synergize with Bmi1 loss.

In this study, we also used cell lines generated from tumor bearing mice as surrogates for advanced disease to interrogate roles for Bmi1. To date, our experiments suggest that Bmi1 loss does not impact the proliferation of mixed populations of cells in culture. However, we continue to optimize conditions for these experiments and expect to develop a more robust system in which to confirm these results. Specifically, we have generated cell lines with inducible hairpins to Bmi1 and results from these experiments are forthcoming. Despite the apparent lack of a critical *in vitro* dependency upon Bmi1, we were particularly intrigued by the behavior of one isogenic Bmi1 null cell line that

displayed no proliferative defects in culture, but grew more slowly in subcutaneous xenografts. Overall, two of three isogenic Bmi1 null cell lines displayed impairment in a xenograft model. This raises interesting possibilities that Bmi1 may mediate other interactions with the tumor microenvironment. There a numerous potential ways in which Bmi1 could modulate growth *in vivo*. Particularly intriguing is the notion that Bmi1 can regulate growth in hypoxic conditions. Dovetailing with our previous observations that Bmi1 may impact the rate of DNA replication, a previous report specifically implicated PRC1 component Ring1b in DNA synthesis in hypoxic conditions (Piunti et al. 2014). However, growth rate differences between Bmi1 proficient and deficient cell lines in this xenograft model could also be secondary to recruitment of vasculature or the capacity to grow in three dimensions. Despite these possibilities, we appreciate that single cell cloning may induce cell line variabilities over generations, even from isogenic parental lines. Therefore, the generation of multiple isogenic clones would be necessary in order to more closely assess these phenotypes.

Together, our work suggests that Bmi1 may enforce tumorigenesis in the lung in multiple ways while being dispensable for others. In particular, we show that substantial fraction of established tumors or advanced lung cells are insensitive to Bmi1 loss. This is reminiscent of our previous work demonstrating a critical role for Bmi1 in grade 2 adenomas. We also present evidence that different subsets of tumors or cell lines may have different dependencies for Bm1. Probing the genetic or environmental contexts that mediate this sensitivity would be a valuable resource to inform potential therapeutic strategies.

MATERIALS AND METHODS

Viral Production

Lentiviral backbone pCMV-CreER.2a.FlpO plasmid was developed by Eric Snyder and obtained from Tyler Jacks (MIT). Lentiviral particles were generated by transfection of 293T cells using TransIT-LT1 (Mirus) with lentiviral backbone plasmid and packaging vectors Δ8.9 (gag/pol) and CMV-VSV-G (Dupage et al. 2009). Supernatant was collected at 48 and 72 hours after transfection, concentrated at 25,000 r.p.m with an Optima L-100 XP ultra-centrifuge (Beckman Coulter), and resuspended in Opti-Mem (Gibco). Viral titer was determined using 3TZ cells (Dupage et al. 2009).

Cre Reporter was a gift from Niels Geijsen (Addgene plasmid # 62732). Lentiviral particles were generated by transfection of 293T cells using TransIT-LT1 (Mirus) with lentiviral backbone plasmid and packaging vectors Δ8.9 (gag/pol) and ecotropic EcoENV (Addgene 15802). Supernatant was collected after 24 and 48 hours and immediately diluted 1:4 in DMEM and added to cells.

Mice and Tumor Initiation

Mice harboring $Kras^{FSF\text{-}G12D}$ (Zhang and Kirsch 2015), $p53^{-}$ (Jacks et al 1994), $R26^{LSL\text{-}Luciferase}$ (Safran et al. 2003), and $Bmi1^{fl}$ (Maynard et al 2014) alleles have been previously described. Mice were intubated intratracheally with lentivirus (described above). $Kras^{G12D/+};R26^{LSL\text{-}Luciferase}$ mice were infected with $5x10^4$ lentiviral particles per mouse. $Kras^{G12D/+};p53^{fl/fl}$ mice were infected with 10^5 or 10^4 lentiviral particles or $6x10^7$

adenoviral particles per mouse. Littermates were invariably used as controls. Animal studies were approved by the Committee for Animal Care, and conducted in compliance with the Animal Welfare Act Regulations and other federal statutes relating to animals and experiments involving animals and adheres to the principles set forth in the Guide for the Care and Use of Laboratory Animals, 8th ed. National Research Council, 2011 (institutional animal welfare assurance no. A-3125-01). All animals were maintained on a mixed C57BL/6J x 129SvJ x Balb/c background.

Tamoxifen treatment

Tamoxifen (Sigma T5648) was dissolved in corn oil (Sigma C8267) at 10mg/ml. Mice were dosed at 0.1g/kg (10ul/g) once per day for four days.

PCR

Recombination of $Bmi1^{fl}$ allele was determined using the following primers: $Bmi1^{fl}$ forward (5'- GCT GCT AGC ATT CCT GGT TTT GC-3'), and $Bmi1^{fl}$ reverse (5'-GGT TCC TCT TCA TAC ATG ACG-3').

qRT-PCR

Isolated tumors were snap frozen in liquid nitrogen and pulverized using Geno/ Grinder 2010 (SPEX SamplePrep). RNA from tumors was extracted from frozen powder using TRIZOL Reagent (Invitrogen) and spun to remove non-soluble fraction. RNA from cell lines was extracted using TRIZOL. Following addition of chloroform and centrifugation per manufacturer's protocol, RNA was purified from the aqueous

phase using an RNeasy Mini Kit (Qiagen) including an on column DNAse I incubation step (Qiagen). cDNA was generated using Superscript III RT (Invitrogen) per manufacturer. Real-Time quantitative PCR reactions were performed using SYBR Green PCR Master Mix (Applied Biosystem) and a Step One Plus Real-Time PCR System (Applied Biosystems). All gene expression was shown relative to 18S and normalized to the average value of Bmi1 proficient controls. Primers qPCR were: 18S forward (5'-CGT CTG CCC TAT CAA CTT TGC-3'), 18S reverse (5'-CTT GGA TGT GGT AGC CGT TTC-3'), $p16^{INK4A}$ forward (5'-GCG GGC ACT GCT GGA AG-3'), $p16^{INK4A}$ reverse (5'-CGT TGC CCA TCA TCA TCA CC-3');

Western Blotting

Samples were loaded in SDS Lysis Buffer (8% SDS, 250mM TrisHCl pH 6.6, 40 %glycerol, 5% 2-Mercaptoethanol, bromophenol blue), separated by SDS-PAGE, transferred to a nitrocellulose membrane, and blocked in 5% nonfat milk. The following antibodies were used in 2.5% nonfat milk: Bmi1 (1:10, 5C9 Lees Lab, MyBioscource MBS588325), HSP90 (1:5000, BD 610418), $p19^{ARF}$ (1:1000, Novus 5-C3-1 or 1:500 Santa Cruz sc-7419), p21(1:200, Santa Cruz sc-6246). Secondary HRP-conjugated antibodies (GE) were used at 1:5000 in 5% nonfat milk.

Animal Imaging

Tumor were imaged using eXplore CT-120-whole mouse μCT (GE Healthcare) and MicroView Software. Volume calculations were determined using ImageJ plugin Multi VFF opener 2.

Histology and Immunohistochemistry

Lungs were perfused with 10% formalin and fixed overnight. Tissue was transferred to 70% ethanol, embedded in paraffin, and 4 micron sections were cut. Immunohistochemistry (IHC) was performed using BMI1(1:100, Millipore F6(05-637)) as follows: Rehydrated slides were washed in PBS 0.15% Triton X-100 followed by inactivation of endogenous peroxidases by incubation with 3% H_2O_2 in PBS. Antigen retrieval was performed by heating in an 800 W microwave for 6.5 min at full power followed by three rounds of 5 min at 60% power using a solution 8.2 mM sodium citrate, 1.8 mM citric acid, pH 6.0. Slides were blocked with PBS containing 5% of the appropriate serum and incubated overnight with the primary antibody diluted in PBS 0.15% Triton X-100 or this buffer alone or a non-specific antiserum as controls. Secondary antibodies (Vectastain ABC kits, Vector laboratories) were diluted 1:200 in PBS containing 0.4% of the appropriate blocking serum and detected using a DAB substrate following the manufacturers instructions (Vector Laboratories). For BMI1 staining, a MOM kit (Vector Laboratories) was used according to the manufacturers instructions and an UltraVision LP Detection System (Thermo) for staining. Slides were counterstained with haematoxylin in a Thermo Gemini stainer and coverslips added using the Thermo Consul cover slipper. Images were captured using a Leica Aperio AT2 Digital Slide Scanner and Aperio ImageScope Software v12.3.0.5056 or on a Nikon Eclipse microscope with a DS Ri2 camera and NIS Elements Software.

Lung adenocarcinoma cell line generation and culture

Individual tumors were isolated from mice, washed in PBS supplemented with Pen-Step, minced with razor blades and dissociated for 10-20 minutes in 0.25% Trypsin-EDTA (Thermo). Cells were then passed through a 40 or 100 micron filter, washed in PBS and plated in DMEM supplemented with 10% FBS (Gibco) and Pen-Strep.

All cells were maintained in DMEM supplemented with 10% FBS and Pen-Strep. For TAM treatments, 4-hydroxytamoxifen was diluted in DMSO and treated at 1 or 10μM concentrations for 24 hours. Growth experiments began 24 hours after TAM. FACS sorting experiments began 24 or 48 hours following removal of TAM. For adenoviral experiments, Adeno-CreGFP or Adeno-GFP (Iowa University Vector Core) were infected MOIs of 30, 100, and 200. Where indicated, cells were exposed to 8.0 Gy and collected after 24 hours. All samples were lysed in RIPA Buffer (150mM NaCl, 50mM Tris, 1% Triton X100, 0.5% Deoxycholate, 0.1% SDS, pH 7.4) supplemented with cOmplete Mini tablets (Roche) and 0.2mM $NaVO_4$.

Soft Agar Colony Formation

6-well dishes were prepared with $5x10^4$ cells per well mixed in sterile 0.3% agar using SeaPlaque Agar (Lonza) in warmed DMEM with 10%FBS. Colonies were counted under a microscope as an average of 3 10x fields of view per well after 2 weeks.

Crystal Violet Growth Assay

Cells were plated at 10^4 cells per well. Day 0 wells were fixed 16 hours after plating using 4% paraformaldehyde pH 7.0 for 10 minutes and kept at 4C in PBS. Wells were

fixed every 24 or 48 hours until confluent. Wells were then stained with 0.1% Crystal Violet (Sigma) in PBS for 30 minutes, then washed in water. After drying, stain was dissolved in 10% acetic acid in water and absorbance measured at OD 590nm. An exponential fit of the average of three replicates was used to determine the doubling time for a cell line.

For Cre Reporter experiments, dsRED expressing cells were collected 24 hours after viral infection using a FACS Aria 2 (BD) running BDFACS Diva Software. After TAM or mock treatment as described above, cells were sorted for eGFP or dsRed respectively. After 24 hours of recovery, cells were plated in 6 well plates as described above.

Mouse transplant experiments

For xenograft growth experiments, six to eight week female NCr nude mice (NCr-Foxn1^{nu}, Taconic) were challenged with 10^5 cells subcutaneously in their flanks. Tumor volume was measured over time as $\pi/6$(length x width x height). For tail vein experiments, $5x10^4$ in Opti-MEM (Gibco) were injected into the tail vein of NCr nude mice. Lungs were collected after 3 weeks. All tissue was fixed in formalin overnight and transferred to 70% ethanol. For the extreme limiting dilution assay experiment, six to eight week female NCr nude mice (Taconic) were injected with cells subcutaneously in their flanks at concentrations of 10^4 (2 per cell line), 10^3 (2 per cell line), 10^2 (4 per cell line), and 10 (2 per cell line).

AKNOWLEDGMENTS

We thank Eric Snider for providing the CreER expressing lentiviral vectors used for tumor initiation. We also thank members of the Lees Lab for input during the study and manuscript preparation. We thank the Koch Institute Swanson Biotechnology Center for technical support, specifically the Tang Histology Facility, Animal Imaging and Preclinical Testing Facility, and the BioMicro Center. This work was supported by a Janssen Transcend Grant to J.A.L. who is a Ludwig Scholar at MIT. D.L.K. was supported by an NSF pre-doctoral fellowship.

REFERENCES

Ahuja N, Sharma AR, Baylin SB. 2016. Epigenetic Therapeutics: A New Weapon in the War Against Cancer. *Annu Rev Med* **67**: 73–89.

Brahmer J, Reckamp KL, Baas P, Crinò L, Eberhardt WEE, Poddubskaya E, Antonia S, Pluzanski A, Vokes EE, Holgado E, et al. 2015. Nivolumab versus Docetaxel in Advanced Squamous-Cell Non-Small-Cell Lung Cancer. **373**: 123–135.

Bruggeman SWM, Hulsman D, Tanger E, Buckle T, Blom M, Zevenhoven J, van Tellingen O, van Lohuizen M. 2007. Bmi1 Controls Tumor Development in an Ink4a/Arf-Independent Manner in a Mouse Model for Glioma. *Cancer Cell* **12**: 328–341.

Chen Z, Fillmore CM, Hammerman PS, Kim CF, Wong K-K. 2014. Non-small-cell lung cancers: a heterogeneous set of diseases. *Nat Rev Cancer* **14**: 535–546.

Collisson EA, Network TCGAR, Campbell JD, Brooks AN, Berger AH, Lee W, Chmielecki J, Beer DG, Cope L, Creighton CJ, et al. 2014. Comprehensive molecular profiling of lung adenocarcinoma. *Nature* **511**: 543–550.

Dupage M, Dooley AL, Jacks T. 2009. Conditional mouse lung cancer models using adenoviral or lentiviral delivery of Cre recombinase. *Nat Protoc* **4**: 1064–1072.

Fillmore CM, Xu C, Desai PT, Berry JM, Rowbotham SP, Lin Y-J, Zhang H, Marquez VE, Hammerman PS, Wong K-K, et al. 2015. EZH2 inhibition sensitizes BRG1 and EGFR mutant lung tumours to TopoII inhibitors. *Nature* **520**: 239–242.

Jacks T, Remington L, Williams BO, Schmitt EM, Halachmi S, Bronson RT, Weinberg RA. 1994. Tumor spectrum analysis in p53-mutant mice. *Curr Biol* **4**: 1–7.

Jacobs JJ, Scheijen B, Voncken JW, Kieboom K, Berns A, van Lohuizen M. 1999. Bmi-1 collaborates with c-Myc in tumorigenesis by inhibiting c-Myc-induced apoptosis via INK4a/ARF. *Genes Dev* **13**: 2678–2690.

Jakopovic M, Thomas A, Balasubramaniam S, Schrump D, Giaccone G, Bates SE. 2013. Targeting the Epigenome in Lung Cancer: Expanding Approaches to Epigenetic Therapy. *Frontiers in Oncology* **3**: 1–12.

Kandoth C, McLellan MD, Vandin F, Ye K, Niu B, Lu C, Xie M, Zhang Q, McMichael JF, Wyczalkowski MA, et al. 2013. Mutational landscape and significance across 12 major cancer types. *Nature* **502**: 333–339.

Kazandjian D, Suzman DL, Blumenthal G, Mushti S, He K, Libeg M, Keegan P, Pazdur R. 2016. FDA Approval Summary: Nivolumab for the Treatment of Metastatic Non-Small Cell Lung Cancer With Progression On or After Platinum-Based Chemotherapy. *Oncologist* **21**: 634–642.

Kerppola TK. 2009. Polycomb group complexes--many combinations, many functions. *Trends Cell Biol* **19**: 692–704.

Knutson SK, Kawano S, Minoshima Y, Warholic NM, Huang K-C, Xiao Y, Kadowaki T, Uesugi M, Kuznetsov G, Kumar N, et al. 2014. Selective inhibition of EZH2 by EPZ-6438 leads to potent antitumor activity in EZH2-mutant non-Hodgkin lymphoma. *Mol Cancer Ther* **13**: 842–854.

Koppens M, van Lohuizen M. 2016. Context-dependent actions of Polycomb repressors in cancer. *Oncogene* **35**: 1341–1352.

Kwak EL, Bang Y-J, Camidge DR, Shaw AT, Solomon B, Maki RG, Ou S-HI, Dezube BJ, Jänne PA, Costa DB, et al. 2010. Anaplastic lymphoma kinase inhibition in non-small-cell lung cancer. *N Engl J Med* **363**: 1693–1703.

Maynard MA, Ferretti R, Hilgendorf KI, Perret C, Whyte P, glurt, Lees JA. 2014. Bmi1 is required for tumorigenesis in a mouse model of intestinal cancer. Oncogene **33**: 3742–3747.

McGranahan N, Favero F, de Bruin EC, Birkbak NJ, Szallasi Z, Swanton C. 2015. Clonal status of actionable driver events and the timing of mutational processes in cancer evolution. - PubMed - NCBI. *Sci Transl Med* **7**: 283ra54–283ra54.

Mok TS, Wu Y-L, Thongprasert S, Yang C-H, Chu D-T, Saijo N, Sunpaweravong P, Han B, Margono B, Ichinose Y, et al. 2009. Gefitinib or carboplatin-paclitaxel in pulmonary adenocarcinoma. *N Engl J Med* **361**: 947–957.

Piotrowska Z, Niederst MJ, Karlovich CA, Wakelee HA, Neal JW, Mino-Kenudson M, Fulton L, Hata AN, Lockerman EL, Kalsy A, et al. 2015. Heterogeneity Underlies the Emergence of EGFRT790 Wild-Type Clones Following Treatment of T790M-Positive Cancers with a Third-Generation EGFR Inhibitor. *Cancer Discov* **5**: 713–722.

Piunti A, Rossi A, Cerutti A, Albert M, Jammula S, Scelfo A, Cedrone L, Fragola G, Olsson L, Koseki H, et al. 2014. Polycomb proteins control proliferation and transformation independently of cell cycle checkpoints by regulating DNA replication. *Nature Communications* **5**: 3649.

Rowbotham SP, Kim CF. 2014. Diverse cells at the origin of lung adenocarcinoma. *Proc Natl Acad Sci USA* **111**: 4745–4746.

Safran M, Kim WY, Kung AL, Horner JW, DePinho RA, Kaelin WG. 2003. Mouse reporter strain for noninvasive bioluminescent imaging of cells that have undergone Cre-mediated recombination. *Mol Imaging* **2**: 297–302.

Serresi M, Gargiulo G, Proost N, Siteur B, Cesaroni M, Koppens M, Xie H, Sutherland KD, Hulsman D, Citterio E, et al. 2016. Polycomb Repressive Complex 2 Is a Barrier to KRAS-Driven Inflammation and Epithelial-Mesenchymal Transition in Non-Small-Cell Lung Cancer. *Cancer Cell* **29**: 17–31.

Siegel RL, Miller KD, Jemal A. 2016. Cancer statistics, 2016. *CA: A Cancer Journal for Clinicians* **66**: 7–30.

Zhang M, Kirsch DG. 2015. The generation and characterization of novel Col1a1FRT-Cre-ER-T2-FRT and Col1a1FRT-STOP-FRT-Cre-ER-T2 mice for sequential mutagenesis. *Dis Model Mech* **8**: 1155–1166.

CHAPTER 4: DISCUSSION AND FUTURE DIRECTIONS

INTRODUCTION

In this thesis, I used mouse models of lung adenocarcinoma to interrogate potential roles for Bmi1 in tumor initiation, progression, and maintenance. I found that Bmi1 appears to be dispensable for tumor initiation but impacts overall survival of tumor bearing animals. I also found that Bmi1 is tumor suppressive by decreasing the proliferative capacity of grade 2 lung adenomas. Gene expression analysis implicated Bmi1 in affecting cell cycle phasing and the repression of developmental regulators. Importantly, I found that Bmi1 contributes to the advancement of tumors toward high grade adenocarcinomas. I also show that the adaptive response to Bmi1 loss results in atypical expression of dedifferentiation markers. Using both mouse models and cell lines, I then presented evidence that a subset of advanced tumors may be sensitive to loss of Bmi1. Taken together, my work clarifies essential roles for Bmi1 in lung tumor biology and suggests that a therapeutic window may exist for the targeted intervention of patients present with this deadly disease. Below I will discuss the implications of my work in more detail, as well as potential ways to address outstanding questions.

Clarifying the role of Bmi1 in maintaining *Cdkn2a* repression in the lung

In this work I used several orthogonal experiments to assess whether Bmi1 loss activates two tumor suppressors transcribed from the *Cdkn2a* locus - $p16^{INK4A}$ and $p19^{ARF}$. I focused my attention on the genes encoded from *Cdkn2a* largely because they are historically tied to Bmi1 as primary targets by which it exerts pro-tumorigenic and self-renewal effects. More importantly for this thesis, though, several previous studies reported that loss of Bmi1 in either lung adenomas or in a lung stem cell populations resulted in the up-regulation of $p19^{ARF}$ (Dovey et al. 2008; Becker et al. 2009; Zacharek et al. 2011; Young and Jacks 2010). One of these studies was previously published from our lab using a Kras driven model of lung adenoma (Dovey et al. 2008). All demonstrated that $p19^{ARF}$ was deregulated after Bmi1 deficiency. One of these studies further identified a critical role for Bmi1 in regulating imprinted loci, with the cell cycle inhibitor p57 emerging as a critical mediator of self-renewal following Bmi1 loss. One study tried to knock down Bmi1 in established Kras driven lung cancer and found modest $p19^{ARF}$ derepression (Young and Jacks 2010).

My results appear to strongly contrast with these reports. I found no evidence of changes in *Cdkn2a* expression by immunohistochemistry or immunofluorescence. I also closely examined $p16^{INK4A}$ and $p19^{ARF}$ levels by isolating RNA from multiple grade 2 tumors - where Bmi1 loss leads to proliferative defects - and did not find any changes after Bmi1 loss. This was confirmed on an independent sample of 48 lesions by high-throughput transcriptome sequencing. Furthermore, a gene signature corresponding to Bmi1 deficiency in lung adenomas did not enrich for human lesions displaying mutations in *Cdkn2a*. Lastly, I either knocked down or ablated Bmi1 in lung

adenocarcinoma cell lines and did not detect transcript or protein differences compared with controls. Together, I show that Bmi1 impacts tumorigenesis independent of maintaining this locus.

Overall, I believe that the differences between my work and previous studies reveal differential requirements for Bmi1 during lung development compared with tumorigenesis. In particular, a main advantage of my work is that I directly address the role for Bmi1 in tumorigenesis by bypassing any role for Bmi1 in development. Although the lungs appear to grossly develop normally in Bmi1 deficient backgrounds - with comparable numbers of different cell types - the previous studies demonstrated that bronchi-alveolar stem cells (BASCS) displayed impaired self renewal capacity both *in vitro* and *in vivo* (Dovey et al. 2008; Zacharek et al. 2011). This implicates Bmi1 in lung development and/or in progenitor maintenance. Furthermore, a review of the literature related to Bmi1's interaction with *Cdkn2a* uncovers an intriguing correlation between *Cdkn2a* derepression and Bmi1 deficiency throughout embryogenesis. This is most striking in the context of the neuronal compartment, but is also found in the other tissues (Jacobs et al. 1999a; Bruggeman et al. 2007; Gargiulo et al. 2013; Fasano et al. 2007; Pietersen et al. 2008; Hoenerhoff et al. 2009) Interestingly, modulation of Bmi1 after development in different hematological compartments suggests that not all lineages maintain a requirement for Bmi1 to restrain *Cdkn2a* (Liu et al. 2012; Jagani et al. 2010; Mourgues et al. 2015). However, an exhaustive examination of Bmi1 knockdown in adult tissues and its effect on *Cdkn2a* has not been performed, so these observations from the literature are limited. Together with my data, I suspect that these studies reveal

an important role for Bmi1 in establishing the long term repression of this loci in progenitors during lung development, but not necessarily in tumorigenesis.

Critically, both *Cdkn2a* and imprinted genes are often regulated by DNA methylation (Herman et al. 1996; Weisenberger 2014; Reik et al. 1987). Several studies have implicated PRC1 in establishing methylation boundaries during development or fate commitment, including one directly linking DNMT1 with Bmi1 (Negishi et al. 2007; Ku et al. 2008; Puschendorf et al. 2008). One hypothesis would be that during lineage commitment, Bmi1 assists in faithful transmission of DNA methylation in the lung. To test this, one could cross the conditional allele of Bmi1 with lineage specific Cre recombinase, isolate the populations and assay genome-wide methylation over a developmental time-course. Such an experiment could inform the community to the extent to which PRC1 and Bmi1 informs the heritability of DNA methylation.

An alternative hypothesis to explain the differences between my findings and some of the previous reports relates to the choice of lung cancer models between the studies. Much of the data related to $p19^{ARF}$ derepression was explored in Bronchi-avleolar Stem Cells (BASCSs), which represent only one potential tumor initiating cell population in the lung. It is possible that viral exposure induced oncogenic Kras preferentially leads to lesions from Alveolar Type II (ATII) cells compared with oncogenic activation through spontaneous recombination. If ATII cells are not dependent on Bmi1 for sustaining $p19^{ARF}$ repression, then perhaps the tumors that arise from this population maintain that independence. A critical examination of the self-renewal capacity of ATII cells in the absence of Bmi1, and an eye on $p19^{ARF}$, may shed light on this possibility.

Bmi1 is dispensable for lung tumor initiation

A central question regarding my work is whether Bmi1 loss enhances overall survival by limiting the number of emerging lesions and/or by impacting the tumors post-initiation. My data clearly demonstrate that at least the latter is true, since I show defects in proliferation and size in Bmi1 deficient lung tumors. Furthermore, the size difference between $Bmi1^{fl/fl}$ and $Bmi1^{+/+}$ lesions is exaggerated over time, implicating the sustained requirement of Bmi1. This can also be seen when I track the tumor burden of individual mice over extended weeks, where I find a long term growth deficiency even after normalizing to a time after tumor establishment. The variability in tumor emergence in these mice prevents me from strongly claiming that Bmi1 does not affect tumor initiation, however overall my data indicate that it is not a critical determinant of overall differences in survival.

Assessing tumor initiation is challenging due to some technical limitations of the model itself. First, there appears to be variability in tumor number from virally induced oncogenic Kras (Dupage et al. 2009). This may be due, in part, to the delivery of the virus. More likely, though, oncogenic Kras requires several cooperating events in order to lead to an overt lesion. This is evidenced by the stochastic nature in which we see tumors arise in the lung, as well as the fact that simultaneous ablation of p53 reduces tumor latency. Regardless, I did not detect significant differences in tumor numbers in early times after infection. If anything, I noticed a trend towards a higher number of lesions in $Bmi1^{fl/fl}$ mice although their sizes are roughly equivalent to wild-type. Interestingly, as I examined tumor number at later times, I noticed that there were

significantly fewer tumors in these mice. Unfortunately this is confounded by the fact that *Bmi1*$^{+/+}$ tumors are larger and therefore may be falsely overrepresented in a given lung section. Since we have no evidence of apoptosis, and few instances of immune destruction of these lesions, I suspect that the tumor number per section largely represents growth defects rather than initiating defects.

To overcome the variability in tumor initiation in this model, I interrogated tumor number in *Bmi1*$^{fl/fl}$ mice more closely in the absence of p53. The reduced latency of tumor onset in these mice results in more consistent tumor emergence soon after infection. In repeat experiments, I looked at tumor numbers 6 weeks post-initiation. While not significant, the data hints at slight trend toward fewer initiating tumors. Size differences between genotypes remains a confounding covariant. Nevertheless, since there are several purported tumor cells of origin, my data formally leaves open the possibility that Bmi1 deficiency is critical for the initiation from one of these cell types. For this to occur, different tumor cells of origin must maintain different kinetics of tumor emergence. In fact, several early papers reported that the onset of one subtype in mice, the papillary subtype, is delayed compared with solid tumors, but when they emerge, they do so more aggressively (Kauffman 1981). Furthermore, a recent report suggested that papillary tumors initiate from a distinct club cell population that expresses the marker CCSP (Sutherland et al. 2014). Interestingly, I noticed a dramatic reduction in the number of tumors displaying a papillary-like phenotype in *Bmi1*$^{fl/fl}$ mice at given times. Therefore, I set out to more carefully assess whether depletion of a hypothetical Bmi1 sensitive papillary tumor initiating population could explain my observations. In brief, I found that tumors with papillary features arise with slower

kinetics in Bmi1 deficient mice, but that this is likely a secondary effect due a prominent role for Bmi1 during tumor progression. I found that papillary-like tumors in Bmi1 proficient mice tend to emerge within solid lesions as they increase in size and as they reach advanced grade. Importantly, I am able to detect Bmi1 deficient papillary-like tumors in our mice but only in advanced lesions. Lastly, when examining the frequency of papillary-like lesions in *Bmi1*$^{fl/+}$ and *Bmi1*$^{fl/fl}$ mice I found comparable levels in grade 3 adenocarcinomas. Together, then, Bmi1 loss is likely not differentially affecting a tumor cell of origin.

While these results clarify the role of Bmi1 in papillary-like tumors, my analysis may also contribute to the better understanding of this tumor phenotype in a *Bmi1*$^{+/+}$ background. I observed an equal proportion of papillary-like adenomas in mice where tumors are either driven by a constitutive Cre and by a Cre from the ATII cell promoter SPC. Confounding the interpretation of this result, BASCs - another tumor initiating cell population - expresses SPC and can reconstitute club cells (Kim et al. 2005). However, if a large fraction of the papillary-like tumors derive from club cells, I would expect to see a partial depletion in papillary-like tumors from this experiment. A more informative experiment would involve initiating tumors from an ATII specific marker such as LysM. A recent paper using such a driver commented in passing that they observe papillary lesions in resulting tumors (Desai et al. 2014).

An important remaining question is whether human papillary tumors are reflective of the peripheral papillary-like lesions we see in our mouse model, or whether they more closely resemble club cell derived papillary tumors. This is particularly relevant for understanding the molecular underpinnings of the micropapillary

histological subtype, since it strongly correlates with poor prognosis in humans (Lee et al. 2015). Therefore, identifying mouse models that may reflect this histological presentation is an unmet need. Notably, I maintained histological data on all 48 tumors that were sequenced for the digital gene expression signature. This dataset includes papillary tumors in which I can run differential expression analysis in order to identify papillary-specific signatures. I have previously identified a human signature from Kras mutant papillary vs solid tumors from publicly available TCGA transcriptomes. Together, this data could be used to assess the extent to which papillary-like tumors in this model reflect this important subtype in human disease. Since I already have evidence of distinct biological outputs from the tumors with this subtype, such as an increase phospho-ERK staining and a higher proliferative index, future experiments may be able to further elucidate any underlying genetic vulnerabilities reflected by this phenotype.

Grade transitions in mouse lung tumors reflect grade transitions in the human disease

Mouse models have been fruitful tools for the study of Kras driven lung adenocarcinoma. This has been particularly true for interrogating late events in tumorigenesis, such as mechanisms contributing to highly advanced and metastatic disease. These studies have clear implications for humans since the majority of cancer patients succumb due to advanced metastatic disease. However, there has been relatively little analysis using this tool to directly compare whether the molecular mechanisms informing lower grade transitions reflect comparable events in human disease. Though this is secondary to the primary nature of my thesis, the role of Bmi1

in lung adenomagenesis, I believe it is worth a brief discussion since my work touches on this topic. Specifically, part of the transcriptomic analysis I performed on the mouse tumors encompassed a comparison of grade 2 and grade 3 lesions. In fact, an unbiased analysis of all 48 tumors extracted a primary signature reflective of grade. When applied to 457 human tumors, this signature was significantly prognostic of poor survival even after adjusting for a number of other covariants. Strikingly, this signature was enriched for higher grade lung adenocarcinoma and borderline intersected in the survival analysis, suggesting that the grade transition in mice may reflect an underlying mechanisms in humans. This result is significant for several reasons. First, this dataset buttresses the use of this mouse model for interrogation of molecular mechanisms underlying grade transitions. These events have clear implications for survival and may represent a distinct set of potentially novel pathways that can prolong lifespan. Furthermore, a significant fraction of patients present with low grade disease at diagnosis (Sun et al. 2006). A more comprehensive understanding of this transition, then, may lead to novel therapeutic interventions that manage disease by blocking tumor progression. It may also assist in clarifying diagnostic decisions concerning patient care and therapy. I demonstrated in this work, for instance, that a tumor suppressive phenotype in early, but not advanced, tumors is prognostic of improved survival of patients with low grade tumors. Lastly, there have been surprisingly few gene signatures that specifically identify differences between histological grades. Therefore, closer interrogation of this dataset may prove valuable for uncovering novel pathways involved in grade transitions.

Bmi1 sustains the proliferative capacity of grade 2 lung adenomas

In this thesis, I showed that Bmi1 deficient tumors display impaired proliferative capacity specifically in grade 2 adenomas. Importantly, once Bmi1 deficient tumors progressed to higher grades, I observed no alterations in the proliferative index between genotypes. This explains the variation in tumor size, tumor burden, and overall survival between $Bmi1^{fl/fl}$ and $Bmi1^{+/+}$ mice after tumor initiation. Intriguingly, there is a dramatic reduction in grade 3 adenocarcinomas in both mouse models of Kras driven lung cancer - those driven by $Kras^{G12D/+}$ with or without $p53^{fl/fl}$. I speculate that the decreased proliferative capacity of Bmi1 deficient tumors may contribute to the delay in tumor progression.

There is a longstanding argument in the cancer community about the interdependence of cancer cell proliferation and tumor progression. This was most recently stoked by a recent report suggesting that the number of stem cell divisions during development for a given tissue directly correlates with the tumor incidence in the tissue (Tomasetti and Vogelstein 2015). While this idea is still not settled in the field, it nevertheless highlights a fundamental idea that the cells are most vulnerable for the acquisition of mutations or copy number alterations during the cell cycle (Loeb 2011). In the context of cancer, this may relate to frequency by which a cell may acquire pro-tumorigenic events, a hypothesis first postulated in 1914 by Theodor Boveri (translated in Boveri 2008). Multi-step acquisition of pro-tumorigenic events is also known to be critical in lung adenomagenesis. Therefore it is reasonable to speculate that in the case of Bmi1 deficient tumors, the number of cell divisions after initiation may partially determine the latency with which tumors progress to advanced grade.

Bmi1 has been implicated in sustaining the proliferation of both stem cells and cancer cells in various tissues. The most common target described is the *Cdkn2a* locus discussed previously. However, Bmi1 has been shown to regulate many other cell cycle inhibitors such as p21, p27, and p57 (Hu et al. 2014; Fasano et al. 2007; Zheng et al. 2014; Zacharek et al. 2011). Close examination of protein and transcript levels suggest these factors are not mediating the proliferative impairment I observe in Bmi1 deficient grade 2 adenomas, though p57 transcript levels were significantly induced in our transcriptomic analysis. Instead, sequencing revealed a clear enrichment of transcripts associated with the cell cycle in Bmi1 deficient tumors. This is particularly surprising given the decreased number of cells that I observed undergoing DNA synthesis at any given time. Indeed, I presented evidence that more cells expressed cell cycle markers such as Ki67 than were actually undergoing DNA synthesis in Bmi1 deficient tumors compared to controls. This suggests that the cell cycle is being delayed or blocked after the restriction point of the cell cycle. While I cannot rule out a role for p57 in this process, it is likely that any delay is independent of cell cycle inhibitors. Recent reports suggest that PRC1 is directly involved in maintaining the rate of replication fork processivity independent of cell cycle inhibitors (Piunti et al. 2014; Bravo et al. 2015). Other reports suggest a role for Bmi1 in directly regulating DNA synthesis after DNA damage (Ginjala et al. 2011; Liu et al. 2009; Chagraoui et al. 2011). My analysis showed that cells from $Bmi1^{fl/fl}$ grade 2 adenomas undergoing DNA replication incorporated less BrdU over a 1 hour pulse than $Bmi1^{+/+}$ controls or $Bmi1^{fl/fl}$ grade 3 lesions from the same lungs. I observed this in both $p53^{fl/fl}$ and $p53^{+/+}$ backgrounds. This work, then, may reveal a less appreciated role for Bmi1 in these processes. Preliminary data suggests

that there is no change in the rate of DNA synthesis in Bmi1 deficient tumor cell lines propagated *in vitro*. Since it is technically difficult to capture cell cycle phasing from isolated grade 2 adenomas, I am currently attempting to analyze the DNA content in grade 2 adenomas on histological sections using several staining or fluorescent methods. Focusing specifically on DNA of cells expressing Ki67, I would develop a tumor cell cycle profile from histological sections. Alternatively, I envision developing an *in vitro* system to test how Bmi1 may modulate the cell cycle in isolated tumor initiating cell populations such as BASCs or ATII cells. These populations are known responders to Kras activation and I have already developed several tools in which to modulate Bmi1 and walk these cells through the cell cycle.

An important feature of tumor progression in both mouse and human lung adenocarcinoma is nuclear atypia and copy number alterations. In fact, this mouse model of Kras driven lung cancer relies on copy number changes to drive tumorigenesis rather than on mutational events (Westcott et al. 2014). One of the reasons that p53 deficient tumors progress more rapidly is that they are able to bypass apoptotic and cell cycle checkpoints induced by these stressful events. Since I observe stark changes in tumor progression dependent on Bmi1 status, it is reasonable to consider a potential role for Bmi1 directly in the toleration of copy number changes. This role might or might not be independent of any cell cycle defect. While I have no direct evidence to support this hypothesis in my mouse model, Bmi1 and Polycomb proteins have been described to play comparable roles in other settings. Bmi1 may be involved in maintaining genomic integrity after DNA damage by recruiting proteins dependent on ubiquitin signaling (Ismail et al. 2010). Polycomb proteins are also classically know to

regulated dosage compensation events on the X chromosome (Wutz 2011). Further, different roles of PcGs in the maintenance of heterochromatin and long term heritable repression of loci are well characterized (Wutz 2011). It would be of interest to test whether similar functions are involved for Bmi1 in the presence of aneuploidy. I anticipate that it would be informative to first determine whether Bmi1 impacts tolerance to aneuploidy in immortalized mouse diploid cell lines before extending this role to lung cell populations.

In the context of lung adenocarcinoma, copy number alterations may pose a similar hurdle as global transcriptional activation. Over-expression of Myc, for instance, correlates with a CpG Island Methylator Phenotype (CIMP) characterized by global hypermethylation in a subset of lung adenocarcinoma (Collisson et al. 2014). In this context, DNA methylation may serve as a mechanism by which cancer cells inhibit the expression of tumor suppressors that would otherwise be induced by over-expressing Myc or hyperactive signaling from Kras (Kress et al. 2015; Zuber et al. 2000). In fact, PRC1 has repeatedly been shown to repress Myc targets in various contexts (Jacobs et al. 1999b; Guney 2006). One of the major putative Bmi1 targets from my analysis is Gata4, that is recurrently methylated in human CIMP tumors, and also a target of Myc in lung adenocarcinoma (Collisson et al. 2014; Castro et al. 2013). These circumstantial data may warrant a closer examination of Bmi1's role in mediating tolerance to global transcriptional activators and copy number alterations in lung adenocarcinoma. I am currently testing this hypothesis by correlating a gene signature based on Bmi1 proficiency with an annotated set of CIMP high, intermediate, and low

human TCGA tumors. If Bmi1 acts, in part, through such a mechanism then inhibiting Bmi1 may synergize with DNMT inhibitors.

Bmi1 sustains the repression of alternative differentiation programs

My transcriptomic analysis of Bmi1 deficient tumors revealed a dramatic enrichment of a small number of non-lung developmental regulators. This is in line with previous data implicating a critical role for PRC1 and Bmi1 in repressing alternative lineages during fate-commitment (Bracken et al. 2006). Bmi1 is also described to restrain transcription at poised promoters of developmental genes (Oguro et al. 2010). Furthemore, loss of the PRC1 core subunit Ring1b derepresses alternate lineages, which in some cases can result in tumor suppression (Chiacchiera et al. 2016). In light of this, I will briefly highlight a few of these candidates and describe known roles.

TBX15

Tbx15 is a member of the T-box family of transcription factors that regulate early fate choice decisions (Naiche et al. 2005). It is expressed in early bone and limb development and *Tbx15* null mice are small in stature displaying skeletal and mesenchymal progenitor defects (Singh et al. 2005). Very little is know about its targets. However, this transcript is strongly induced in nearly all of the Bmi1 deficient samples, and not expressed in Bmi1 proficient samples. Fortuitously, one of the few reports of a role for Tbx15 in tumorigenesis identified it as a direct Bmi1 target by chromatin immuno-precipitation (Yuan et al. 2011). Derepression of Tbx15 was found to be a potent tumor suppressive independent of *Cdkn2a*. Together, my data and the literature

implicate this protein as good candidate to pursue as a potential tumor suppressor in lung adenocarcinoma.

ZFHX4

Similar to Tbx15, there are few reports describing roles for Zfhx4. It is thought to act as as a transcription factor in neuronal differentiation and is suppressed in muscle lineages (Hemmi et al. 2006). However, it was described as a factor that mediates the self-renewal capacity of glioma tumor initiating cell populations by mediation of differentiation (Chudnovsky et al. 2014). Furthermore, it is mutated in 27% of TCGA lung tumors - the seventh most frequently mutated gene in 522 human lung adenocarcinoma. There are also several recurrent mutations sites.

GATA4

Gata4 is in some ways the most intriguing target identified. As mentioned, it is a known target of Myc in adenocarcinoma and recurrently repressed in CIMP high lesions (Castro et al. 2013; Collisson et al. 2014). Similar to the other transcription factors I described, Gata4 is not expressed in the lung but is involved in lineage specification during development (Lowry and Atchley 2000). It plays a prominent role in cardiac differentiation, and a recent paper identified Bmi1 as a main barrier in cardiac reprograming due to its direct repression of Gata4 (Zhou et al. 2016). Interestingly, Gata4 has been described as a tumor suppressor in some contexts, but one report hinted that marks advanced disease in lung cancer (Hellebrekers et al. 2009; Castro et al. 2013).

Other Developmental Regulators

In addition to these factors, I found a number of other deregulated transcripts from developmental factors in Bmi1 deficient tumors. Given the broad roles for

polycomb and other epigenetic regulators, a tumor suppressive effect may depend on the deregulation of multiple of these factors in concert. Testing all candidates in mice individually would be exhaustive, though there is strong incentive to do so for the top three candidates described above. To determine whether potential derepression of developmental targets contributes to the tumor suppressive phenotype after Bmi1 loss, I would express tiled guide RNAs targeting these factors packaged with Cre during viral delivery and infect $Bmi1^{fl/fl}$ and $Bmi1^{+/+}$ mice in the context of $Kras^{LSL\text{-}G12D/+}$;$R26^{LSL\text{-}Cas9}$ mouse. After identifying whether or not any of these act as mediators of the Bmi1 dependent phenotype, I would use a pooling strategy to interrogate which candidates are major contributors. Conversely, I could attempt to over-express these factors in $Bmi1^{+/+}$ tumors, individually or as a group, to determine whether they act as tumor suppressors. Recent advances in transplant models may facilitate these experiments (Zheng et al. 2013).

Adaptation to BMI1 loss

Among the most striking findings in this work is the apparent adaptive response by tumors to Bmi1 deficiency. While I observe a consistent tumor suppressive phase that correlates with grade 2 adenomas, mice with Bmi1 deficient tumors eventually succumb to disease. Further, many of these tumors broadly express Hmga2 in an atypical manner compared with progression in $Bmi1^{+/+}$ tumors. It is tempting, then, to speculate that Hmga2 expression is a compensatory mechanism to Bmi1 loss.

Hmga2 is a chromatin regulator involved in restructuring and organizing the nucleus in embryogenesis. It is often expressed in advanced cancers and may indicate

progression to an advanced stage disease, particularly in lung adenocarcinoma. Hmga2 is typically detected after a decrease in the expression of Nkx2.1, a lung lineage marker and tumor suppressor in this model (Winslow et al. 2011). This suggests that Hmga2 reflects a more dedifferentiated phenotype. Interestingly, Bmi1 expression decreases in grade 3 lesions, the inverse of Hmga2 expression. Furthermore, Hmga2 is known to repress similar targets in other contexts, such as *Cdkn2a* (Tzatsos and Bardeesy 2008). Thus, Hmga2 might be co-opting a Bmi1-like oncogenic function in the context of advanced dedifferentiated tumors.

One of the highest differentially expressed genes between grade 2 $Bmi1^{fl/fl}$ and $Bmi1^{+/+}$ tumors is Porcn, which is a regulator and general co-activator of Wnt signaling (Clevers and Nusse 2012). Wnt activation has been reported to lead to Hmga2 expression (Cheng et al. 2015). Interestingly, we also find Plag1, an activator of Wnt and Igf2 expression, overexpressed in Bmi1 deficient tumors (Declercq et al. 2008). Indeed, Igf2 stands out as one of the most differentially expressed genes only when comparing grade 3 $Bmi1^{fl/fl}$ and $Bmi1^{+/+}$ tumors. Perhaps, then, these connected pathways are being deregulated as a consequence of Bmi1 ablation, are selected for during adenomagenesis, and contribute to tumor adaptation and progression. I have little functional evidence directly arguing for these roles in adaptation mechanisms. Before interrogating these further, I would examine our histological sections for protein expression of these pathways during tumor progression. Ultimately, there are several small molecule modulators of the Wnt pathway that may synergize with Bmi1 loss and inhibit progression to advanced disease. Nevertheless, careful mining of the transcriptomic

landscape that I describe in this thesis may prove fruitful for uncovering the molecular basis of an adaptive response by tumors to Bmi1 loss.

Therapeutic implications of targeting BMI1 in lung adenocarcinoma

In many ways my thesis project was designed to probe the therapeutic benefit of targeting Bmi1 or it downstream effectors. Overall, the data I present in Chapter 2 suggests that the bulk of the therapeutic window exists in lower grade lesions, before they progress to advanced disease. In Chapter 3, I presented evidence that Bmi1 is dispensable for the majority of advanced cancer cells such as those that propagate *in vitro*. However, my data does not preclude the possibility that a subset of more advanced tumors might be sensitive to Bmi1 inhibition. Below I will describe alternative strategies for assessing roles for Bmi1 in established lung adenocarcinomas.

Autochthonous mouse models are valuable resources for interrogating tumor responses in a context that best mimics those in human patients. However, the key feature of spontaneously arising tumors is inter-tumoral heterogeneity, such as unique dependencies and genetic alterations. I explicitly saw this variation reflected in my transcriptomic analysis. A major technical limit that I encountered in my attempts to ablate Bmi1 in an established autochthonous setting was the variable silencing of the viral locus expressing CreER. Even in settings where CreER remained expressed, though, I found it difficult to entirely ablate Bmi1. This could be due to the fact that the Bmi1 locus is sterically protected from Cre access. Interestingly, in a chromatin immuno-precipitation experiment in the intestine that I did not discuss in this thesis, I found that a major target of Bmi1 is its own locus. Inaccessibility may explain why cells

can regularly recombine a reporter allele, but maintain Bmi1 expression over many generations. This also raises the formal possibility that one alleles is repressed and I am consistently observing heterozygous loss of Bmi1 in culture. Regardless, I am confident that part of the technical difficulties of ablating Bmi1 in established tumors *in vivo* lie in the frequent repression of the viral integration site in tumors.

I propose two strategies to overcome these technical hurdles. Firstly, the lab has developed two mouse alleles of doxycycline inducible hairpins targeting Bmi1. In data that I did not present, I have demonstrated that these alleles knock down Bmi1 *in vivo* and that global Bmi1 knockdown is well tolerated over extended time frames. To test whether Bmi1 is required for tumor maintenance, I propose crossing this mouse with $Kras^{G12D/+}$ and inducing tumors with adenovirally packaged Cre Recombinase. Low titer infection would allow me to track individual tumors by μCT and IVIS depending an included Cre reporter. In the presence of a global rtTA allele, doxycycline mimics the effects of a system small molecule inhibitor against Bmi1. Additionally, since these adenomas universally express SPC, I would cross the Bmi1 hairpin allele with an allele expressing rtTA from the SPC promoter. This would restrict Bmi1 knockdown to the lung epithelium and tumors, thereby avoiding any secondary effects from targeting Bmi1 in the microenvironment. An alternative strategy would be to continue to rely on CreER and the $Bmi1^{fl}$ allele, but to express CreER from a germ-line allele instead of a viral integration. In order to restrict CreER expression to the tumor, I would cross $Kras^{FSF\text{-}G12D/+}$ mice with $R26^{FSF\text{-}CreER}$ mice in the context of a $Bmi1^{fl/fl}$ or $Bmi1^{+/+}$ background. Therefore, initiating tumors with adenovirus packaging Flp recombinase would lead to CreER expression in initiated tumors. I suspect this strategy would

reduce the technical challenges of assessing the therapeutic window of Bmi1 modulation *in vivo*.

Concluding Remarks

Due in part to its widely described oncogenic roles, there is broad interest in assessing the therapeutic benefit of targeting Bmi1. Indeed, there are now small molecules reported to specifically inhibit Bmi1 in humans (Kreso et al. 2014). This thesis sheds light on potential therapeutic windows in which targeting Bmi1 may be efficacious. It also probes potential mechanisms by which Bmi1 loss confers a tumor suppressive effect and offers resources to further interrogate this complicated biology. Understanding the genetic dependencies of Bmi1 as well as further insights into the mechanisms by which tumors evade Bmi1 loss may broaden that window.

REFERENCES

Becker M, Korn C, Sienerth AR, Voswinckel R, Luetkenhaus K, Ceteci F, Rapp UR. 2009. Polycomb group protein Bmi1 is required for growth of RAF driven non-small-cell lung cancer. *PLoS ONE* **4**: e4230.

Boveri T. 2008. Concerning the Origin of Malignant Tumours by Theodor Boveri. Translated and annotated by Henry Harris. *J Cell Sci* **121**: 1–84.

Bracken AP, Dietrich N, Pasini D, Hansen KH, Helin K. 2006. Genome-wide mapping of Polycomb target genes unravels their roles in cell fate transitions. *Genes Dev* **20**: 1123–1136.

Bravo M, Nicolini F, Starowicz K, Barroso S, Calés C, Aguilera A, Vidal M. 2015. Polycomb RING1A- and RING1B-dependent histone H2A monoubiquitylation at pericentromeric regions promotes S-phase progression. *J Cell Sci* **128**: 3660–3671.

Bruggeman SWM, Hulsman D, Tanger E, Buckle T, Blom M, Zevenhoven J, van Tellingen O, van Lohuizen M. 2007. Bmi1 Controls Tumor Development in an Ink4a/Arf-Independent Manner in a Mouse Model for Glioma. *Cancer Cell* **12**: 328–341.

Castro IC, Breiling A, Luetkenhaus K, Ceteci F, Hausmann S, Kress S, Lyko F, Rudel T, Rapp UR. 2013. MYC-induced epigenetic activation of GATA4 in lung adenocarcinoma. *Mol Cancer Res* **11**: 161–172.

Chagraoui J, Hébert J, Girard S, Sauvageau G. 2011. An anticlastogenic function for the Polycomb Group gene Bmi1. *Proc Natl Acad Sci USA* **108**: 5284–5289.

Cheng Y, Phoon YP, Jin X, Chong SYS, Ip JCY, Wong BWY, Lung ML. 2015. Wnt-C59 arrests stemness and suppresses growth of nasopharyngeal carcinoma in mice by inhibiting the Wnt pathway in the tumor microenvironment. *Oncotarget* **6**: 14428–14439.

Chiacchiera F, Rossi A, Jammula S, Piunti A, Scelfo A, Ordóñez-Morán P, Huelsken J, Koseki H, Pasini D. 2016. Polycomb Complex PRC1 Preserves Intestinal Stem Cell Identity by Sustaining Wnt/β-Catenin Transcriptional Activity. *Stem Cell* **18**: 91–103.

Chudnovsky Y, Kim D, Zheng S, Whyte WA, Bansal M, Bray M-A, Gopal S, Theisen MA, Bilodeau S, Thiru P, et al. 2014. ZFHX4 Interacts with the NuRD Core Member CHD4 and Regulates the Glioblastoma Tumor-Initiating Cell State. *Cell Reports* **6**: 313–324.

Clevers H, Nusse R. 2012. Wnt/β-Catenin Signaling and Disease. *Cell* **149**: 1192–1205.

Collisson EA, Network TCGAR, Campbell JD, Brooks AN, Berger AH, Lee W, Chmielecki J, Beer DG, Cope L, Creighton CJ, et al. 2014. Comprehensive molecular profiling of lung adenocarcinoma. *Nature* **511**: 543–550.

Declercq J, Van Dyck F, Van Damme B, Van de Ven WJM. 2008. Upregulation of Igf and Wnt signalling associated genes in pleomorphic adenomas of the salivary glands in PLAG1 transgenic mice. *Int J Oncol* **32**: 1041–1047.

Desai TJ, Brownfield DG, Krasnow MA. 2014. Alveolar progenitor and stem cells in lung development, renewal and cancer. *Nature* **507**: 190–194.

Dovey JS, Zacharek SJ, Kim CF, Lees JA. 2008. Bmi1 is critical for lung tumorigenesis and bronchioalveolar stem cell expansion. *Proc Natl Acad Sci USA* **105**: 11857–11862.

Dupage M, Dooley AL, Jacks T. 2009. Conditional mouse lung cancer models using adenoviral or lentiviral delivery of Cre recombinase. *Nat Protoc* **4**: 1064–1072.

Fasano CA, Dimos JT, Ivanova NB, Lowry N, Lemischka IR, Temple S. 2007. shRNA Knockdown of Bmi-1 Reveals a Critical Role for p21-Rb Pathway in NSC Self-Renewal during Development. *Cell Stem Cell* **1**: 87–99.

Gargiulo G, Cesaroni M, Serresi M, de Vries N, Hulsman D, Bruggeman SW, Lancini C, van Lohuizen M. 2013. In vivo RNAi screen for BMI1 targets identifies TGF-β/BMP-ER stress pathways as key regulators of neural- and malignant glioma-stem cell homeostasis. *Cancer Cell* **23**: 660–676.

Ginjala V, Nacerddine K, Kulkarni A, Oza J, Hill SJ, Yao M, Citterio E, van Lohuizen M, Ganesan S. 2011. BMI1 is recruited to DNA breaks and contributes to DNA damage-induced H2A ubiquitination and repair. *Mol Cell Biol* **31**: 1972–1982.

Guney I. 2006. Reduced c-Myc signaling triggers telomere-independent senescence by regulating Bmi-1 and p16INK4a. *Proc Natl Acad Sci USA* **103**: 3645–3650.

Hellebrekers DMEI, Lentjes MHFM, van den Bosch SM, Melotte V, Wouters KAD, Daenen KLJ, Smits KM, Akiyama Y, Yuasa Y, Sanduleanu S, et al. 2009. GATA4 and GATA5 are potential tumor suppressors and biomarkers in colorectal cancer. - PubMed - NCBI. *Clin Cancer Res* **15**: 3990–3997.

Hemmi K, Ma D, Miura Y, Kawaguchi M, Sasahara M, Hashimoto-Tamaoki T, Tamaoki T, Sakata N, Tsuchiya K. 2006. A homeodomain-zinc finger protein, ZFHX4, is expressed in neuronal differentiation manner and suppressed in muscle differentiation manner. *Biol Pharm Bull* **29**: 1830–1835.

Herman JG, Graff JR, Myöhänen S, Nelkin BD, Baylin SB. 1996. Methylation-specific PCR: a novel PCR assay for methylation status of CpG islands. *Proc Natl Acad Sci USA* **93**: 9821–9826.

Hoenerhoff MJ, Chu I, Barkan D, Liu Z-Y, Datta S, Dimri GP, Green JE. 2009. BMI1 cooperates with H-RAS to induce an aggressive breast cancer phenotype with brain metastases. *Oncogene* **28**: 3022–3032.

Hu X, Feng Y, Zhang D, Zhao SD, Hu Z, Greshock J, Zhang Y, Yang L, Zhong X, Wang L-P, et al. 2014. A Functional Genomic Approach Identifies FAL1 as an Oncogenic Long Noncoding RNA that Associates with BMI1 and Represses p21 Expression in Cancer. *Cancer Cell* **26**: 344–357.

Ismail IH, Andrin C, McDonald D, Hendzel MJ. 2010. BMI1-mediated histone ubiquitylation promotes DNA double-strand break repair. *J Cell Biol* **191**: 45–60.

Jacobs JJ, Kieboom K, Marino S, DePinho RA, van Lohuizen M. 1999a. The oncogene and Polycomb-group gene bmi-1 regulates cell proliferation and senescence through the ink4a locus. *Nature* **397**: 164–168.

Jacobs JJ, Scheijen B, Voncken JW, Kieboom K, Berns A, van Lohuizen M. 1999b. Bmi-1 collaborates with c-Myc in tumorigenesis by inhibiting c-Myc-induced apoptosis via INK4a/ARF. *Genes Dev* **13**: 2678–2690.

Jagani Z, Wiederschain D, Loo A, He D, Mosher R, Fordjour P, Monahan J, Morrissey M, Yao YM, Lengauer C, et al. 2010. The Polycomb Group Protein Bmi-1 Is Essential for the Growth of Multiple Myeloma Cells. *Cancer Res* **70**: 5528–5538.

Kauffman SL. 1981. Histogenesis of the papillary Clara cell adenoma. *Am J Pathol* **103**: 174–180.

Kim CFB, Jackson EL, Woolfenden AE, Lawrence S, Babar I, Vogel S, Crowley D, Bronson RT, Jacks T. 2005. Identification of bronchioalveolar stem cells in normal lung and lung cancer. *Cell* **121**: 823–835.

Kreso A, van Galen P, Pedley NM, Lima-Fernandes E, Frelin C, Davis T, Cao L, Baiazitov R, Du W, Sydorenko N, et al. 2014. Self-renewal as a therapeutic target in human colorectal cancer. *Nat Med* **20**: 29–36.

Kress TR, Sabò A, Amati B. 2015. MYC: connecting selective transcriptional control to global RNA production. *Nat Rev Cancer* **15**: 593–607.

Ku M, Koche RP, Rheinbay E, Mendenhall EM, Endoh M, Mikkelsen TS, Presser A, Nusbaum C, Xie X, Chi AS, et al. 2008. Genomewide Analysis of PRC1 and

PRC2 Occupancy Identifies Two Classes of Bivalent Domains ed. B. Van Steensel. *PLoS Genet* **4**: e1000242.

Lee G, Lee HY, Jeong JY, Han J, Cha MJ, Lee KS, Kim J, Shim YM. 2015. Clinical impact of minimal micropapillary pattern in invasive lung adenocarcinoma: prognostic significance and survival outcomes. *Am J Surg Pathol* **39**: 660–666.

Liu J, Cao L, Chen J, Song S, Lee IH, Quijano C, Liu H, Keyvanfar K, Chen H, Cao L-Y, et al. 2009. Bmi1 regulates mitochondrial function and the DNA damage response pathway. *Nature* **459**: 387–392.

Liu Y, Liu F, Yu H, Zhao X, Sashida G, Deblasio A, Harr M, She Q-B, Chen Z, Lin H-K, et al. 2012. Akt Phosphorylates the Transcriptional Repressor Bmi1 to Block Its Effects on the Tumor-Suppressing Ink4a-Arf Locus. *Science Signaling* **5**: ra77.

Loeb LA. 2011. Human cancers express mutator phenotypes: origin, consequences and targeting. *Nat Rev Cancer* **11**: 450–457.

Lowry JA, Atchley WR. 2000. Molecular Evolution of the GATA Family of Transcription Factors: Conservation Within the DNA-Binding Domain. *J Mol Evol* **50**: 103–115.

Mourgues L, Imbert V, Nebout M, Colosetti P, Neffati Z, Lagadec P, Verhoeyen E, Peng C, Duprez E, Legros L, et al. 2015. The BMI1 polycomb protein represses cyclin G2-induced autophagy to support proliferation in chronic myeloid leukemia cells. *Leukemia* **29**: 1993–2002.

Naiche LA, Harrelson Z, Kelly RG, Papaioannou VE. 2005. T-box genes in vertebrate development. *Annu Rev Genet* **39**: 219–239.

Negishi M, Saraya A, Miyagi S, Nagao K, Inagaki Y, Nishikawa M, Tajima S, Koseki H, Tsuda H, Takasaki Y, et al. 2007. Bmi1 cooperates with Dnmt1-associated protein 1 in gene silencing. *Biochem Biophys Res Commun* **353**: 992–998.

Oguro H, Yuan J, Ichikawa H, Ikawa T, Yamazaki S, Kawamoto H, Nakauchi H, Iwama A. 2010. Poised lineage specification in multipotential hematopoietic stem and progenitor cells by the polycomb protein Bmi1. *Cell Stem Cell* **6**: 279–286.

Pietersen AM, Evers B, Prasad AA, Tanger E, Cornelissen-Steijger P, Jonkers J, van Lohuizen M. 2008. Bmi1 regulates stem cells and proliferation and differentiation of committed cells in mammary epithelium. *Curr Biol* **18**: 1094–1099.

Piunti A, Rossi A, Cerutti A, Albert M, Jammula S, Scelfo A, Cedrone L, Fragola G, Olsson L, Koseki H, et al. 2014. Polycomb proteins control proliferation and transformation independently of cell cycle checkpoints by regulating DNA replication. *Nature Communications* **5**: 3649.

Puschendorf M, Terranova R, Boutsma E, Mao X, Isono K-I, Brykczynska U, Kolb C, Otte AP, Koseki H, Orkin SH, et al. 2008. PRC1 and Suv39h specify parental asymmetry at constitutive heterochromatin in early mouse embryos. *Nat Genet* **40**: 411–420.

Reik W, Collick A, Norris ML, Barton SC, Surani MA. 1987. Genomic imprinting determines methylation of parental alleles in transgenic mice. *Nature* **328**: 248–251.

Singh MK, Petry M, Haenig B, Lescher B, Leitges M, Kispert A. 2005. The T-box transcription factor Tbx15 is required for skeletal development. *Mech Dev* **122**: 131–144.

Sun Z, Aubry M-C, Deschamps C, Marks RS, Okuno SH, Williams BA, Sugimura H, Pankratz VS, Yang P. 2006. Histologic grade is an independent prognostic factor for survival in non-small cell lung cancer: an analysis of 5018 hospital- and 712 population-based cases. *J Thorac Cardiovasc Surg* **131**: 1014–1020.

Sutherland KD, Song J-Y, Kwon M-C, Proost N, Zevenhoven J, Berns A. 2014. Multiple cells-of-origin of mutant K-Ras-induced mouse lung adenocarcinoma. *Proc Natl Acad Sci USA* **111**: 4952–4957.

Tomasetti C, Vogelstein B. 2015. Variation in cancer risk among tissues can be explained by the number of stem cell divisions. *Science* **347**: 78–81.

Tzatsos A, Bardeesy N. 2008. Ink4a/Arf regulation by let-7b and Hmga2: a genetic pathway governing stem cell aging. *Cell Stem Cell* **3**: 469–470.

Weisenberger DJ. 2014. Characterizing DNA methylation alterations from The Cancer Genome Atlas. *J Clin Invest* **124**: 17–23.

Westcott PMK, Halliwill KD, To MD, Rashid M, Rust AG, Keane TM, Delrosario R, Jen K-Y, Gurley KE, Kemp CJ, et al. 2014. The mutational landscapes of genetic and chemical models of Kras-driven lung cancer. *Nature* **517**: 489–492.

Winslow MM, Dayton TL, Verhaak RGW, Kim-Kiselak C, Snyder EL, Feldser DM, Hubbard DD, DuPage MJ, Whittaker CA, Hoersch S, et al. 2011. Suppression of lung adenocarcinoma progression by Nkx2-1. *Nature* **473**: 101–104.

Wutz A. 2011. Gene silencing in X-chromosome inactivation: advances in understanding facultative heterochromatin formation. *Nat Rev Genet* **12**: 542–553.

Young NP, Jacks T. 2010. Tissue-specific p19Arf regulation dictates the response to oncogenic K-ras. *Proc Natl Acad Sci USA* **107**: 10184–10189.

Yuan J, Takeuchi M, Negishi M, Oguro H, Ichikawa H, Iwama A. 2011. Bmi1 is essential for leukemic reprogramming of myeloid progenitor cells. *Leukemia* **25**: 1335–1343.

Zacharek SJ, Fillmore CM, Lau AN, Gludish DW, Chou A, Ho JWK, Zamponi R, Gazit R, Bock C, Jäger N, et al. 2011. Lung Stem Cell Self-Renewal Relies on BMI1-Dependent Control of Expression at Imprinted Loci. *Cell Stem Cell* **9**: 272–281.

Zheng X, Wang Y, Liu B, Liu C, Liu D, Zhu J, Yang C, Yan J, Liao X, Meng X, et al. 2014. Bmi-1-shRNA inhibits the proliferation of lung adenocarcinoma cells by blocking the G1/S phase through decreasing cyclin D1 and increasing p21/p27 levels. *Nucleic Acid Ther* **24**: 210–216.

Zheng Y, la Cruz de CC, Sayles LC, Alleyne-Chin C, Vaka D, Knaak TD, Bigos M, Xu Y, Hoang CD, Shrager JB, et al. 2013. A rare population of CD24(+)ITGB4(+)Notch(hi) cells drives tumor propagation in NSCLC and requires Notch3 for self-renewal. *Cancer Cell* **24**: 59–74.

Zhou Y, Wang L, Vaseghi HR, Liu Z, Lu R, Alimohamadi S, Yin C, Fu J-D, Wang GG, Liu J, et al. 2016. Bmi1 Is a Key Epigenetic Barrier to Direct Cardiac Reprogramming. *Cell Stem Cell* **18**: 382–395.

Zuber J, Tchernitsa OI, Hinzmann B, Schmitz A-C, Grips M, Hellriegel M, Sers C, Rosenthal A, Schäfer R. 2000. A genome-wide survey of RAS transformation targets. *Nat Genet* **24**: 144–152.